INTERNATIONAL ATOMIC ENERGY AGENCY
UNITED NATIONS EDUCATIONAL, SCIENTIFIC AND CULTURAL ORGANIZATION
**INTERNATIONAL CENTRE FOR THEORETICAL PHYSICS**
**I.C.T.P., P.O. BOX 586, 34100 TRIESTE, ITALY, CABLE: CENTRATOM TRIESTE**

UNITED NATIONS INDUSTRIAL DEVELOPMENT ORGANIZATION

**INTERNATIONAL CENTRE FOR SCIENCE AND HIGH TECHNOLOGY**
c/o INTERNATIONAL CENTRE FOR THEORETICAL PHYSICS 34100 TRIESTE (ITALY) VIA GRIGNANO, 9 (ADRIATICO PALACE) P.O. BOX 586 TELEPHONE 040-224572 TELEFAX 040-224575 TELEX 460449 APH I

**H4.SMR/537-9**

# *SECOND COLLEGE ON THEORETICAL AND EXPERIMENTAL RADIOPROPAGATION PHYSICS*

**(7 January - 1 February 1991)**

***Co-sponsered by ICTP, URSI, ICSU***
***and with the participation of ICS***

## *Characteristics and applications of atmospheric radio noise data*

A. D. Spaulding
Institute for Telecommunication Sciences
U.S. Department of Commerce
Boulder, Colorado

COMITÉ CONSULTATIF INTERNATIONAL DES RADIOCOMMUNICATIONS
INTERNATIONAL RADIO CONSULTATIVE COMMITTEE
COMITÉ CONSULTIVO INTERNACIONAL DE RADIOCOMUNICACIONES

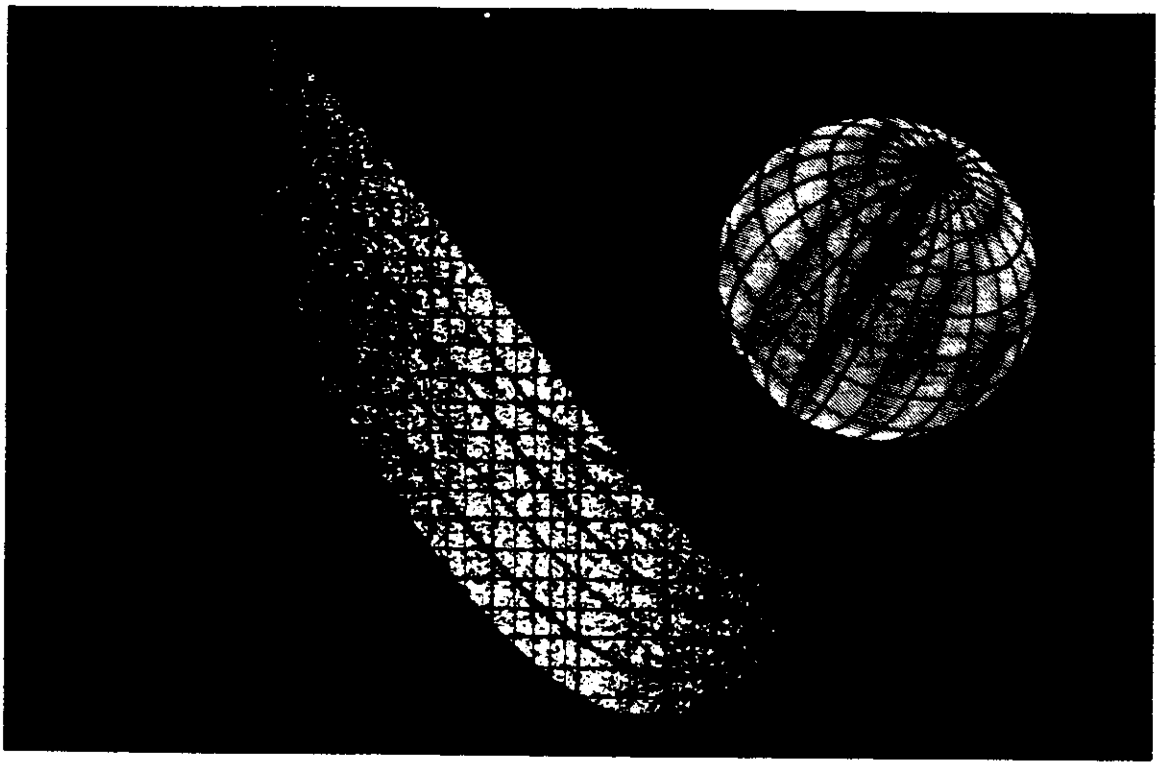

# CARACTÉRISTIQUES DU BRUIT ATMOSPHÉRIQUE RADIOÉLECTRIQUE ET APPLICATIONS

# CHARACTERISTICS AND APPLICATIONS OF ATMOSPHERIC RADIO NOISE DATA

# CARACTERÍSTICAS DEL RUIDO ATMOSFÉRICO RADIOELÉCTRICO Y APLICACIONES

UNION INTERNATIONALE DES TÉLÉCOMMUNICATIONS
INTERNATIONAL TELECOMMUNICATION UNION
UNIÓN INTERNACIONAL DE TELECOMUNICACIONES

Genève, 1988

## TABLE DES MATIÈRES

Page

Liste des notations . . . . . . . . 3
1. Introduction . . . . . . . . 4
2. Evaluations du bruit radioélectrique . . . . . . . . 5
3. Définition des paramètres utilisés . . . . . . . . 5
4. Méthodes utilisées pour obtenir les évaluations . . . . . . . . 7
5. Données de bruit et estimation du bruit . . . . . . . . 8
6. Application des données de bruit a l'évaluation des systèmes . . . . . . . . 9
7. Influence de la directivité et de la polarisation des antennes . . . . . . . . 13

## CONTENTS

Page

List of symbols . . . . . . . . 15
1. Introduction . . . . . . . . 16
2. Radio noise estimates . . . . . . . . 17
3. Description of the parameters used . . . . . . . . 17
4. Methods used to obtain the estimates . . . . . . . . 19
5. The noise data or estimates . . . . . . . . 20
6. Application of noise data to system evaluation . . . . . . . . 21
7. The influence of the directivity and polarization of antennas . . . . . . . . 25

## ÍNDICE

Página

Notación . . . . . . . . 27
1. Introducción . . . . . . . . 28
2. Estimaciones del ruido radioeléctrico . . . . . . . . 29
3. Descripción de los parámetros utilizados . . . . . . . . 29
4. Métodos utilizados para obtener estimaciones . . . . . . . . 31
5. Los datos del ruido o estimaciones . . . . . . . . 32
6 Aplicación de los datos de ruido a la evaluación de un sistema

## REPORT 322-3[*]

# CHARACTERISTICS AND APPLICATIONS OF ATMOSPHERIC RADIO NOISE DATA

(Study Programme 29B/6)

(1963-1974-1982-1986)

## LIST OF SYMBOLS

Where a symbol is shown in both lower case and capital letters, the capital letter is used to represent the equivalent, in decibels, of the quantity denoted by the lower case letter.

| | |
|---|---|
| $A$ | Instantaneous amplitude of the noise envelope (dB) |
| $A_{rms}$ | Root-mean-square value of the noise envelope voltage (dB) |
| $APD$ | Amplitude-probability distribution of received noise envelope (exceedance probability) |
| $b$, $B$ | Effective receiver noise bandwidth (Hz) ($B = 10 \log b$) |
| $D$ | Deviation of a random variable from its median value (dB) |
| $D_l$ | Lower decile, value of the average noise power exceeded 90% of the hours within a time block (dB below the median value for the time block) |
| $D_R$ | Upper decile of signal-to-noise ratio (dB value exceeded 10% of the time) |
| $D_S$ | Upper decile of the received signal power (dB value exceeded 10% of the time) |
| $D_u$ | Upper decile, value of the average noise power exceeded 10% of the hours within a time block (dB above the median value for the time block) |
| $E_e$ | Expected value of the signal field strength required for a given grade of service (dB($\mu$V/m)) |
| $E_n$ | Root-mean-square noise field strength for a bandwidth $b$ (dB($\mu$V/m)) |
| $f$ | Operating noise factor of a receiving system |
| $F$ | Operating noise figure of a receiving system ($F = 10 \log f$) |
| $f_a$ | Effective antenna noise factor that results from the external noise power available from a loss-free antenna |
| $F_a$ | Effective antenna noise figure ($F_a = 10 \log f_a$) |
| $F_{am}$ | Median of the hourly values of $F_a$ within a time block |
| $f_c$ | Noise factor of the antenna circuit (its loss in available power) |
| $f_{MHz}$ | Frequency (MHz) |
| $f_r$ | Receiver noise factor |
| $f_t$ | Noise factor of the transmission line (its loss in available power) |
| $k$ | Boltzmann's constant $= 1.38 \times 10^{-23}$ J/K |
| $K$ | Temperature (Kelvin) |
| $P$ | Received signal power available from an equivalent loss-free antenna (dBW) |
| $P_e$ | Expected median value of $P$ (dBW) |
| $p_n$, $P_n$ | Noise power available from an equivalent loss-free antenna ($P_n = 10 \log p_n$) |
| $p_s$, $P_s$ | Received signal power required for a given signal-to-noise ratio, from a loss-free antenna ($P_s = 10 \log p_s$) |
| $pdf$ | Probability density function |
| $r$, $R$ | Signal-to-noise power ratio required ($R = 10 \log r$) |
| $R_m$ | Median value of $R$ |
| $t$ | Standard normal deviate |
| $T_a$ | Effective antenna temperature in the presence of external noise (K) |
| $T_0$ | Reference temperature = 288 K |

---

[*] This new version of Report 322 was adopted by the XVIth Plenary Assembly (Dubrovnik, 1986) for the purpose of facilitating further studies to be carried out by Study Group 6 (see Recommendation 372-4).

| | |
|---|---|
| $V_d$ | Voltage deviation: the ratio (dB) of the root-mean-square envelope voltage to the average noise envelope voltage |
| $V_{dm}$ | Time-block median value of $V_d$ |
| $\sigma_D$ | Standard deviation of $D$ |
| $\sigma_{Dl}$ | Standard deviation of $D_l$ |
| $\sigma_{D_u}$ | Standard deviation of $D_u$ |
| $\sigma_{DR}$ | Standard deviation of $D_R$ |
| $\sigma_{F_{am}}$ | Standard deviation of $F_{am}$ |
| $\sigma_P$ | Standard deviation of the expected received signal power |
| $\sigma_R$ | Standard deviation of $R$ |
| $\sigma_T$ | Total standard deviation; total uncertainty of $P_e$ |
| $\sigma_{V_d}$ | Standard deviation of $V_d$ |

## 1. Introduction

The determination of radio communication system performance and the resulting minimum signal level required for satisfactory reception is a matter of the proper statistical treatment of both the desired signal and the real-world noise (and interference) processes. System performance is highly dependent on the detailed statistical characteristics of both the signal and the noise. It has long been recognized that the ultimate limitation to a properly designed communication link will usually be the radio noise.

There are a number of types of radio noise that must be considered in any design; though, in general, one type will be the predominant noise and will be the deciding design factor. In broad categories, the noise can be divided into two types – noise internal to the receiving system and noise external to the receiving antenna. The internal noise is due to antenna and transmission line losses, or is generated in the receiver itself and has the characteristics of thermal noise (i.e., white Gaussian noise). Noise power is generally the most significant parameter (but seldom sufficient) in relating the interference potential of the noise to system performance. Since the noise level often results from a combination of external and internal noise, it is convenient to express the resultant noise by means of an overall operating noise factor that characterizes the performance of the entire receiving system. In so doing, it is then possible to make decisions concerning required receiving system sensitivity; that is, a receiver need have no more sensitivity than that dictated by the external noise. Indeed, world-wide minimum noise levels have been estimated for this purpose (Report 670). Also, the noise levels can then be compared to the desired signal level to determine the pre-detection signal-to-noise ratio. The pre-detection signal-to-noise ratio is an important system design parameter and is always required knowledge (required but seldom sufficient) when determining the effects of the external noise on system performance.

External noise can be divided into several types, each having its own characteristics. The most usual types are of atmospheric, galactic, and man-made origin. All these types are considered here, but since atmospheric noise usually predominates at frequencies below about 30 MHz, this Report deals primarily with this type and with its influence on the reception of signals. Unlike the internal noise, the external noise is generally highly non-Gaussian in character, usually being impulsive in nature.

The purpose of this Report is to present values of noise power and of other noise parameters, and to show, by example, the method of using these noise parameters and their statistical variations in the evaluation of the performance of a radio circuit. Additional examples of the use of the noise data in this Report and a summary of the effects of atmospheric radio noise (and similar forms of impulsive noise) on telecommunication systems performance are given in Spaulding [1982]. Also, recent results concerning atmospheric noise from lightning and means of developing appropriate communication systems to perform in this noise are summarized by URSI [198[illegible]], in Report 254 and in the references therein. Finally, Reports 258 and 670 give additional information concerning man-made and atmospheric noise, and Recommendation 339 gives required signal energy to noise power spectral density ratios for various systems operating in the presence of atmospheric noise.

The estimates for atmospheric noise levels given in this Report are for the average background noise level due to lightning in the absence of other signals, whether intentionally or unintentionally radiated. In addition, the noise due to local thunderstorms can be important for a significant percentage of the time. This local noise can also be significant at frequencies well above 30 MHz. Some information pertaining to local thunderstorm noise is available in Hagn and Shepherd [1984], Kotaki and Katoh [1983] and Kotaki [1984].

## 2. Radio noise estimates

This Report gives:

- estimates that take account of major reliable programmes of noise measurements,
- statistical information on the accuracy of the estimates,
- a statistical description of the fine structure of the noise,
- examples of using the estimates in the determination of system performance.

The data used were obtained from the 15 stations that used standardized recording equipment, the ARN-2 radio noise recorder, which was operated by a number of organizations in an international cooperative programme [URSI, 1962], a measurement station in Thailand that used equipment equivalent to the ARN-2, and 10 measurement stations within the USSR. The measurement station locations are shown in Fig. 1. Data from the stations during the period 1957 to 1966 inclusive were used in the analysis. Not all the stations produced data for the entire period. Data from the Southern Hemisphere are sparse. Details on the specifics of this data base of long-term atmospheric radio noise measurements and the analysis of these data are given in Spaulding and Washburn [1985].

For these predictions, the data were grouped into four seasons of the year and six four-hour periods of the day in each season. The aggregate of corresponding four-hour periods of the day throughout a season was defined as a time block. Thus, there are in the year twenty-four time blocks, each consisting of about 360 hours (four hours in each day for about ninety days).

The division of the year into four seasons of three months each was made in the following way, although it was realized that the seasonal pattern of noise variations existing in temperate regions was not necessarily followed at lower latitudes.

| Month | Season | |
|---|---|---|
| | *Northern Hemisphere* | *Southern Hemisphere* |
| December, January, February | Winter | Summer |
| March, April, May | Spring | Autumn |
| June, July, August | Summer | Winter |
| September, October, November | Autumn | Spring |

The main parameter presented is the median hourly value of the average noise power for each time block, and the variations in this parameter show systematic diurnal and seasonal variations of the noise. The variations of the hourly values within a time block have been treated statistically.

To facilitate the use of the noise data in this Report, computer programs are available from the CCIR Secretariat that give "exact" numerical representations of all the noise characteristics contained in this Report.

## 3. Description of the parameters used

As noted above, the single most important and basic noise parameter is noise power, although this single parameter (or any other single parameter) is almost never sufficient to determine the effects of the noise on system performance. Also, it is convenient to express the external noise in a form that allows for its combination with the internal noise, thereby given an overall operating noise threshold for a receiving system. Report 670 details how this noise threshold is obtained.

The noise power received from sources external to the antenna is expressed in terms of an effective antenna noise factor, $f_a$, which is defined by:

$$f_a = p_n / k T_0 b = T_a / T_0 \qquad (1)$$

where:

$p_n$ : noise power available from an equivalent loss free antenna (W),

$k$ : Boltzmann's constant $= 1.38 \times 10^{-23}$ J/K,

$T_0$ : reference temperature, taken as 288 K,

$b$ : effective receiver noise bandwidth (Hz),

$T_a$ : effective antenna temperature in the presence of external noise.

Equation (1) gives two equivalent methods of specifying the noise power, by the effective noise factor or by the effective noise temperature of the antenna. The value of $T_0$ has been taken as 288 K so that 10 log $kT_0$ is 204 dB below one Joule.

Since atmospheric noise is a spectrally broadband process, both $f_a$ and $T_a$ are independent of bandwidth (for normal communications bandwidths). Note that $f_a$ is a dimensionless quantity, being the ratio of two powers (or, equivalently, two temperatures). The quantity $f_a$, however, gives, numerically, the available power spectral density in terms of $kT_0$ or the available power in terms of $kT_0b$. The noise factor $f_a$ is commonly given by the corresponding noise figure $F_a$, i.e., $F_a = 10 \log f_a$.

The antenna noise figure, $F_a$, in decibels, in this Report is for a lossless short vertical antenna over a perfectly conducting ground plane. Means of obtaining the appropriate antenna noise figure, $F_a$, for other types of antennas from the data in this Report are given in Report 670, the references therein, Hagn and Shepherd [1984] and Lauber and Bertrand [1977]. $F_a$ is simply related to the vertical r.m.s. field strength (for the short vertical antenna) by:

$$E_n = F_a - 95.5 + 20 \log f_{MHz} + 10 \log b \qquad (2)$$

where:

$E_n$ : r.m.s. noise field strength (dB(μV/m)) in bandwidth $b$ (Hz),

$F_a$ : noise figure for the centre frequency $f_{MHz}$ (MHz).

Atmospheric radio noise is characterized by large, rapid fluctuations, but if the noise power is averaged over a period of several minutes, the average values are found to be nearly constant during a given hour, variations rarely exceeding ± 2 dB except near sunrise or sunset, or when there are local thunderstorms. The ARN-2 radio noise recorder yielded values of average power at each of eight frequencies for fifteen minutes each hour, and it is assumed that the resulting values of $F_a$ used in the analysis were representative of the hourly values. Similar assumptions are made to obtain hourly $F_a$ values for the other measurements (non-ARN-2) used in the analysis.

In predicting the expected noise level, the systematic trends, that is, the trends with time of day, season, frequency, and geographical location, are taken into account explicitly. There are other variations that must be taken into account statistically. The value of $F_a$ for a given hour of the day varies from day to day, because of random changes in thunderstorm activity and propagation conditions. The median of the hourly values within a time block (the time-block median), is designated as $F_{am}$. Variations of the hourly values during the time block can be represented by the values exceeded for 10% and 90% of the hours, expressed as deviations $D_u$ and $D_l$ from the time block median. When plotted on a normal probability graph (level in dB), the amplitude distribution of the deviations, $D$, above the median can be represented with reasonable accuracy by a straight line through the median and upper decile values, and a corresponding line through the median and lower decile values can be used to represent values below the median.

It is natural to expect some correlation of atmospheric radio noise with sunspot activity, since both propagation conditions and thunderstorm activity seem to be affected by solar activity. Some measurements at very low frequencies, made many years ago, did seem to show such a correlation [Austin, 1932]. A thorough examination of the data for Boulder, Colorado (1957-1966) did not reveal any systematic variation of the noise with sunspot activity.

So far, we have dealt with the average power as represented by $F_a$ (or $T_a$) as the most useful and common way of specifying the external noise level. When one is concerned with determining the effects of the external noise on system performance, more information about the received noise process than just its energy content (level) is almost always required. An exception would be if the external noise were a white Gaussian noise process, but this is almost never the case. Atmospheric noise (and man-made noise) is a random process. The fact that we are dealing with a random process means that the noise can be described only in probabilistic or statistical terms and cannot be represented by a deterministic waveform or any collection of deterministic waveforms.

The basic description of any random process is its probability density function (pdf) or distribution function. The first-order pdf of the received interference process is almost always required in order to determine system performance (although sometimes it is not sufficient). The received atmospheric noise process under consideration here is a bandpass process in that it is describable by an envelope process and a phase process. Since the phase process is known (phase uniformly distributed), the required pdf of the instantaneous amplitude can be obtained from the envelope amplitude pdf. Usually, also, the envelope pdf can be used directly in system performance analyses. The atmospheric noise envelope statistic is usually given as (and measured as) a cumulative exceedance distribution, termed the "amplitude probability distribution" or APD. For some envelope level, $A_i$, the APD is the fraction of the total measurement time, $T$, for which the envelope was above level $A_i$.

A large number of APDs have been measured in several countries, and reasonably consistent results have been obtained [URSI, 1962; Clarke, 1962; Science Council of Japan, 1960; see also URSI, 1975, 1978, 1981, 1984, and references therein]. For presenting the data in an operationally useful form, it is convenient to construct a family of idealized curves, one of which can be chosen to represent a practical APD to a sufficient accuracy. This has been done by using a system of coordinates in which a Rayleigh distribution (representing the envelope of thermal-type noise), is a straight line with a slope of $-0.5$. The low amplitude parts of an atmospheric noise curve have this slope, the high amplitude parts are represented by a second straight line, with a greater slope, and the two lines are joined by an arc of a circle. The construction of these curves involved the use of quantities related to the r.m.s. average, and mean logarithmic values of the distribution, parameters that have been recorded in routine noise measurements [Crichlow *et al.*, 1960a, 1960b]. In practice, because the average voltage and mean logarithmic voltage are found to be closely correlated, the ratio of r.m.s. to average voltage, $V_d$(dB), is sufficient to specify the curve that can be used to represent the distribution [Spaulding *et al.*, 1962]. A set of the APD curves is reproduced in Fig. 27, which gives the probability (× 100) that an envelope level $A_0$ (given relative to the envelope r.m.s. level, $A_{rms}$) will be exceeded. Figure 27 represents one "model" for the APD parametric in the parameter $V_d$. Many other models for atmospheric noise statistics have been developed, and a historical summary of the various main models and their interrelationships has been given by Spaulding [1977, 1982] and by Shaver *et al.* [1972]. Numerical representation (coefficients and computer programs) of the APD model in this Report is available in Spaulding and Washburn [1985]. It should be noted that the actual noise power is one-half the envelope power (as given by $A_{rms}$).

The APD curves (Fig. 27) can be used for a wide range of bandwidths. The estimates of $V_d$ given in this Report, however, are for a bandwidth of 200 Hz, so a means to convert the 200 Hz $V_d$ to other bandwidths is needed. Herman and De Angelis [1987] conducted an extensive study in order to develop a $V_d$ bandwidth relationship. Figure 26 gives the results of this study and gives a means to convert the 200 Hz $V_d$ to the corresponding $V_d$ in other bandwidths. The results of Fig. 26 are strictly valid only at MF, although recent results indicate they are valid also at HF. Care should be exercised, therefore, when applying these results to lower frequencies (i.e., LF, VLF, ELF).

## 4. Methods used to obtain the estimates

Values of $F_a$, collected from the measurement stations previously mentioned, were edited to remove, as far as possible, the effects of man-made noise and unwanted signals. The remaining values were considered to represent actual atmospheric radio noise. The time block median 1 MHz values were compared with the Report 322-2 values and corrections derived. The means for obtaining the 1 MHz values from the [illegible] of measurements at all the measurement frequencies and the numerical interpolation and mapping procedures used to obtain the world-wide 1 MHz $F_{am}$ values for each time block are detailed in Spaulding and Washburn [illegible]

Only data from measurement stations that employed ARN-2 equipment were used to obtain the variation of $F_{am}$ with frequency (i.e., for frequencies other than 1 MHz). An analysis of these data indicated no significant difference from the frequency variations given in Report 322-2. The same is true for the deviations, $D_u$, $D_l$, of the decile value of $F_a$ from the median value $F_{am}$, for each time block, and also for the median value, $V_{dm}$, of the voltage deviation $V_d$.

To obtain a measure of the variability of the noise with respect to the predicted values in each time block, standard deviations of $F_{am}$, $D_u$, $D_l$, and $V_d$, as functions of frequency, were found.

## 5. The noise data or estimates

World charts, showing the expected median values of background atmospheric radio noise, $F_{am}$ in dB above $kT_0b$, at 1 MHz for each season, 4-hour-time block, in local time, are shown in Figs. 2a to 25a. The only geographical variation given is for the 1 MHz $F_{am}$. The variation of $F_{am}$ with frequency for each season-time block is given in Figs. 2b to 25b and the variation with frequency of the other noise parameters is given in Figs. 2c to 25c.

Galactic noise levels, from Cottony and Johler [1952] and verified using a vertical antenna, are shown on the frequency curves (Figs. 2b to 25b). Within a ± 2 dB temporal variation (neglecting ionospheric shielding), the values shown will be the upper limit of galactic noise but in any given situation the received noise should be determined considering critical frequencies and the directional properties of the antenna.

In many locations and at some frequencies, man-made noise is a limiting factor in radiocommunication for at least part of the time. Although this type of noise depends on local conditions, a curve of expected values at a quiet receiving location has been added. The values shown are the "average" of the man-made values recorded at sites chosen to ensure a minimum amount of man-made noise (the ARN-2 sites). Man-made noise levels, in terms of $F_a$, and their variations for various environmental categories (business, residential, rural and quiet rural, etc.) are given in Report 258. The noise levels for "quiet rural" locations given in Report 258 are taken from this Report. Additional information concerning man-made noise is summarized in Hagn [1982], Skomal [1978] and URSI [1975, 1978, 1981, 1984].

It will be observed that values of atmospheric noise are indicated that are below the expected levels of man-made noise and galactic noise. These values should be used with caution, as they represent only estimates of what atmospheric noise levels would be recorded if the other types of noise were not present. An examination of the data, however, shows that such low levels were, on rare occasions, actually measured.

On Figs. 2c to 25c are the estimated values of $D_u$, $D_l$, $V_{dm}$, $\sigma_{D_u}$, $\sigma_{D_l}$, $\sigma_{V_d}$, and $\sigma_{F_{am}}$. $D_u$ will normally be used for assessing minimum required signal strengths, but $D_l$ may be needed to determine whether the internal noise of a receiving system is negligible under the quieter external noise conditions.

The variation of $F_{am}$ with frequency (Figs. 2b to 25b) is given by a least squares numerical mapping of the totality of ARN-2 data for all the measurement frequencies [Spaulding and Washburn, 1985]. The parameter $\sigma_{F_{am}}$ represents, as a function of frequency, the variation of the $F_{am}$ data about the "mapped" (or estimated) values. The curves for $\sigma_{F_{am}}$ will be seen to extend only up to 10 MHz, since at higher frequencies the predominant noise at many measurement locations was often of galactic origin.

Originally, separate curves for $D_u$, $D_l$, $\sigma_{D_u}$, and $\sigma_{D_l}$ were derived using data from measurement locations in temperate and tropical zones. No statistically significant difference between the two zones was obtained and, therefore, this Report gives a single curve for the entire Earth's surface. These curves should be used with some caution, especially at the higher frequencies

APD curves corresponding to various values of $V_d$, are given in Fig. 27, in which the r.m.s. envelope voltage, $A_{rms}$, is taken as the reference. The measured values of $V_d$ vary about the predicted median value, $V_{dm}$, and their variation is given by $\sigma_{V_d}$. The $V_{dm}$ estimates given are for a 200 Hz bandwidth. The corresponding $V_{dm}$ for other bandwidth can be obtained from Fig. 26. As noted earlier, this bandwidth conversion should be used with caution at the lower frequencies (VLF and LF).

The figures are used in the following way. The value of $F_{am}$ for 1 MHz is found from the noise charts (Figs. 2a to 25a) for the season under consideration. Using this value as the noise grade, the value of $F_{am}$ for the required frequency is determined from the frequency curves (Figs. 2b to 25b). The variability parameters $\sigma_{F_{am}}$, $D_u$, $\sigma_{D_u}$, etc., are obtained for the required frequency from Figs. 2c to 25c. If the value of $D (= F_a - F_{am})$ or the value of $\sigma_D$ is required for any percentage (less than 50%) of time other than 10%, the values can be found by plotting $D_u$ and $\sigma_{D_u}$ on a normal probability graph (with ordinate values in decibels) and drawing straight lines through 0 dB at 50% and the 10% values, as shown in Fig. 28. That is, the noise power is log-normally distributed (above 50%). Values at percentages greater than 50% can be obtained in the same manner using $D_l$ and $\sigma_{D_l}$.

## 6. Application of noise data to system evaluation

The treatment here is not intended to be comprehensive; however, it is considered desirable to give some indication of how the data may be used in the study of telecommunication system performance. Additional examples and information are given in Spaulding [1982], URSI [1975, 1978, 1981, 1984], and the references therein.

As noted earlier, it is desirable to express the external noise as an antenna noise factor, so that it can be combined with the noise generated within the receiving system to give an overall operating noise factor, $f$ (Report 670) [Barsis *et al.*, 1961]. If the receiver is free from spurious responses and all elements prior to the receiver are at the reference temperature $T_0$, then $f$ is given by:

$$f = f_a - 1 + f_c f_t f_r \qquad (3)$$

where:

$f_c$ : noise factor of the antenna (its loss in available power),

$f_t$ : noise factor of the transmission line (its loss in available power), and

$f_r$ : noise factor of the receiver (10 log $f_r$ is the familiar receiver noise figure).

The operating noise factor, $f$, is useful in determining the relation between the signal power, $p_s$, available from a loss-free antenna and the corresponding signal-to-noise ratio, $r$, at the intermediate frequency output of the receiver, since:

$$p_s = f r k T_0 b \qquad (4)$$

or:

$$P_s = R + F + B - 204 \qquad (5)$$

where:

$F = 10 \log f$

$B = 10 \log b$, etc.

In evaluating the operating noise figure, $F$, for use in equation (5), it is necessary to consider all of the parameters in equation (3). However, in many cases, one source of noise will predominate, and only one of the component noise factors will be important. At low frequencies, a receiving system with poor internal noise characteristics may be used, since the values of $f_a$ are large, and will determine the value of $f$. In general, $F_a$ will decrease with increasing frequency, and, at the higher frequencies, the antenna tends to become more efficient and $f_c$ approaches unity. Under these conditions, $f_t$ and/or $f_r$ may become important in the determination of $f$ (Report 670).

The relation (5) is used to obtain the required average signal power from the required signal-to-noise ratio, $R$ (dB). The required $R$ always depends on the detailed statistical characteristics of both the noise and signal processes. For the noise, the APD (or statistics derivable from it) is almost always required (but sometimes not sufficient) information. Also, since the determination of system performance involves predicting the future (statistically) and such predictions are subject to error, it is common to define system performance in terms of three independent component parts: grade of service, time availability, and service probability [Barsis *et al.*, 1961; Spaulding, 1982].

6.1 *Grade of service* represents the average performance for stationary noise and signal processes. Typical examples are probability of symbol error versus signal-to-noise ratio for digital systems, articulation index versus signal-to-noise ratio for voice systems, etc.

6.2 *Time availability* is the percentage of time a given grade of service or better will be achieved.

6.3 *Service probability* is the probability that a specified grade of service or better will be achieved for a specified time availability. It is the "standard" statistical confidence factor required for any statistical description.

When the desired performance of a system has been defined, it is necessary to evaluate the various factors affecting this performance. For the sake of clarity and simplicity, the performance will, in the following two examples, be evaluated in terms of the characteristics of the available signal and noise powers at the terminals of the equivalent loss-free receiving antenna. In both examples it will be assumed that a short vertical rod antenna is used and that the predominant noise is atmospheric noise external to the system. In the first example, ground-wave propagation is assumed, so that the signal level is constant and only the noise level is variable. The second example involves sky-wave propagation and thus both the signal and noise levels vary with time. In both examples, the variation of the noise power is log-normal (i.e., dB values normally distributed) and the signal power is also log-normal (but constant, zero variance, in the first example). This results, then, in the signal-to-noise ratio, $r$, also being log-normal. This means that the standard procedures (based on the normal distribution) to determine statistical confidence factors (service probability) can be followed. The determination of the service probability involves not only uncertainties associated with the noise parameters but also the uncertainties of all values involved in the prediction process.

### 6.4 *Example I*

Determine the performance of a binary symmetric non-coherent frequency shift keying (NCFSK) system with reception at Geneva, Switzerland, under the following conditions.

| | |
|---|---|
| Frequency: | 50 kHz |
| Time of day: | 2000-2400 local time |
| Season: | summer |
| Bandwidth: | 100 Hz |
| Propagation: | ground wave (resulting in a constant signal) |
| Grade of service: | probability of bit error of $5 \times 10^{-4}$. This corresponds approximately to 1% teletype errors in a five unit start-stop system. |

The problem is to assess the probability that a given received signal power will provide the specified grade of service for any given percentage of time.

The expected value (mean value) of received power, $P_e$, required for a particular grade of service for a given external noise figure, $F_a$, is from relation (5):

$$P_e = F_a + R + B - 204 \qquad \text{dBW} \tag{6}$$

where $R$ is the required pre-detection signal-to-noise ratio (dB) for the given bandwidth.

When the receiving antenna is a short vertical rod over a ground plane, the corresponding field strength, $E_e$, is given by:

$$E_e = P_e + 20 \log f_{MHz} + 108.5 \qquad \text{dB}(\mu\text{V/m}) \tag{7}$$

The first step is to determine the required $R$ (and its variation). Following Montgomery [1954], we have the following results for any arbitrary additive noise that is independent from one integration period (bit length) to the next and that has uniformly distributed phase. For the symmetric binary NCFSK system, the probability of a bit being in error is given by one half the probability that the noise envelope exceeds the signal envelope. Therefore, the required signal-to-noise ratio can be obtained directly from the APD (Fig. 27) for the appropriate $V_d$. From Fig. 19c, the 200 Hz $V_{dm}$ at 50 kHz is 8.5 dB and $\sigma_{V_d}$ is 1.2 dB. Using Fig. 26, this translates to the 100 Hz $V_d$ ranging between 6.6 and 8.9 dB (from the 200 Hz $V_d$ range of 7.3 to 9.7 dB) with the 100 Hz $V_{dm}$ being 7.7 dB. The APDs can be used directly to determine the median required signal-to-noise ratio ($R$) and its variation. However, this is also available in Akima *et al.* [1969] where probability of bit error versus signal-to-noise characteristics for various $V_d$'s is given (using the APDs of Fig. 27 of this Report). The required $R$ for a $V_d$ of 7.7 is 20.3 dB with a variation of approximately 0.8 dB based on the above expected $V_d$ range; that is, $\sigma_R$ = 0.8 dB. It should be noted [Akima *et al.*, 1969] that if the signal was Rayleigh fading the required $R$ will be 28 dB and $\sigma_R$ would be 0 dB, since for small probability of errors, probability of error is independent of $V_d$. This is not true for other forms of fading (e.g., log-normal) or if diversity reception is employed. In these cases, probability of error is quite dependent on the APD (i.e., $V_d$).

$F_a$ must now be derived from the median value $F_{am}$ plus a deviation $D$ consistent with the percentage of time during which satisfactory service must be obtained (time availability). From Fig. 19a, the 1 MHz value is 74 dB and the value of $F_{am}$ at 50 kHz is 133 dB with a standard deviation, $\sigma_{F_{am}}$, of 3.4 dB (Fig. 19b, 19c). To obtain values of $F_a$ for percentages of time other than 50% (given by $F_{am}$), $D_u$ (6.4 dB from Fig. 19c) is used to obtain $D = F_a - F_{am}$ as shown on Fig. 28. Likewise, $\sigma_D$ is obtained using $\sigma_{D_u}$ (1.9 dB from Fig. 19c) as also shown on Fig. 28.

Equation (6) is next evaluated (with $F_a = F_{am} + D$) using the appropriate $D$ for the required time availability. From equation (6), then, with $R = 20.3$ dB, $F_{am} = 133$ dB, and $B = 20$ dB, we obtain:

$$P_e = D - 30.7 \qquad \text{dBW} \tag{8}$$

This is the usual prediction of the signal power required (or required field strength from equation (7)) to produce the specified grade of service for various time availabilities. The required signal power for various time availabilities is shown on Fig. 29. Since, however, the prediction uncertainties have not been taken into account yet, only one-half of such circuits will meet the design criteria.

The uncertainties to consider are given by the following standard deviations:

$\sigma_P$: the standard error of achieving the expected "constant" received signal power. This must be derived from propagation and other data and, for the purposes of this example, is assumed to be 2 dB;

$\sigma_R$: uncertainty in the required signal-to-noise ratio 0.8 dB as derived above;

$\sigma_{F_{am}} = 3.4$ dB (from Fig. 19c);

$\sigma_D$: standard deviation of $D$ (from Fig. 28).

The resulting standard deviation, $\sigma_T$, is obtained, since the errors are uncorrelated from:

$$\sigma_T^2 = \sigma_P^2 + \sigma_R^2 + \sigma_{F_{am}}^2 + \sigma_D^2 \tag{9}$$

$\sigma_T$ is also shown on Fig. 29 and enables us to determine the service probability (confidence) that the indicated time availability will be achieved, as follows.

Since, as noted earlier, only log-normal distributions are involved, for any given value of received power, $P$, the time availability can be determined as a function of the service probability from:

$$t = (P - P_e)/\sigma_T \tag{10}$$

where $t$ is the standard normal deviate. Figure 30 gives the values of $t$ as a function of service probability.

If a probability of only 0.5 (50% confidence) is required that a specified time availability will be achieved, $t = 0$, $P = P_e$, and the required powers are given by Fig. 29. Suppose, however, we specify that we want to be 90% confident (service probability of 0.9) that our grade of service (probability of bit error of $5 \times 10^{-4}$) or better will be achieved 90% of the time (or better), then $t = 1.3$ (Fig. 30), $\sigma_T = 4.45$ dB (Fig. 29), $P_e = 24.3$ dBW (Fig. 29) so that, from equation (10), the required signal strength is −18.5 dBW. In general, using equation (8) and equation (10):

$$P = D - 30.7 + t\,\sigma_T \tag{11}$$

Results for service probabilities of 0.5, 0.8, 0.9 and 0.99 are shown on Fig. 31.

### 6.5 *Example II*

Determine the performance of an A3E telephony double-sideband system with reception at Geneva, Switzerland, under the following conditions:

| | |
|---|---|
| Frequency: | 5 MHz |
| Time of day: | 2000-2400 local time |
| Season: | summer |
| Bandwidth: | 6 kHz |
| Propagation: | ionospheric (resulting in a fading signal) |
| Grade of service: | marginally commercial. |

Again the problem is to assess the probability that a given received signal power will provide the specified grade of service or better for any given percentage of time. Here, both the signal and atmospheric noise have statistical variation. For ionospheric propagation, it is usually noted that the short-term (within an hour, say) distribution of the signal is Rayleigh and the long-term fading of the hourly (say) median values is log-normal (Report 266). The resulting normal distribution of signal median dB values, for this example, has a standard deviation of 8 dB (Report 266), which results in an upper decile value for the signal, $D_S$, of 1.27 × 8 = 10 dB. Based on the variation noted in Report 266 for the standard deviation of the long-term signal fading distribution, a value of $\sigma_{D_S} = 2$ dB is used.

Recommendation 339 gives a median required carrier power to noise power in a 1 Hz bandwidth of 64 dB for marginally commercial A3E emissions. This gives a median required signal-to-noise ratio $R$ of 26 dB. For analogue systems these performance requirements are based on white Gaussian noise. In general, a given voice understandability can be achieved with a smaller $R$ in impulsive (e.g., atmospheric) noise than in white Gaussian noise [Spaulding, 1982]. Figure 19c gives a $V_{dm}$ of 4.5 dB at 5 MHz and a 200 Hz bandwidth. This translates to a 6 kHz bandwidth $V_{dm}$ of 7.5 dB (Fig. 26). Spaulding [1982] gives results for AM voice systems in atmospheric noise ($V_d = 12$ dB). These results indicate that we can probably safely reduce the required $R_m$ by about 6 dB (at least, assuming no noise limiting). We, therefore, will specify a required $R_m$ of 20 dB, with a $\sigma_R$ of 3 dB.

As in Example I, the 1 MHz $F_{am}$ value for Geneva for June, July, August and 2000-2400 h is 74 dB. From Figs. 19b and 19c; the 5 MHz $F_{am}$ value is 56 dB with a standard deviation $\sigma_{F_{am}}$ of 4.1 dB. Also from Fig. 19c, $D_u = 4.8$ dB and $\sigma_{D_u} = 1.3$ dB. Since the signal-to-noise ratio is log-normally distributed (as it was in Example I), we proceed as before. The upper decile for $R$ is given by:

$$D_R^2 = D_S^2 + D_u^2 \tag{12}$$

since the signal and noise processes are independent. The deviation $D = R - R_m$ ($D_R = 11.1$ dB) and $\sigma_D$ (using a decile value given by $\sigma_{D_R} = \sqrt{\sigma_{D_u}^2 + \sigma_{D_S}^2} = 2.4$ dB) are shown on Fig. 32.

The deviation, $D$, now accounts for the long-term statistical variation of both the signal power and the noise power.

In order to obtain the service probability, the prediction uncertainties are given by the following standard deviations:

$\sigma_P$: standard deviation in the expected received signal power. We have specified the short-term and long-term fading distributions of $P$, but there still is a prediction error for the expected value, due to, for example, errors in the ionospheric propagation prediction method used. We will use 5 dB for $\sigma_P$;

$\sigma_R$: uncertainty in the required $R$, 3 dB as discussed earlier;

$\sigma_{F_{am}} = 4.1$ dB (Fig. 19c);

$\sigma_D$: standard deviation of $D$ (Fig. 32), which is a function of the required time availability.

The standard deviation $\sigma_T$ is shown on Fig. 33. Also shown on Fig. 33 is the expected median value of the received signal power, $P_e$, for the different time availabilities, from equation (6), given by:

$$P_e = F_{am} + R_m + D + B - 204$$

or: (13)

$$P_e = D - 90.2 \qquad \text{dBW}$$

Finally, Fig. 34 shows the required received signal power versus time availability for service probabilities of 0.5, 0.8, 0.9 and 0.99 using, as in Example I:

$$P = P_e + t\,\sigma_T \tag{14}$$

## 7. The influence of the directivity and polarization of antennas

All the noise information presented in this Report, including the examples given in the last section, relates to a short vertical receiving antenna. Although such an antenna may be used in practice at low frequencies, long-distance communication at high frequencies is normally achieved by the use of a highly-directional antenna. Some allowance must therefore be made for the effects of directivity and polarization on the signal-to-noise ratio.

It is assumed that the signal gain is reasonably well known, although it is dependent on the relative importance of the various propagation modes, which vary with time. The effective noise factor of the antenna, insofar as it is determined by atmospheric noise, may be influenced in several ways. If the noise sources were distributed isotropically, the noise factor would be independent of the directional properties. In practice, however, the azimuthal direction of the beam may coincide with the direction of an area where thunderstorms are prevalent, and the noise factor will be increased correspondingly, compared with the omnidirectional antenna. On the other hand, the converse may be true. The directivity in the vertical plane may be such as to differentiate in favour of, or against, the reception of noise from a strong source. The movement of storms in and out of the antenna beam may be expected to increase the variability of the noise, even if the average intensity is unchanged.

Experimental information on the effects of directivity is scarce, and in some respects conflicting. In an equatorial region (Singapore), the median value of $F_a$ for certain directional antennas was found to be somewhat higher (about 4 dB on the average), than that for a vertical rod antenna over the same period [Bradley and Clarke, 1964]. This figure is considerably lower than the maximum possible antenna gain, as would be expected from the widespread nature of the storms, but the fact that there was, on the average, some gain in noise in a wide range of storm conditions suggests that there was a tendency for the noise to be received more from the lower angles of elevation. In the Federal Republic of Germany also, directional antennas had, on the average, higher noise factors [Kronjäger and Vogt, 1959]. In order to determine the effects of antenna directivity on the signal-to-noise ratio, it is necessary to take into account the storm locations and the critical frequency of the ionosphere in addition to the antenna polar diagram. Rather detailed information on thunderstorm locations is now available [e.g., Kotaki and Katoh, 1983; Kotaki, 1984; Crichlow *et al.*, 1971].

Even less information is available on the effects of antenna polarization but for a first approximation, it may be assumed that the received noise would be comparable with either polarization, provided the antenna height is large compared with the wavelength. Some limited data on polarization (and directivity) for antennas "close" to the ground is available in Hagn *et al.* [1968] and Hagn and Shepherd [1984]. Additional information is also available (primarily in the references) from URSI [1975, 1978, 1981, 1984].

## REFERENCES

AKIMA, H., AX, G. G. and BEERY, W. M. [1969] Required signal-to-noise ratios for HF communication systems. ESSA Tech. Rep. ERL 131-ITS 92 (NTIS Order No. AD-697579).

AUSTIN, L. W. [1932] Solar activity and radio telegraphy. *Proc. IRE*, Vol. 20, 280.

BARSIS, A. P., NORTON, K. A., RICE, P. L. and ELDER, P. H. [1961] Performance predictions for single tropospheric communication links and for several links in tandem. NBS Tech. Note 102.

BRADLEY, P. A. and CLARKE, C. [1964] Atmospheric radio noise and signals received on directional aerials at high frequencies. *Proc. IEE*, Vol. III, 1534-1540.

CLARKE, C. [1962] Atmospheric radio noise studies based on amplitude probability measurements at Slough, England, during the International Geophysical Year. *Proc. IEE*, Vol. 109B, 393.

COTTONY, H. V. and JOHLER, J. R. [1952] Cosmic radio noise intensities in the VHF band. *Proc. IRE*, Vol. 40, 1053.

CRICHLOW, W. Q., DAVIS, R. C., DISNEY, R. T. and CLARK, M. W. [1971] Hourly probability of world-wide thunderstorm occurrence. Office of Telecommunications Research Report OT/ITS RR 12 (NTIS Order No. COM75-11202).

CRICHLOW, W. Q., ROUBIQUE, C. J., SPAULDING, A. D. and BEERY, W. M. [1960a] Determination of the amplitude-probability distribution of atmospheric radio noise from statistical moments. *NBS J. Res.*, Vol. 64D, 49.

CRICHLOW, W. Q., SPAULDING, A. D., ROUBIQUE, C. J. and DISNEY, R. T. [1960b] Amplitude-probability distributions for atmospheric radio noise. NBS Monograph 23.

HAGN, G. H. [1982] Man-made electromagnetic noise. *Handbook of Atmospherics*, Chapter 7. Ed. H. Volland, CRC Press, Boca Raton, FL, USA.

HAGN, G. H., CHINDAHPORN, R. and YARBORROUGH, J. M. [1968] HF atmospheric radio noise on horizontal dipole antennas in Thailand. Special Technical Report 47, Stanford Research Institute, Menlo Park, CA 94025, USA (NTIS Order No. AD68-1879).

HAGN, G. H. and SHEPHERD, R. A. [1984] Selected radio noise topics. Final Report, Contract NT83 RAC-36001, SRI-5002-FR/84, SRI International, Arlington, VA, USA (NTIA Order No. PB86 173218).

HERMAN, J. R. and DE ANGELIS, X. A. [January-February, 1987] Bandwidth expansion effects on the voltage deviation parameter ($V_d$) of MF and HF atmospheric radio noise. *Radio Sci.*, Vol. 22, **1**, 26-36.

KOTAKI, M. [1984] Global distribution of atmospheric radio noise derived from thunderstorm activity. *J. Atmos. Terr. Phys.*, Vol. 46, **10**, 867-877.

KOTAKI, M. and KATOH, C. [1983] The global distribution of thunderstorm activity observed by the Ionospheric Sounding Satellite (ISS-b). *J. Atmos. Terr. Phys.*, Vol. 45, **12**, 833-847.

KRONJÄGER, W. and VOGT, K. [1959] Über das Aussengeräusch kommerzieller Antennenanlagen (On the external noise of commercial antenna installations). *NTZ*, **12**, 371.

LAUBER, W. R. and BERTRAND, J. M. [28-30 June, 1977] Preliminary urban VHF/UHF radio noise intensity measurements in Ottawa, Canada. Proc. 2nd Symposium on Electromagnetic Compatibility, Montreux, Switzerland, 357-362 (IEEE Catalog No. 77CH1224-5EMC).

MONTGOMERY, G. F. [1954] A comparison of amplitude and angle modulation for narrow-band communication of binary-coded messages in fluctuation noise. *Proc. IRE*, Vol. 42, 447.

SCIENCE COUNCIL OF JAPAN [1960] Compilation of data in Japan for atmospheric radio noise during the IGY, 1957/58. Japanese National Committee for IGY.

SHAVER, H. N., HATFIELD, V. E. and HAGN, G. H. [1972] Man-made radio noise parameter identification task. Final Report, Contract N00039-71-A-0223, Standard Research Institute, Menlo Park, CA, USA (NTIS Order No. AD904405).

SKOMAL, E. N. [1978] *Man-Made Radio Noise*. Van Nostrand Reinhold, New York, NY, USA.

SPAULDING, A. D. [12-15 June, 1977] Stochastic modelling of the electromagnetic interference environment. Conf. Record, 42.2-114-42.2-123. IEEE International Conference on Communications (ICC '77), Chicago, ILL, USA (IEEE Catalog No. 77CH1209-6C SCB).

SPAULDING, A. D. [1982] Atmospheric radio noise and its effects on telecommunication systems. *Handbook of Atmospherics*, Chapter 6. Ed. H. Volland, CRC Press, Boca Raton, FL, USA.

SPAULDING, A. D., ROUBIQUE, C. J. and CRICHLOW, W. Q. [1962] Conversion of the amplitude-probability distribution function for atmospheric radio noise from one bandwidth to another. *NBS J. Res.*, Vol. 66D, 713.

SPAULDING, A. D. and WASHBURN, J. S. [1985] Atmospheric radio noise: Worldwide levels and other characteristics. National Telecommunications and Information Administration Report 85-173 (NTIS Order No. PB85-212942).

URSI [1962] The measurement of characteristics of terrestrial radio noise. Special Report No. 7. Elsevier, London, UK.

URSI [1975] *Review of Radio Science 1972-1974*, Radio noise of terrestrial origin, 127-133. International Union of Radio Science, Brussels, Belgium.

URSI [1978] *Review of Radio Science 1975-1977*, Interference environment, 57-66. International Union of Radio Science, Brussels, Belgium.

URSI [1981] *Review of Radio Science 1978-1980*, EM noise and interference, E1-E13. International Union of Radio Science, Brussels, Belgium.

URSI [1984] *Review of Radio Science 1981-1983*, Electromagnetic noise and interference, E1-E15. International Union of Radio Science, Brussels, Belgium.

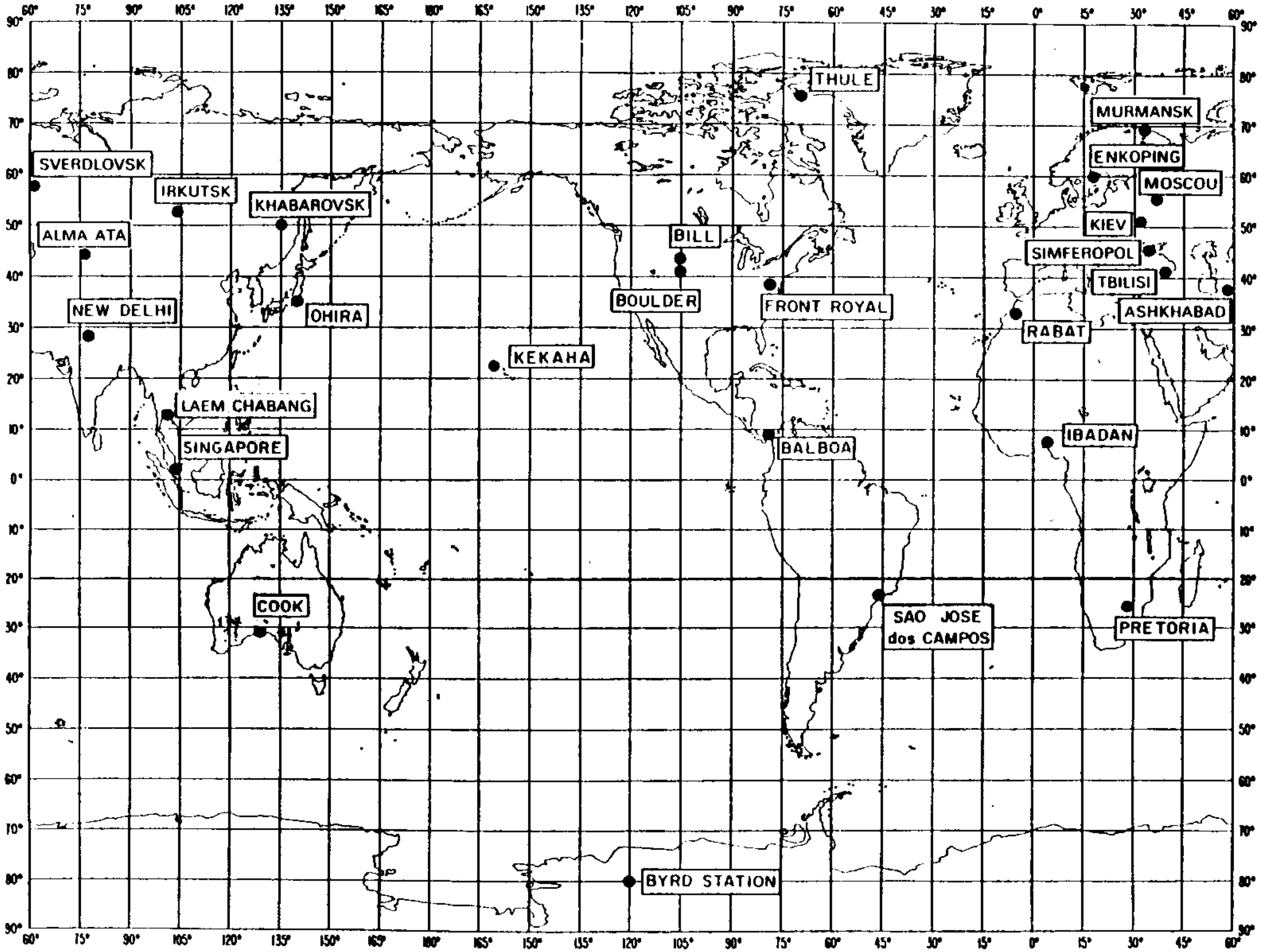
THULE
MURMANSK
ENKOPING
MOSCOU
SVERDLOVSK
IRKUTSK
KHABAROVSK
KIEV
ALMA ATA
BILL
SIMFEROPOL
TBILISI
BOULDER
FRONT ROYAL
ASHKHABAD
NEW DELHI
OHIRA
RABAT
KEKAHA
LAEM CHABANG
IBADAN
SINGAPORE
BALBOA
COOK
SAO JOSE
dos CAMPOS
PRETORIA
BYRD STATION
60° 75° 90° 105° 120° 135° 150° 165° 180° 165° 150° 135° 120° 105° 90° 75° 60° 45° 30° 15° 0° 15° 30° 45° 60°
90° 80° 70° 60° 50° 40° 30° 20° 10° 0° 10° 20° 30° 40° 50° 60° 70° 80° 90°

FIGURE 1 – *Stations qui ont fourni des données de bruit radioélectrique*
FIGURE 1 – *Stations which provided radio noise data*
FIGURA 1 – *Estaciones de medida que han suministrado datos del ruido radioeléctrico*

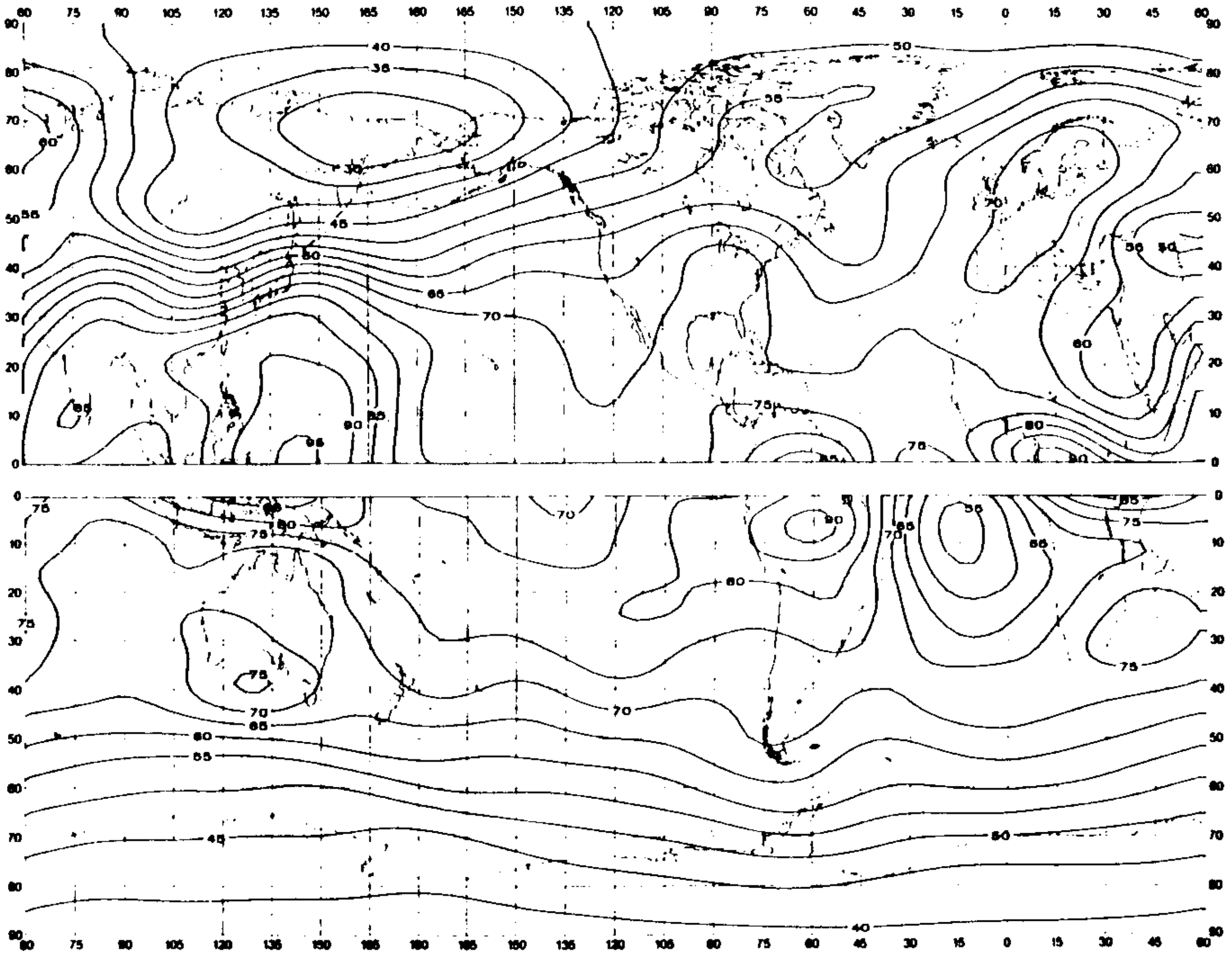
60
75
90
105
120
135
150
165
180
165
150
135
120
105
90
75
60
45
30
15
0
15
30
45
60
90
80
70
60
50
40
30
20
10
0
40
35
30
45
50
55
60
65
70
75
80
85
90
40
45
50
55
60
65
70
75
80
85
90

FIGURE 2a — *Valeurs attendues du bruit atmosphérique radioélectrique, $F_{am}$, en dB au-dessus de $kT_0b$ à 1 MHz (Hiver; 0000-0400 heure locale)*

FIGURE 2a — *Expected values of atmospheric radio noise, $F_{am}$ (dB above $kT_0b$ at 1 MHz) (Winter; 0000-0400 LT)*

FIGURA 2a — *Valores probables del ruido atmosférico, $F_{am}$, en dB por encima de $kT_0b$ en 1 MHz (Invierno; 0000-0400 hora local)*

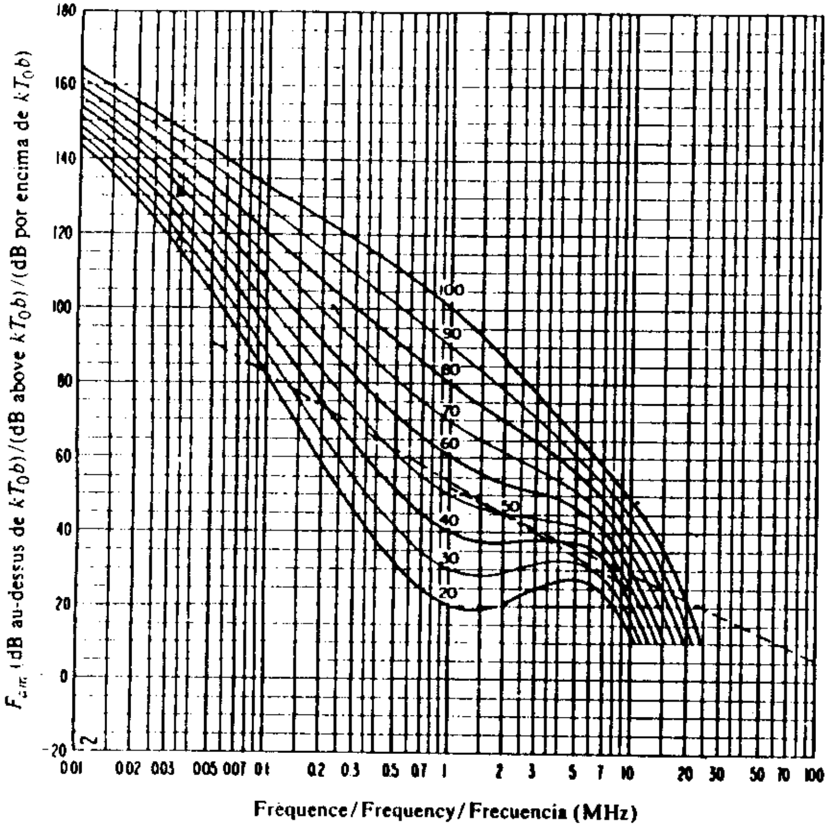

FIGURE 2b *Variation du bruit radioélectrique en fonction de la fréquence*
*(Hiver; 0000-0400 heure locale)*

FIGURE 2b – *Variation of radio noise with frequency (Winter; 0000-0400 LT)*

FIGURA 2b – *Variaciones del ruido radioeléctrico con la frecuencia*
*(Invierno; 0000-0400 hora local)*

——— Valeurs attendues du bruit atmosphérique/Expected values of atmospheric noise/Valores probables del ruido atmosférico

—·—·— Valeurs attendues du bruit artificiel en un emplacement de réception calme/Expected values of man made noise at a quiet receiving location/Valores probables del ruido artificial en un punto de recepción tranquilo

- - - - - Valeurs attendues du bruit galactique/Expected values of galactic noise/Valores probables del ruido galáctico

*Note* – Pour des raisons d'ordre pratique, le point anglais a été utilisé dans cette version trilingue au lieu de la virgule décimale

*Nota* – Por razones prácticas se ha utilizado un punto en lugar de una coma para indicar las cifras decimales

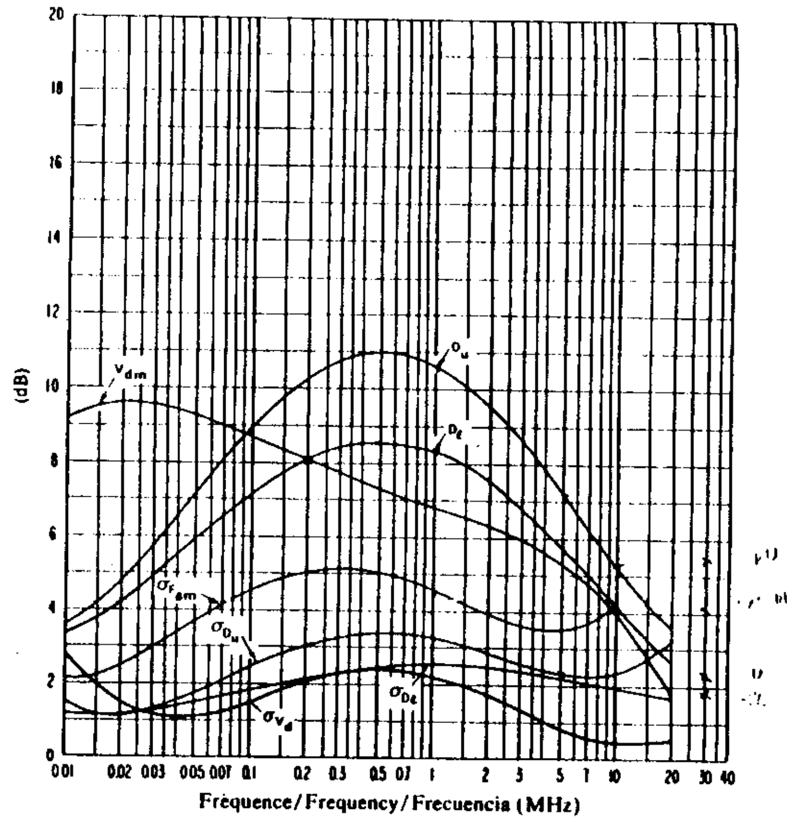

FIGURE 2c – *Données sur la variabilité et le caractère du bruit*
*(Hiver; 0000-0400 heure locale)*

FIGURE 2c – *Data on noise variability and character (Winter; 0000-0400 LT)*

FIGURA 2c – *Datos sobre la variabilidad y el carácter del ruido*
*(Invierno; 0000-0400 hora local)*

$\sigma_{F_{am}}$ – Ecart type des valeurs de $F_{am}$/Standard deviation of values of $F_{am}$/Desviación típica de los valores de $F_{am}$

$D_u$ – Rapport du décile supérieur à la valeur médiane de $F_{am}$/Ratio of upper decile to median value, $F_{am}$/Relación del decilo superior al valor mediano, $F_{am}$

$\sigma_{D_u}$ – Ecart type des valeurs de $D_u$/Standard deviation of values of $D_u$/Desviación típica de los valores de $D_u$

$D_l$ – Rapport de la valeur médiane de $F_{am}$ au décile inférieur/Ratio of median value, $F_{am}$, to lower decile/Relación del valor mediano $F_{am}$ al decilo inferior

$\sigma_{D_l}$ – Ecart type des valeurs de $D_l$/Standard deviation of value of $D_l$/Desviación típica de los valores de $D_l$

$V_{dm}$ – Valeur attendue de l'écart médian de la tension moyenne (valeurs pour une largeur de bande de 200 Hz)/Expected value of median deviation of average voltage. The values shown are for a bandwidth of 200 Hz/Valor probable de la desviación mediana de la tensión media (valores para una anchura de banda de 200 Hz)

$\sigma_{V_d}$ – Ecart type de $V_d$/Standard deviation of $V_d$/Desviación típica de $V_d$

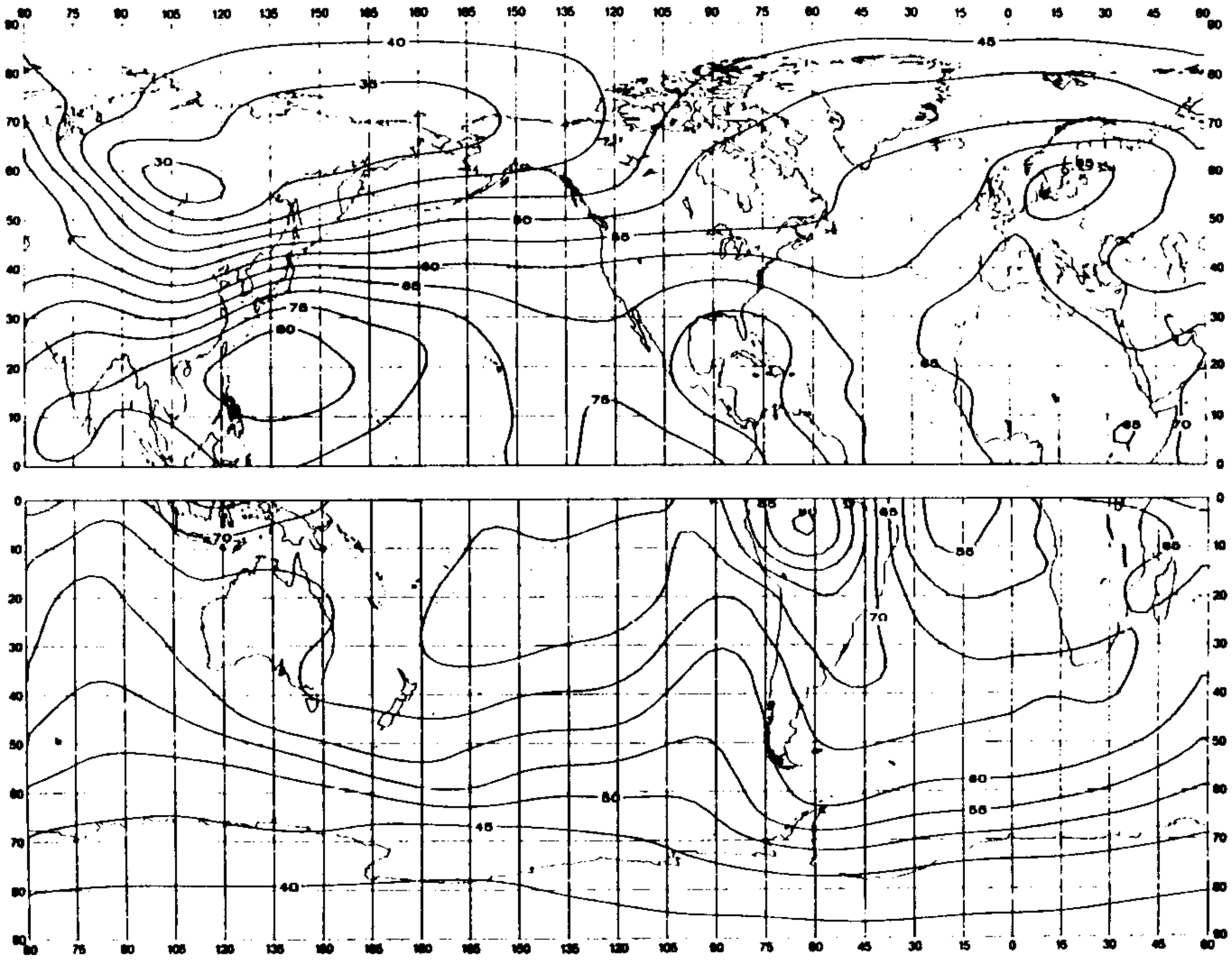
40
45
35
30
60
65
70
75
80
85
90
50
55
60
65
70
75
80
85
90
45
40
60
55
50
50
60
65
70
80
70
65
55
55
60
45
40

FIGURE 3a – *Valeurs attendues du bruit atmosphérique radioélectrique, $F_{am}$, en dB au-dessus de $kT_0b$ à 1 MHz (Hiver; 0400-0800 heure locale)*

FIGURE 3a – *Expected values of atmospheric radio noise, $F_{am}$ (dB above $kT_0b$ at 1 MHz) (Winter; 0400-0800 LT)*

FIGURA 3a – *Valores probables del ruido atmosférico, $F_{am}$, en dB por encima de $kT_0b$ en 1 MHz (Invierno; 0400-0800 hora local)*

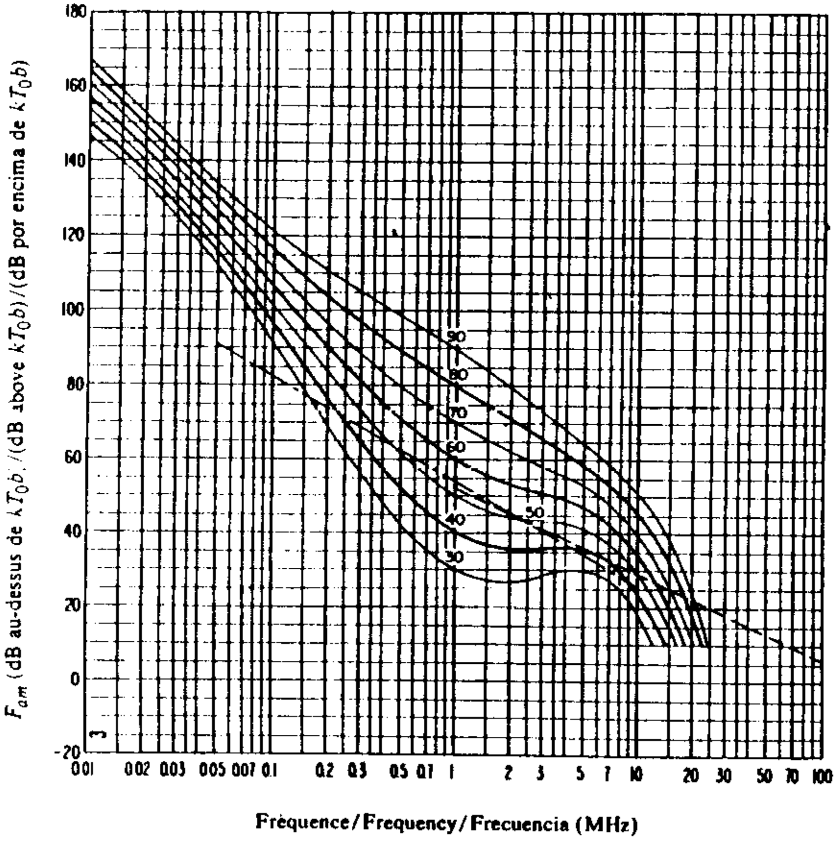

FIGURE 3b – *Variation du bruit radioélectrique en fonction de la fréquence (Hiver; 0400-0800 heure locale)*

FIGURE 3b – *Variation of radio noise with frequency (Winter; 0400-0800 LT)*

FIGURA 3b – *Variaciones del ruido radioeléctrico con la frecuencia (Invierno; 0400-0800 hora local)*

Voir la légende de la Fig. 2b/See legend of Fig. 2b/Véase la leyenda de la fig. 2b

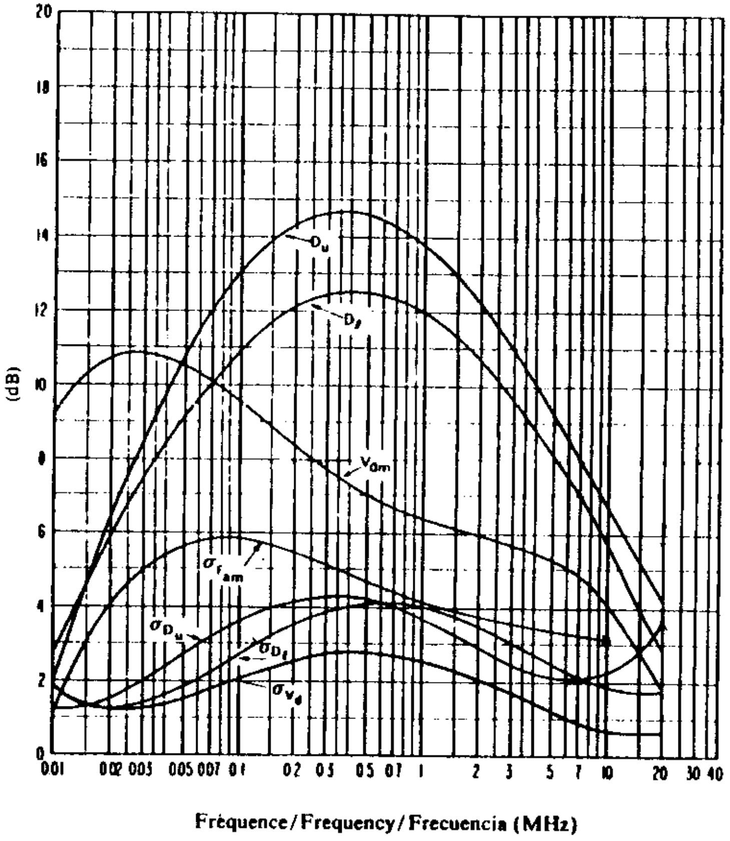

FIGURE 3c – *Données sur la variabilité et le caractère du bruit (Hiver; 0400-0800 heure locale)*

FIGURE 3c – *Data on noise variability and character (Winter; 0400-0800 LT)*

FIGURA 3c – *Datos sobre la variabilidad y el carácter del ruido (Invierno; 0400-0800 hora local)*

Voir la légende de la Fig. 2c/See legend of Fig. 2c/Véase la leyenda de la fig. 2c

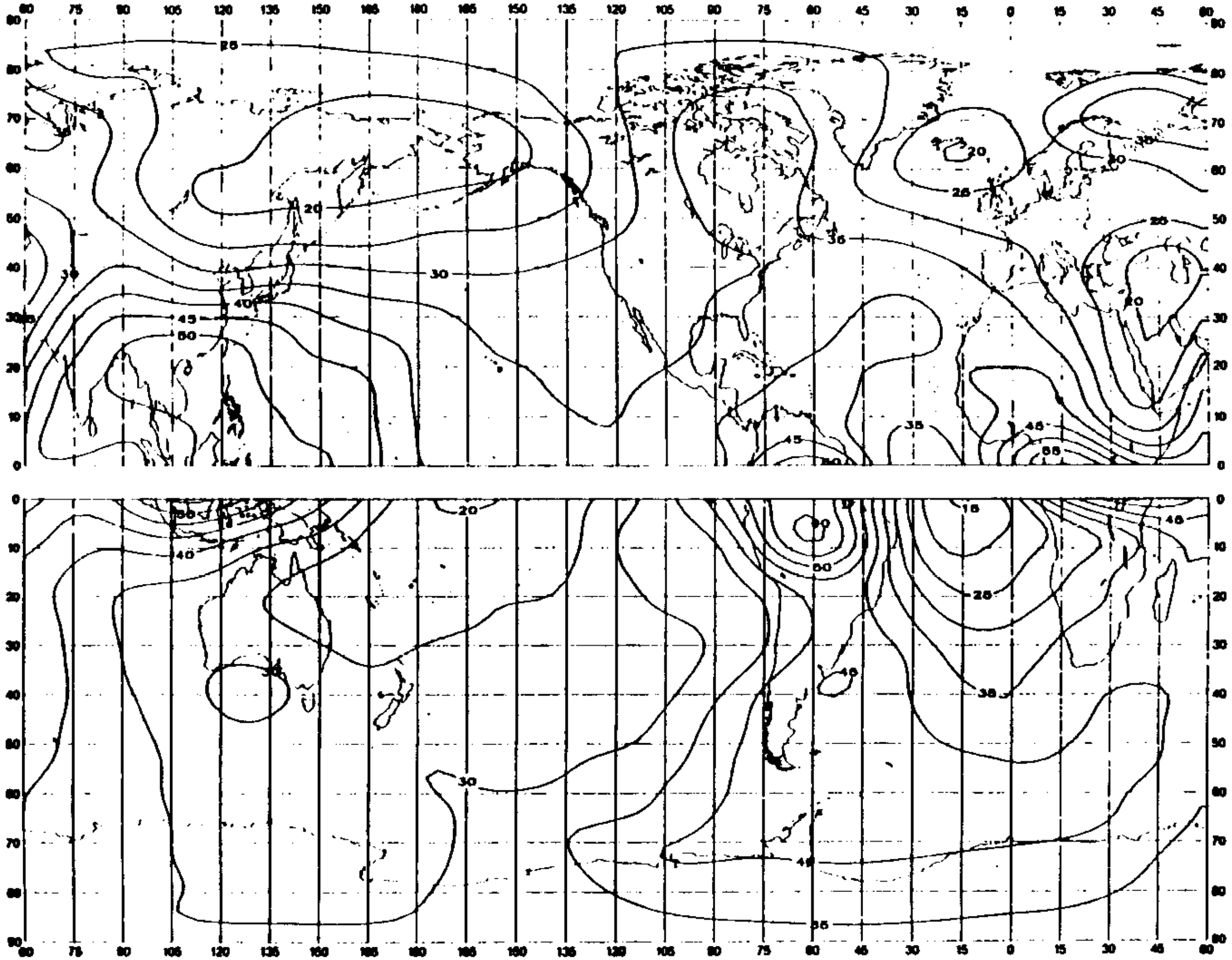
80
75
90
105
120
135
150
165
180
165
150
135
120
105
90
75
60
45
30
15
0
15
30
45
60
80
70
60
50
40
30
20
10
0
25
20
30
35
40
45
50
55
60
15
36
46

FIGURE 4a – *Valeurs attendues du bruit atmosphérique radioélectrique,* $F_{am}$, *en dB au-dessus de* $kT_0b$ *à 1 MHz (Hiver; 0800-1200 heure locale)*
FIGURE 4a – *Expected values of atmospheric radio noise,* $F_{am}$ *(dB above* $kT_0b$ *at 1 MHz) (Winter; 0800-1200 LT)*
FIGURA 4a – *Valores probables del ruido atmosférico,* $F_{am}$, *en dB por encima de* $kT_0b$ *en 1 MHz (Invierno; 0800-1200 hora local)*

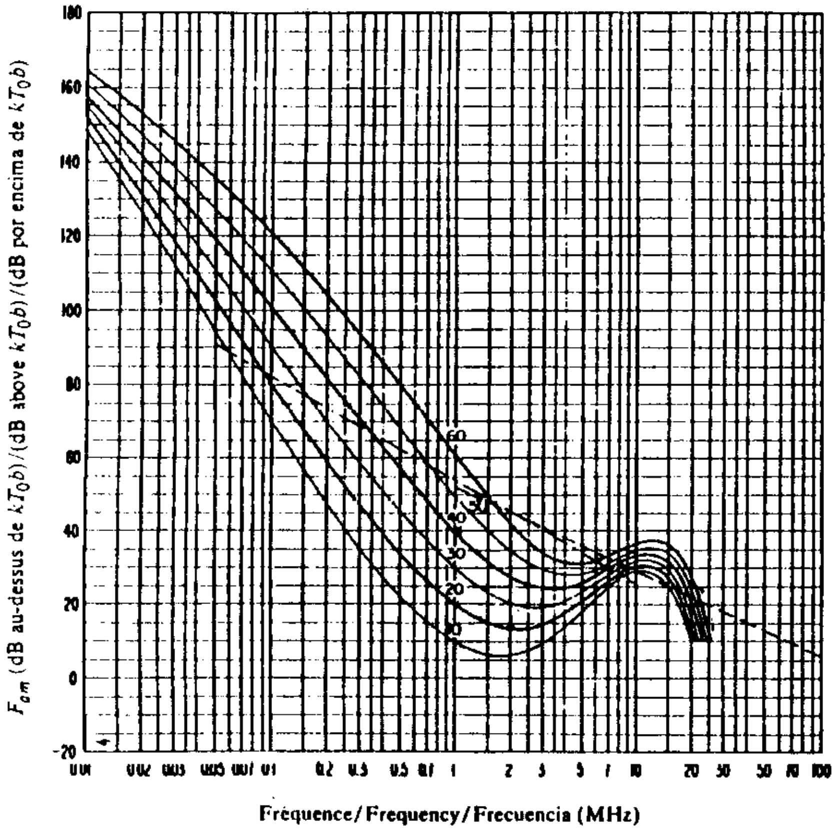

FIGURE 4b – *Variation du bruit radioélectrique en fonction de la fréquence (Hiver; 0800-1200 heure locale)*

FIGURE 4b – *Variation of radio noise with frequency (Winter; 0800-1200 LT)*

FIGURA 4b – *Variaciones del ruido radioeléctrico con la frecuencia (Invierno; 0800-1200 hora local)*

Voir la légende de la Fig. 2b/See legend of Fig. 2b/Véase la leyenda de la fig. 2b

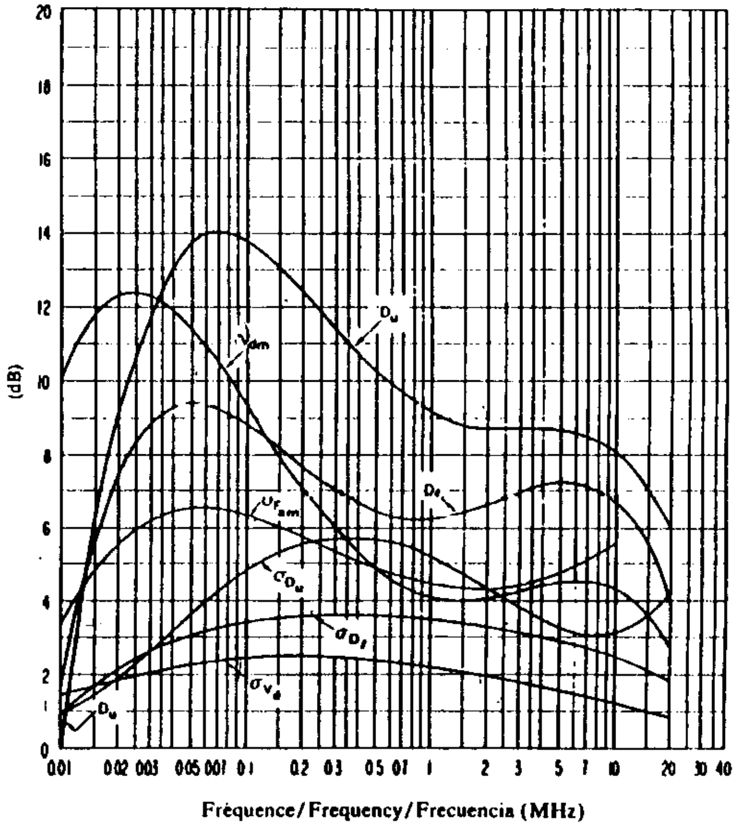

FIGURE 4c – *Données sur la variabilité et le caractère du bruit (Hiver; 0800-1200 heure locale)*

FIGURE 4c – *Data on noise variability and character (Winter; 0800-1200 LT)*

FIGURA 4c – *Datos sobre la variabilidad y el carácter del ruido (Invierno; 0800-1200 hora local)*

Voir la légende de la Fig. 2c/See legend of Fig. 2c/Véase la leyenda de la fig. 2c

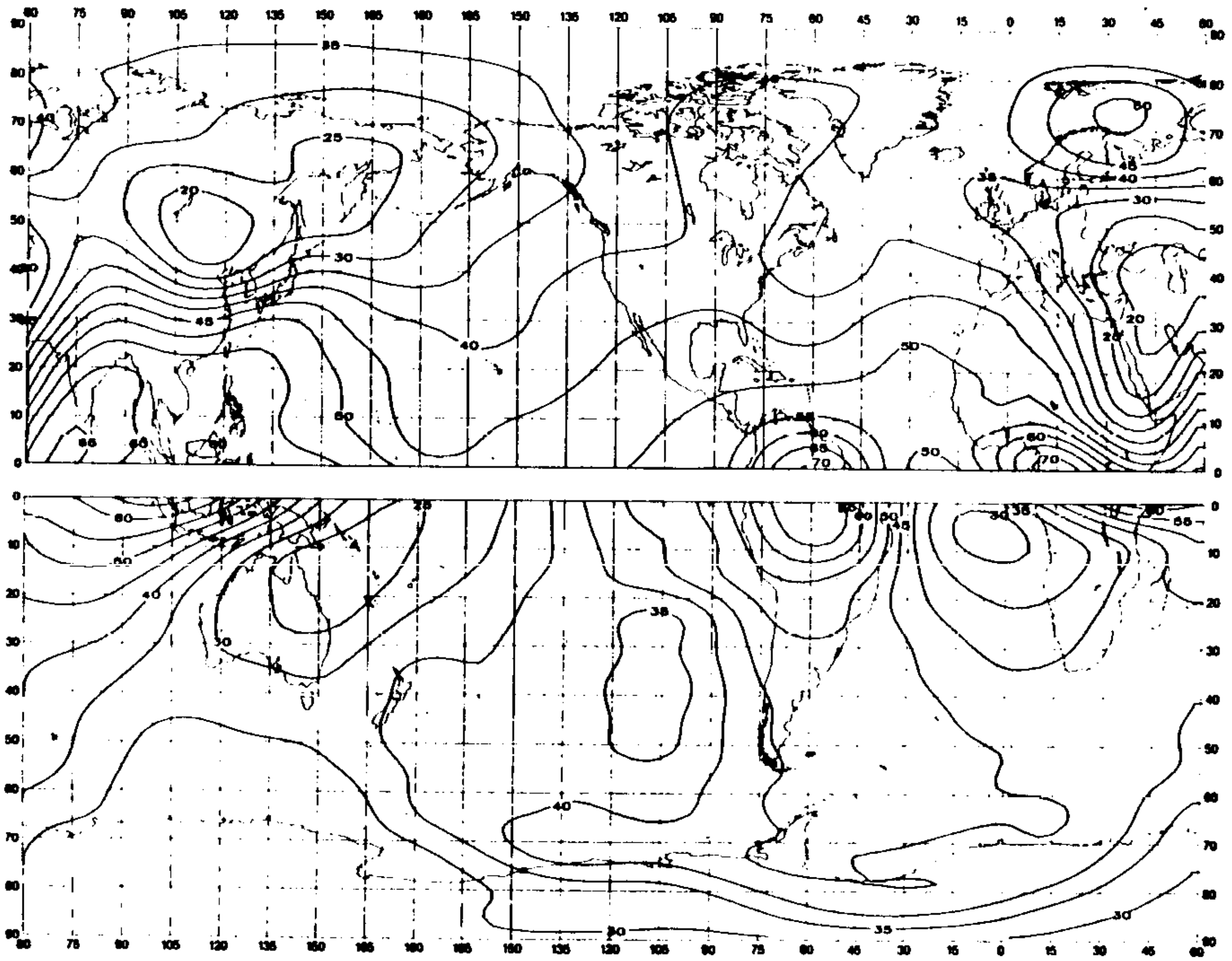
180
75
90
105
120
135
150
165
180
165
150
135
120
105
90
75
60
45
30
15
0
15
30
45
60
90
80
70
60
50
40
30
20
10
0
0
10
20
30
40
50
60
70
80
90

FIGURE 5a – *Valeurs attendues du bruit atmosphérique radioélectrique, $F_{am}$, en dB au-dessus de $kT_0b$ à 1 MHz (Hiver; 1200-1600 heure locale)*

FIGURE 5a – *Expected values of atmospheric radio noise, $F_{am}$ (dB above $kT_0b$ at 1 MHz) (Winter; 1200-1600 LT)*

FIGURA 5a – *Valores probables del ruido atmosférico, $F_{am}$, en dB por encima de $kT_0b$ en 1 MHz (Invierno; 1200-1600 hora local)*

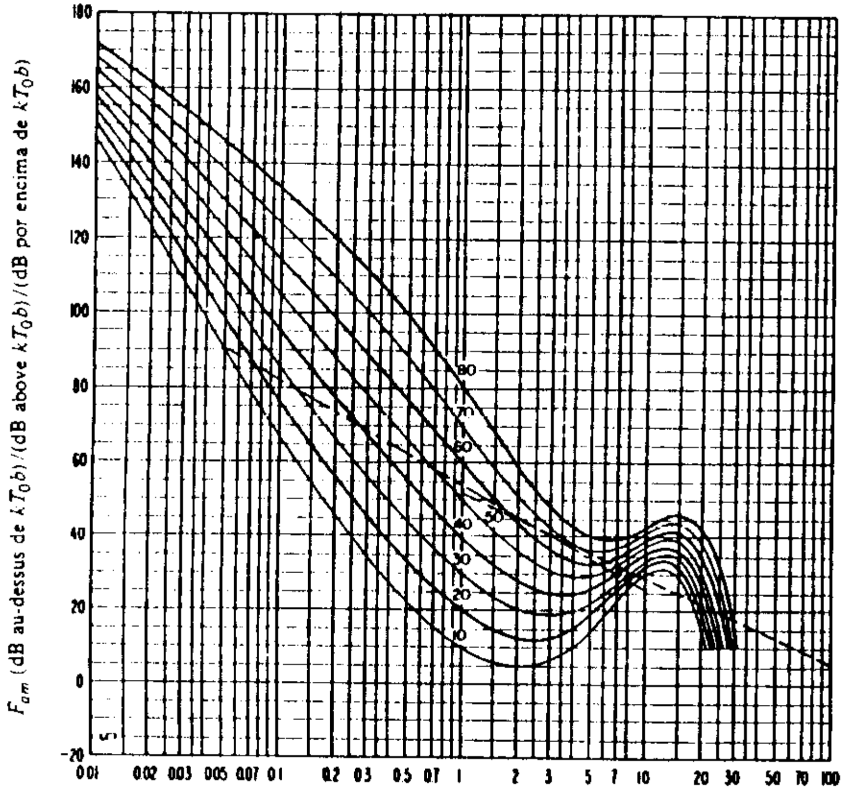

Fréquence/Frequency/Frecuencia (MHz)

FIGURE 5b – *Variation du bruit radioélectrique en fonction de la fréquence (Hiver; 1200-1600 heure locale)*

FIGURE 5b – *Variation of radio noise with frequency (Winter; 1200-1600 LT)*

FIGURA 5b – *Variaciones del ruido radioeléctrico con la frecuencia (Invierno; 1200-1600 hora local)*

Voir la légende de la Fig. 2b/See legend of Fig. 2b/Véase la leyenda de la fig. 2b

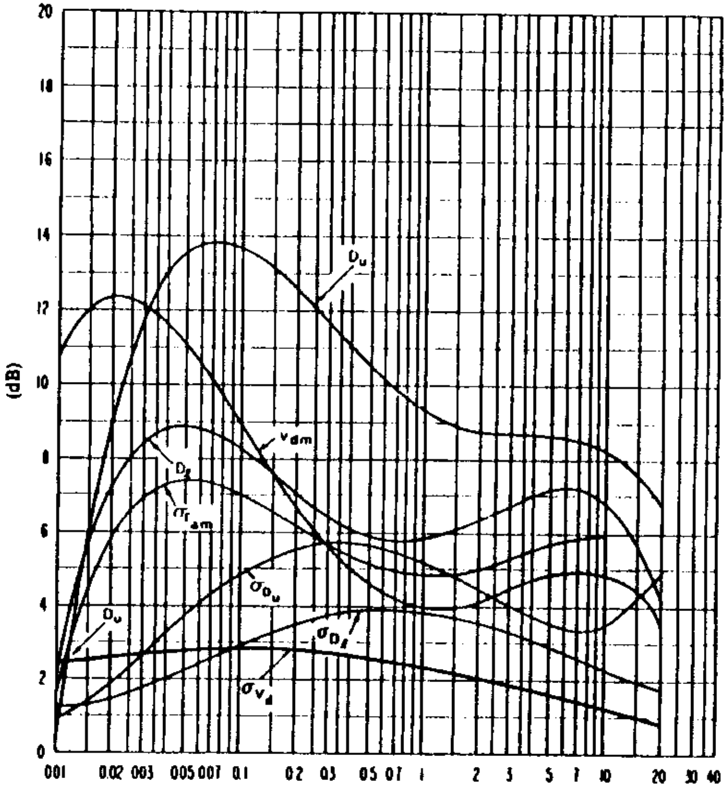

Fréquence/Frequency/Frecuencia (MHz)

FIGURE 5c – *Données sur la variabilité et le caractère du bruit (Hiver; 1200-1600 heure locale)*

FIGURE 5c – *Data on noise variability and character (Winter; 1200-1600 LT)*

FIGURA 5c – *Datos sobre la variabilidad y el carácter del ruido (Invierno; 1200-1600 hora local)*

Voir la légende de la Fig. 2c/See legend of Fig. 2c/Véase la leyenda de la fig. 2c

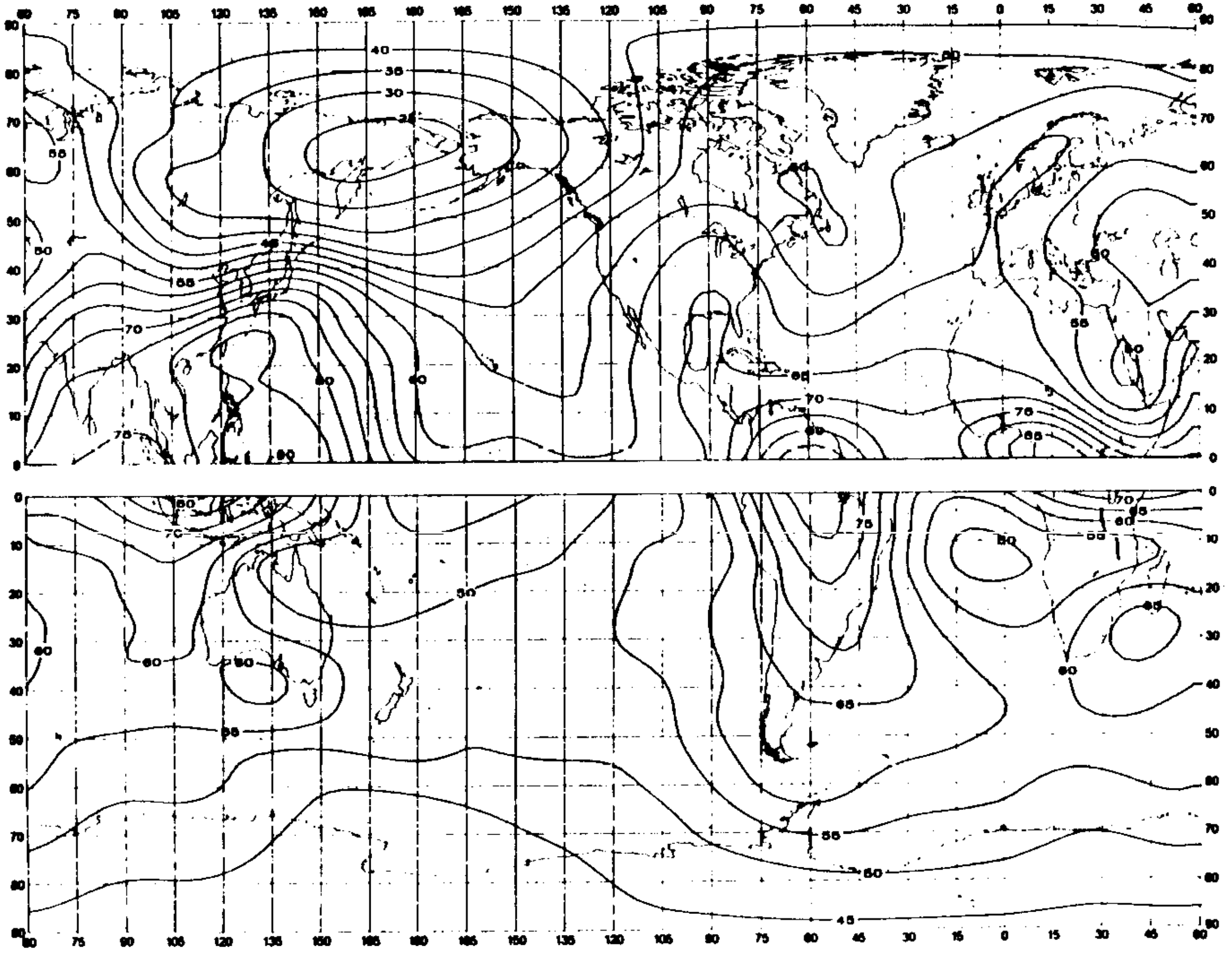
60
75
90
105
120
135
150
165
180
165
150
135
120
105
90
75
60
45
30
15
0
15
30
45
60
90
80
70
60
50
40
30
20
10
0
10
20
30
40
50
60
70
80
90
40
35
30
25
45
50
55
60
65
70
75
80
45

FIGURE 6a – *Valeurs attendues du bruit atmosphérique radioélectrique, $F_{am}$, en dB au-dessus de $kT_0b$ à 1 MHz (Hiver; 1600-2000 heure locale)*

FIGURE 6a – *Expected values of atmospheric radio noise, $F_{am}$ (dB above $kT_0b$ at 1 MHz) (Winter; 1600-2000 LT)*

FIGURA 6a – *Valores probables del ruido atmosférico, $F_{am}$, en dB por encima de $kT_0b$ en 1 MHz (Invierno; 1600-2000 hora local)*

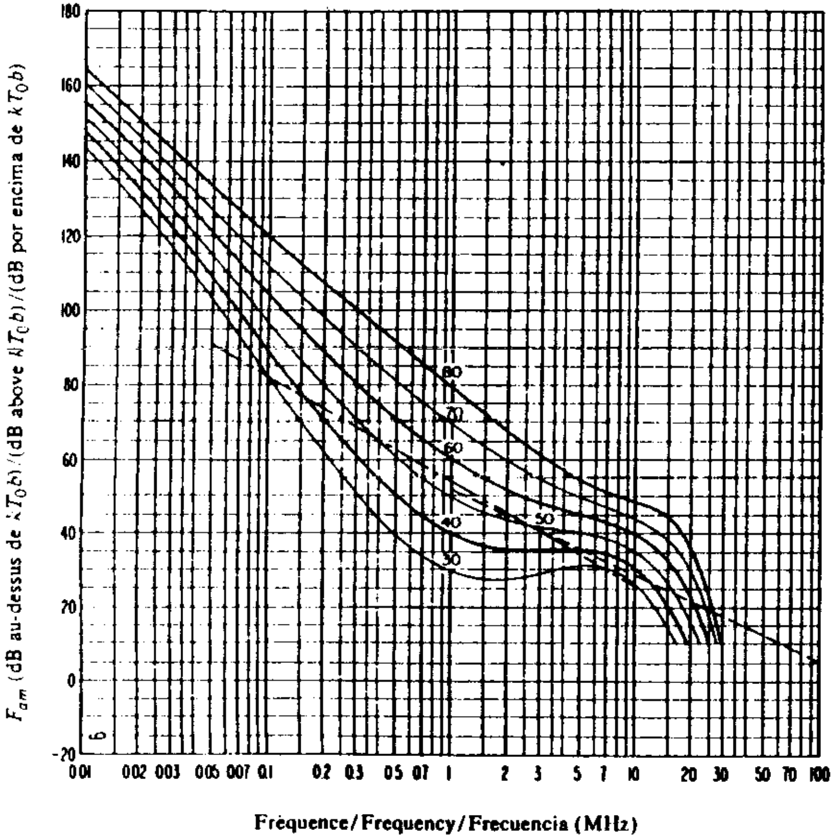

FIGURE 6b – *Variation du bruit radioélectrique en fonction de la fréquence (Hiver; 1600-2000 heure locale)*

FIGURE 6b – *Variation of radio noise with frequency (Winter; 1600-2000 LT)*

FIGURA 6b – *Variaciones del ruido radioeléctrico con la frecuencia (Invierno; 1600-2000 hora local)*

Voir la légende de la Fig. 2b/See legend of Fig. 2b/Véase la leyenda de la fig. 2b

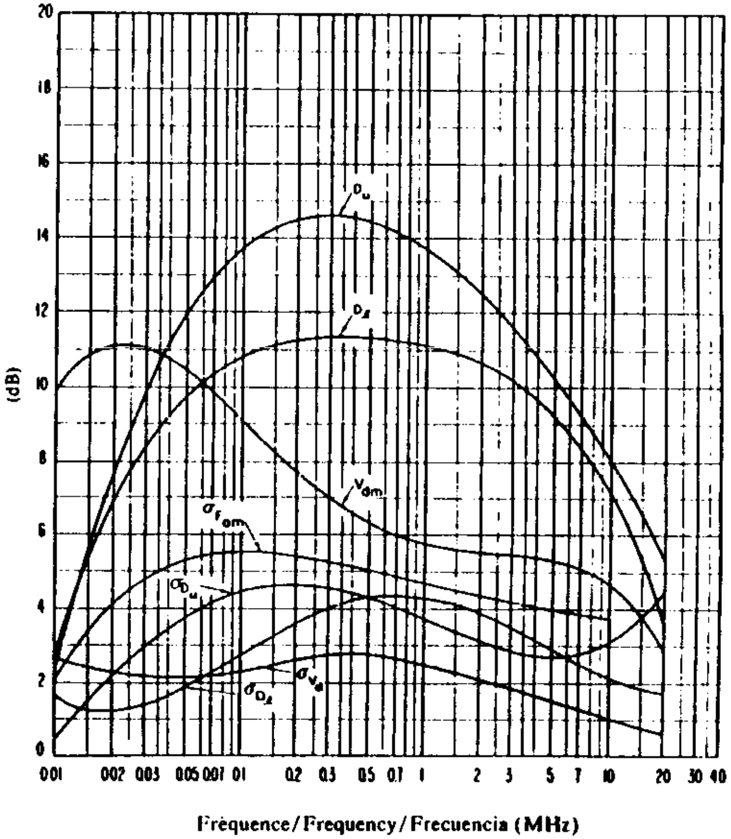

FIGURE 6c – *Données sur la variabilité et le caractère du bruit (Hiver; 1600-2000 heure locale)*

FIGURE 6c – *Data on noise variability and character (Winter; 1600-2000 LT)*

FIGURA 6c – *Datos sobre la variabilidad y el carácter del ruido (Invierno; 1600-2000 hora local)*

Voir la légende de la Fig. 2c/See legend of Fig. 2c/Véase la leyenda de la fig. 2c

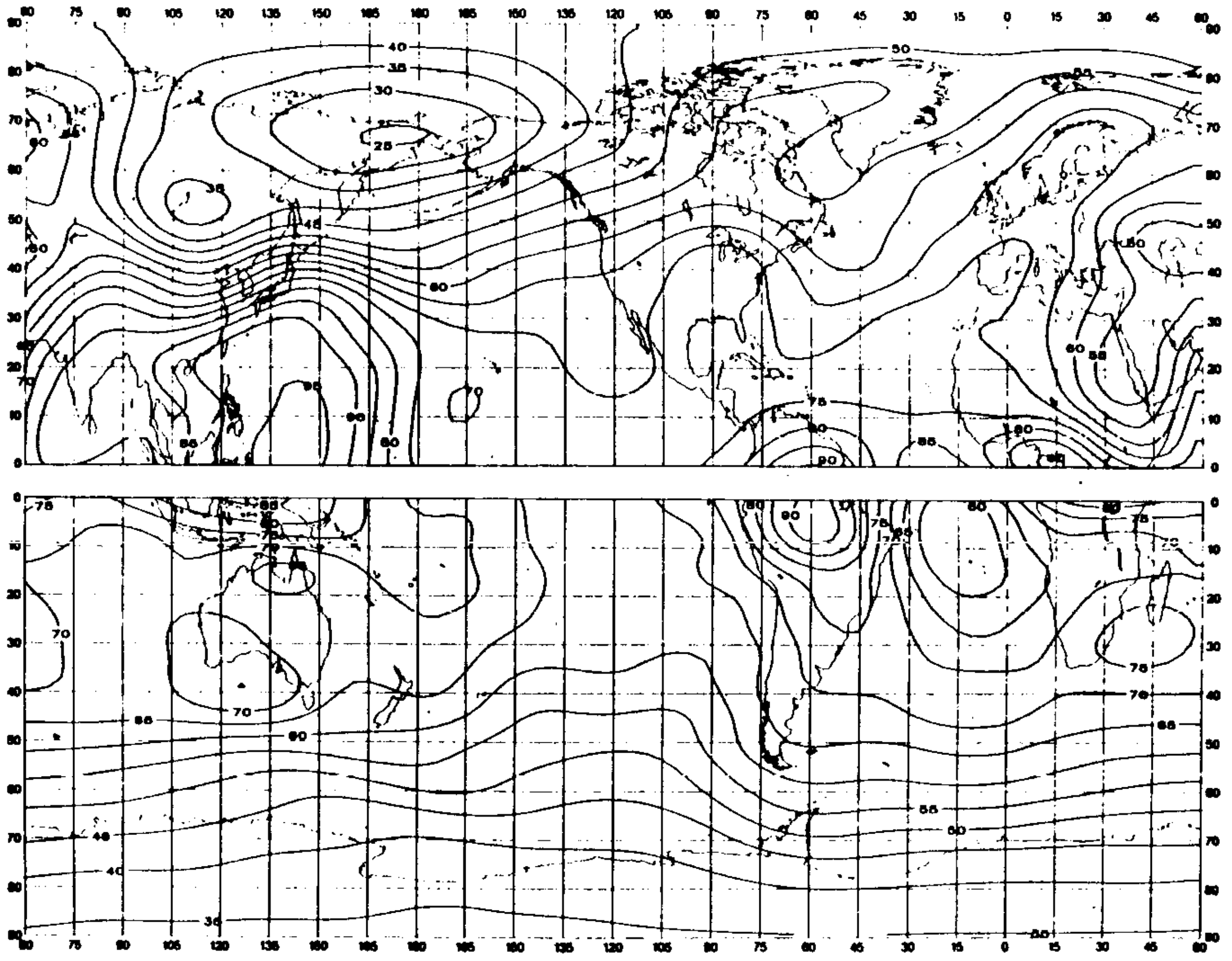
80
75
90
105
120
135
150
165
180
165
150
135
120
105
90
75
60
45
30
15
0
15
30
45
60
80
70
60
50
40
30
20
10
0
10
20
30
40
50
60
70
80
90
40
35
30
25
50
55
60
65
70
75
80
85
90
45
36
40
55
60
65
70
75
76
80

FIGURE 7a – *Valeurs attendues du bruit atmosphérique radioélectrique, $F_{am}$, en dB au-dessus de $kT_0b$ à 1 MHz (Hiver; 2000-2400 heure locale)*

FIGURE 7a – *Expected values of atmospheric radio noise, $F_{am}$ (dB above $kT_0b$ at 1 MHz) (Winter; 2000-2400 LT)*

FIGURA 7a – *Valores probables del ruido atmosférico, $F_{am}$, en dB por encima de $kT_0b$ en 1 MHz (Invierno; 2000-2400 hora local)*

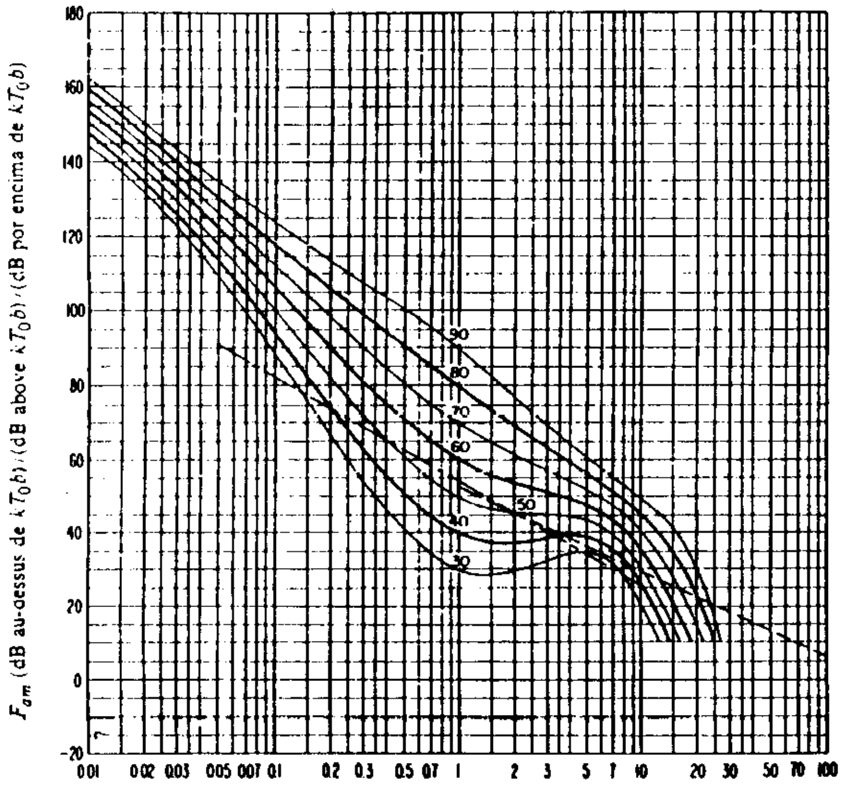

FIGURE 7b – *Variation du bruit radioélectrique en fonction de la fréquence (Hiver; 2000-2400 heure locale)*

FIGURE 7b – *Variation of radio noise with frequency (Winter; 2000-2400 LT)*

FIGURA 7b – *Variaciones del ruido radioeléctrico con la frecuencia (Invierno; 2000-2400 hora local)*

Voir la légende de la Fig. 2b/See legend of Fig. 2b/Véase la leyenda de la fig. 2b

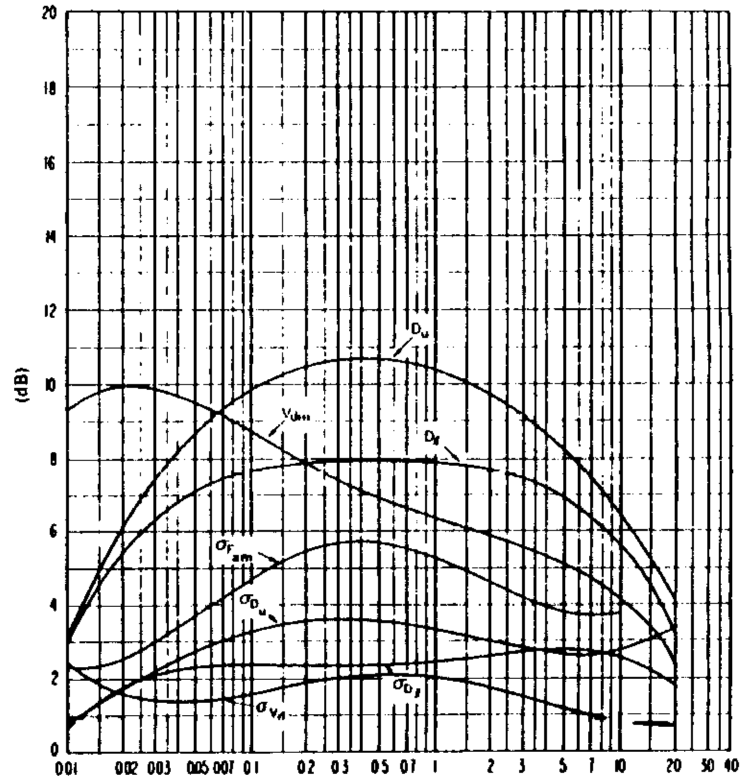

FIGURE 7c – *Données sur la variabilité et le caractère du bruit (Hiver; 2000-2400 heure locale)*

FIGURE 7c – *Data on noise variability and character (Winter; 2000-2400 LT)*

FIGURA 7c – *Datos sobre la variabilidad y el carácter del ruido (Invierno; 2000-2400 hora local)*

Voir la légende de la Fig. 2c/See legend of Fig. 2c/Véase la leyenda de la fig. 2c

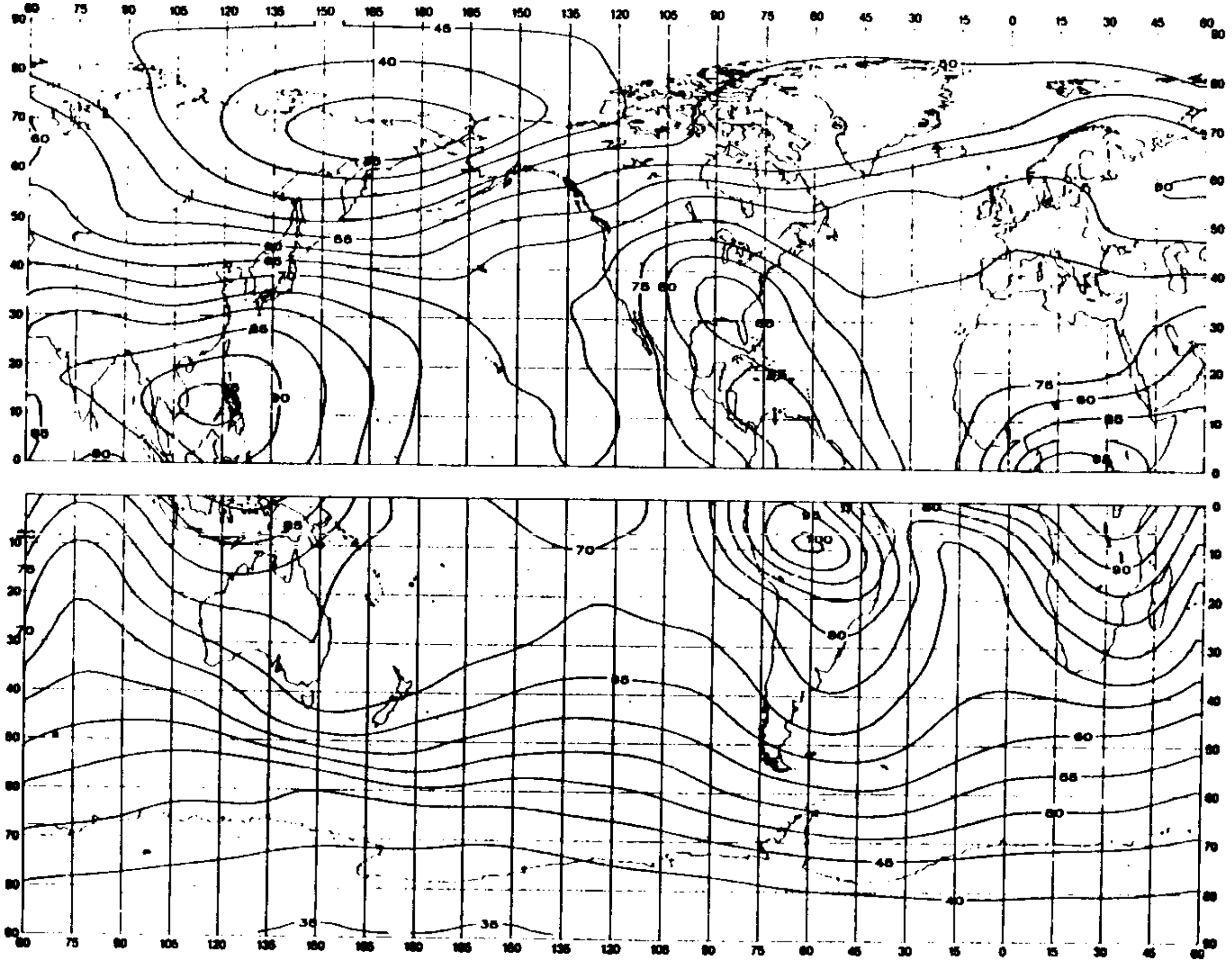
90
75
60
45
30
15
0
45
40
55
60
65
70
75
80
85
90
100
36

FIGURE 8a – *Valeurs attendues du bruit atmosphérique radioélectrique, $F_{am}$, en dB au-dessus de $kT_0b$ à 1 MHz (Printemps; 0000-0400 heure locale)*

FIGURE 8a – *Expected values of atmospheric radio noise, $F_{am}$ (dB above $kT_0b$ at 1 MHz) (Spring; 0000-0400 LT)*

FIGURA 8a – *Valores probables del ruido atmosférico, $F_{am}$, en dB por encima de $kT_0b$ en 1 MHz (Primavera; 0000-0400 hora local)*

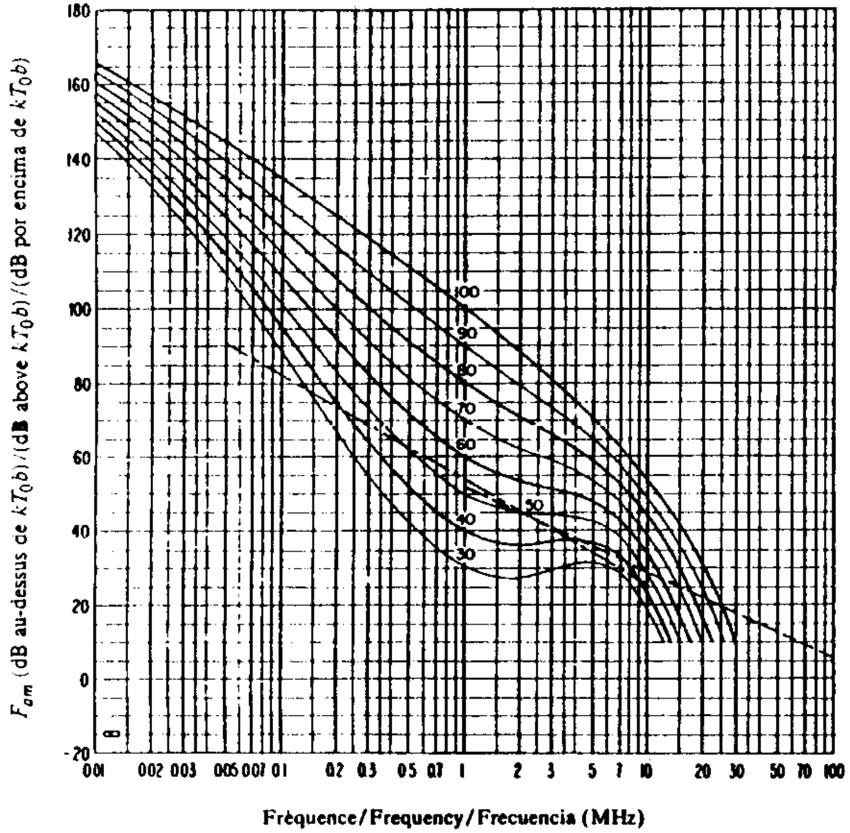

FIGURE 8b – *Variation du bruit radioélectrique en fonction de la fréquence (Printemps; 0000-0400 heure locale)*

FIGURE 8b – *Variation of radio noise with frequency (Spring; 0000-0400 LT)*

FIGURA 8b – *Variaciones del ruido radioeléctrico con la frecuencia (Primavera; 0000-0400 hora local)*

Voir la légende de la Fig. 2b/See legend of Fig. 2b/Véase la leyenda de la fig. 2b

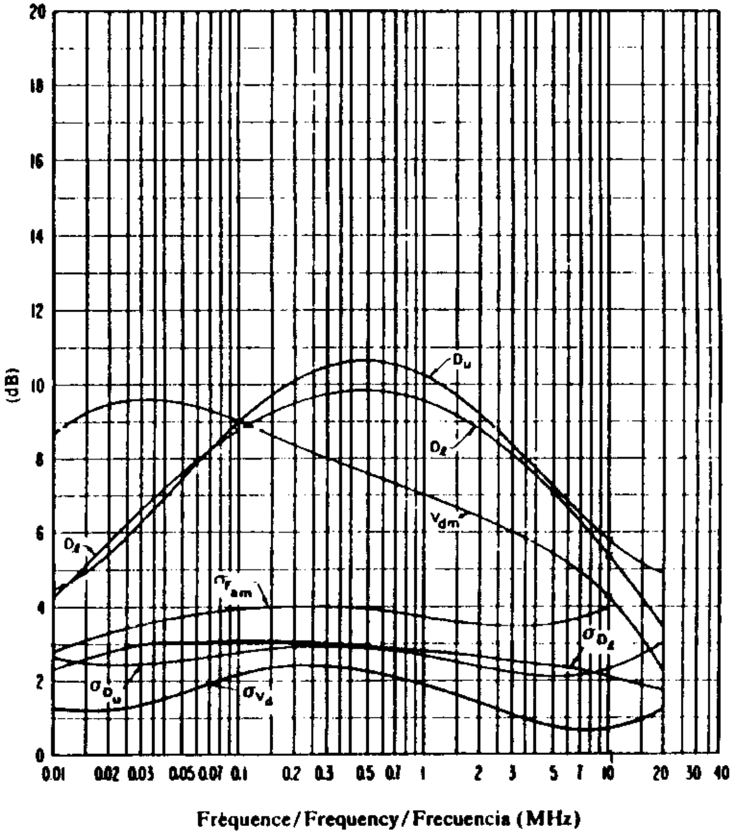

FIGURE 8c – *Données sur la variabilité et le caractère du bruit (Printemps; 0000-0400 heure locale)*

FIGURE 8c – *Data on noise variability and character (Spring; 0000-0400 LT)*

FIGURA 8c – *Datos sobre la variabilidad y el carácter del ruido (Primavera; 0000-0400 hora local)*

Voir la légende de la Fig. 2c/See legend of Fig. 2c/Véase la leyenda de la fig. 2c

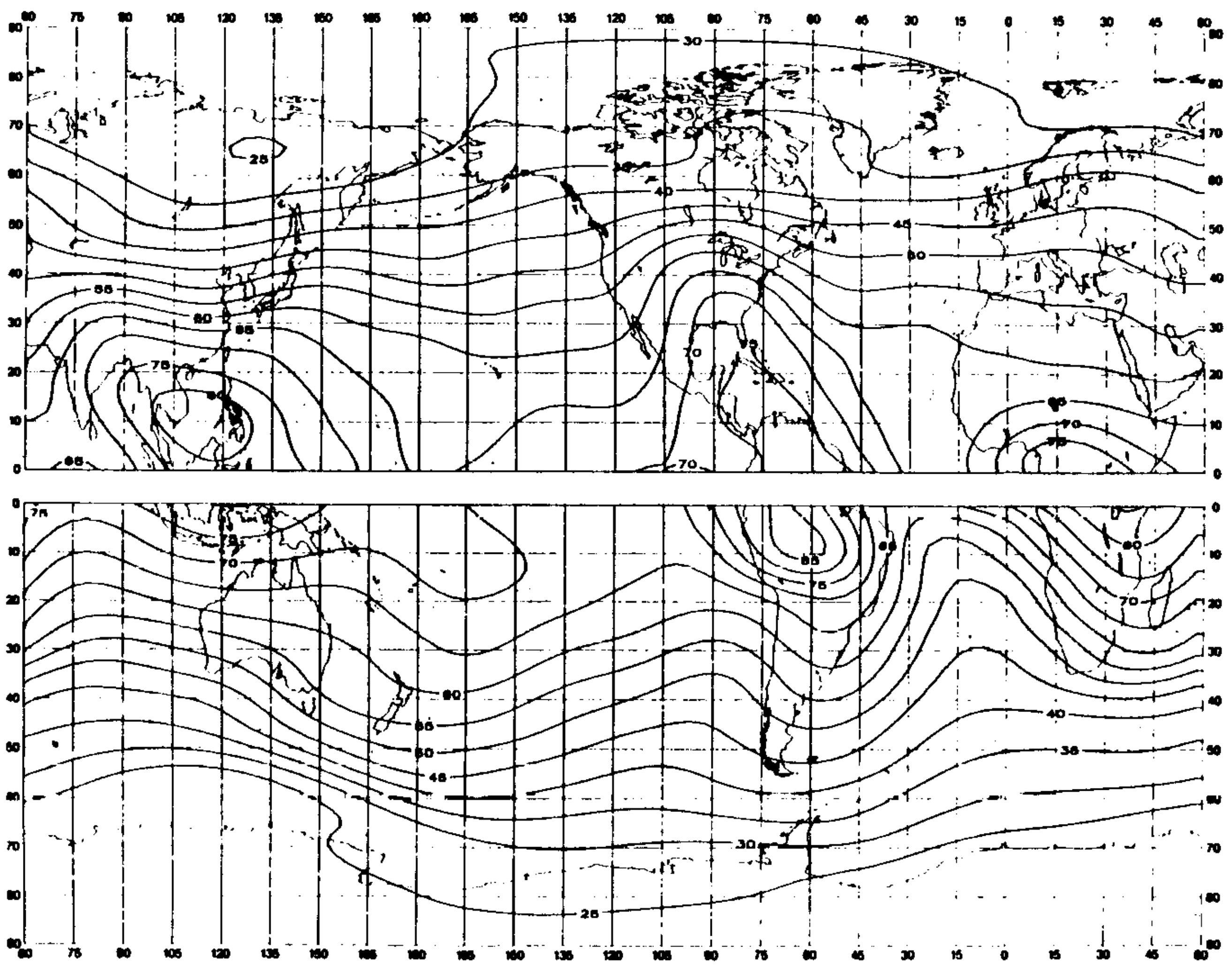
30
25
40
45
50
55
60
65
70
75
80
85
36
28
90
75
60
45
30
15
0
15
30
45
60
75
90
105
120
135
150
165
180
165
150
135
120
105
90
75
60
45
30
15
0
15
30
45
60
80
70
60
50
40
30
20
10
0
10
20
30
40
50
60
70
80

FIGURE 9a – *Valeurs attendues du bruit atmosphérique radioélectrique, $F_{am}$, en dB au-dessus de $kT_0b$ à 1 MHz (Printemps; 0400-0800 heure locale)*

FIGURE 9a – *Expected values of atmospheric radio noise, $F_{am}$ (dB above $kT_0b$ at 1 MHz) (Spring; 0400-0800 LT)*

FIGURA 9a – *Valores probables del ruido atmosférico, $F_{am}$, en dB por encima de $kT_0b$ en 1 MHz (Primavera; 0400-0800 hora local)*

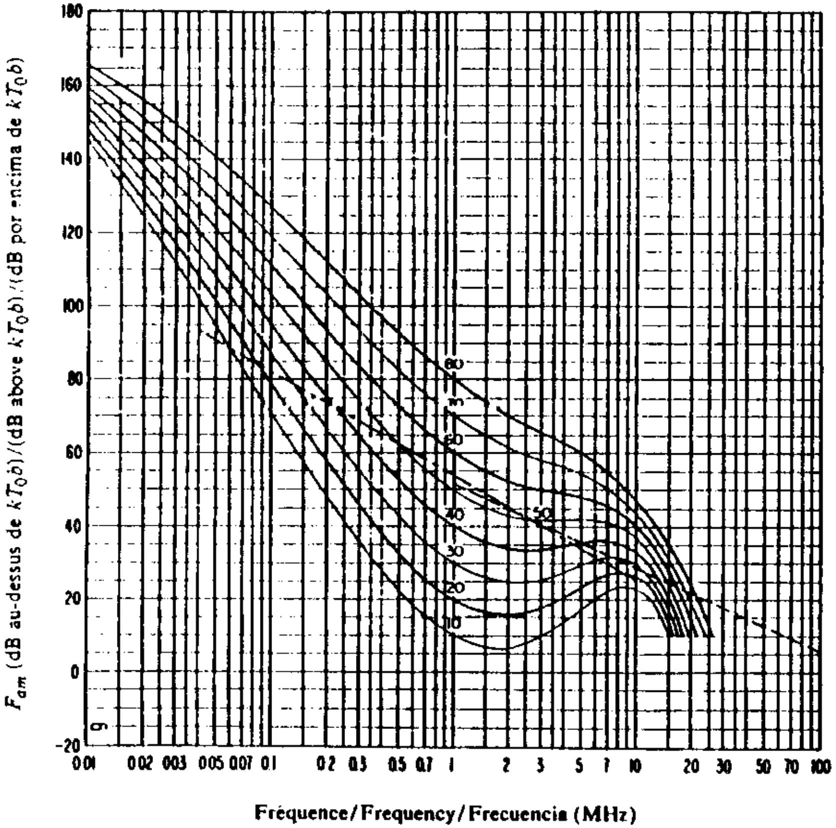

FIGURE 9b – *Variation du bruit radioélectrique en fonction de la fréquence (Printemps; 0400-0800 heure locale)*

FIGURE 9b – *Variation of radio noise with frequency (Spring; 0400-0800 LT)*

FIGURA 9b – *Variaciones del ruido radioeléctrico con la frecuencia (Primavera; 0400-0800 hora local)*

Voir la légende de la Fig. 2b/See legend of Fig. 2b/Véase la leyenda de la fig. 2b

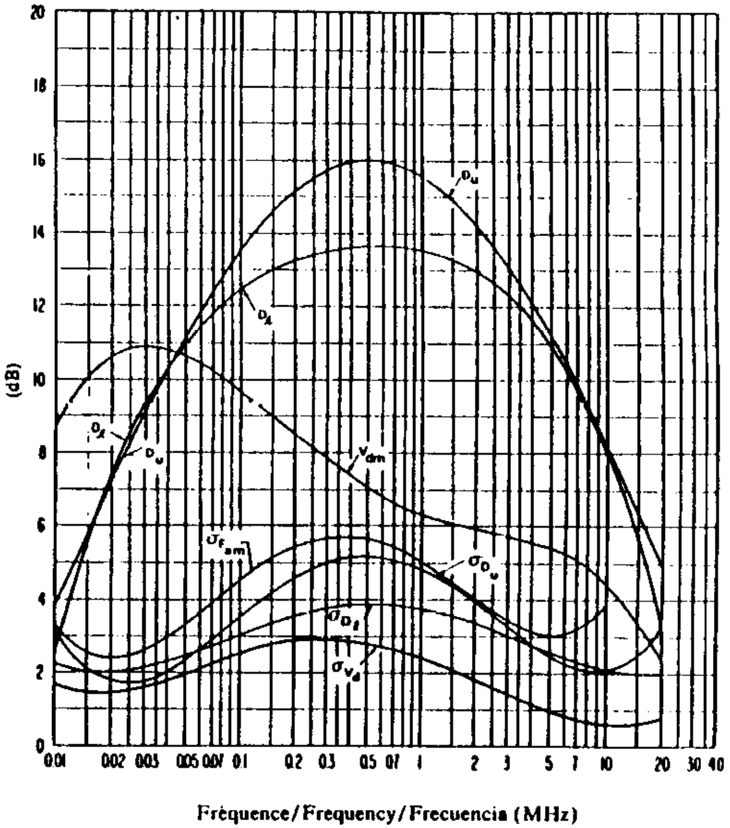

FIGURE 9c – *Données sur la variabilité et le caractère du bruit (Printemps; 0400-0800 heure locale)*

FIGURE 9c – *Data on noise variability and character (Spring; 0400-0800 LT)*

FIGURA 9c – *Datos sobre la variabilidad y el carácter del ruido (Primavera; 0400-0800 hora local)*

Voir la légende de la Fig. 2c/See legend of Fig. 2c/Véase la leyenda de la fig. 2c

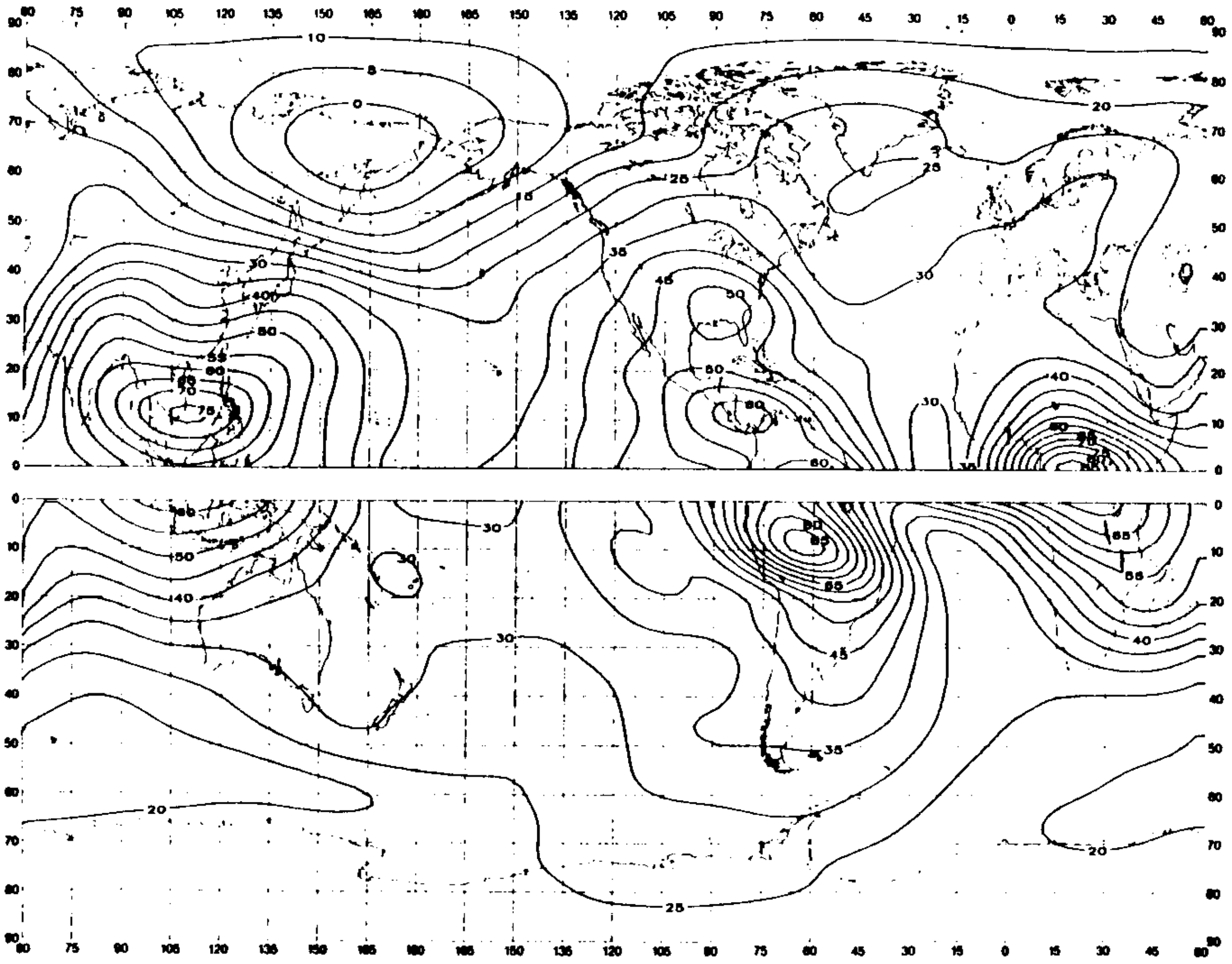
60
75
90
105
120
135
150
165
180
165
150
135
120
105
90
75
60
45
30
15
0
15
30
45
60
90
80
70
60
50
40
30
20
10
0
10
20
30
40
50
60
70
80
90
10
5
0
20
25
15
30
35
45
50
60
40
55
65
70
75
80
85
30
35
40
45
50
55
60
25
20
30

FIGURE 10a – *Valeurs attendues du bruit atmosphérique radioélectrique, $F_{am}$, en dB au-dessus de $kT_0b$ à 1 MHz (Printemps; 0800-1200 heure locale)*

FIGURE 10a – *Expected values of atmospheric radio noise, $F_{am}$ (dB above $kT_0b$ at 1 MHz) (Spring; 0800 1200 LT)*

FIGURA 10a – *Valores probables del ruido atmosférico, $F_{am}$, en dB por encima de $kT_0b$ en 1 MHz (Primavera; 0800-1200 hora local)*

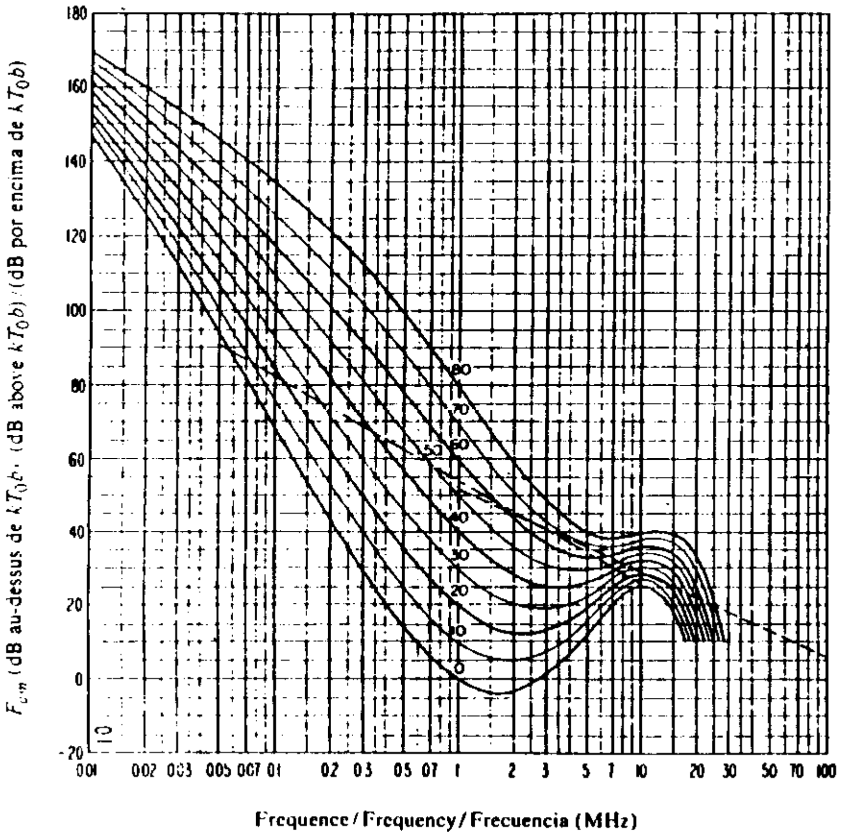

FIGURE 10b – *Variation du bruit radioélectrique en fonction de la fréquence (Printemps; 0800-1200 heure locale)*

FIGURE 10b – *Variation of radio noise with frequency (Spring; 0800-1200 LT)*

FIGURA 10b – *Variaciones del ruido radioeléctrico con la frecuencia (Primavera; 0800-1200 hora local)*

Voir la legende de la Fig. 2b/See legend of Fig. 2b/Vease la leyenda de la fig. 2b

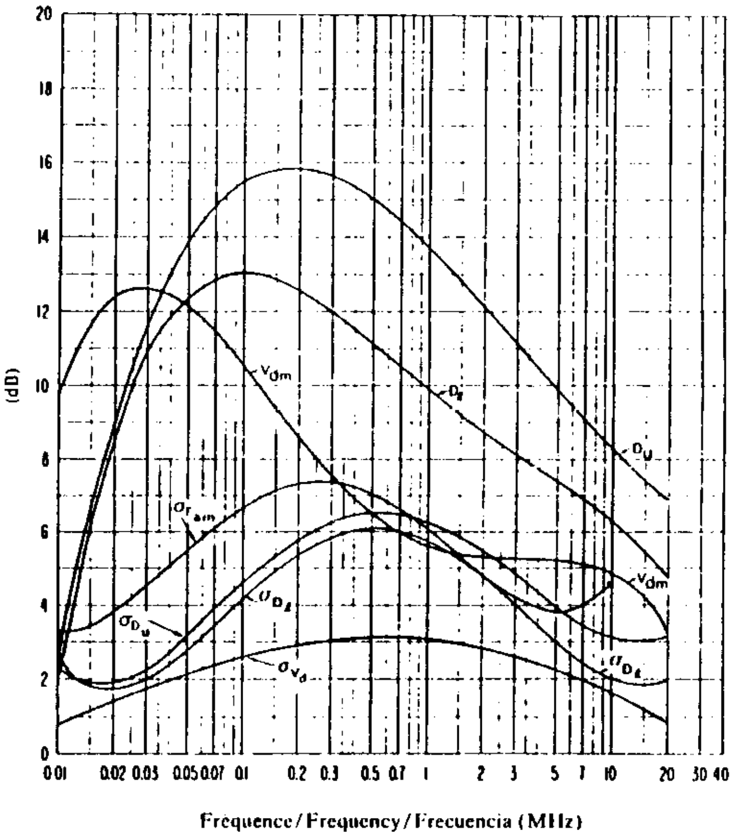

FIGURE 10c – *Données sur la variabilité et le caractère du bruit (Printemps; 0800-1200 heure locale)*

FIGURE 10c – *Data on noise variability and character (Spring; 0800-1200 LT)*

FIGURA 10c – *Datos sobre la variabilidad y el carácter del ruido (Primavera; 0800-1200 hora local)*

Voir la legende de la Fig. 2c/See legend of Fig. 2c/Vease la leyenda de la fig. 2c

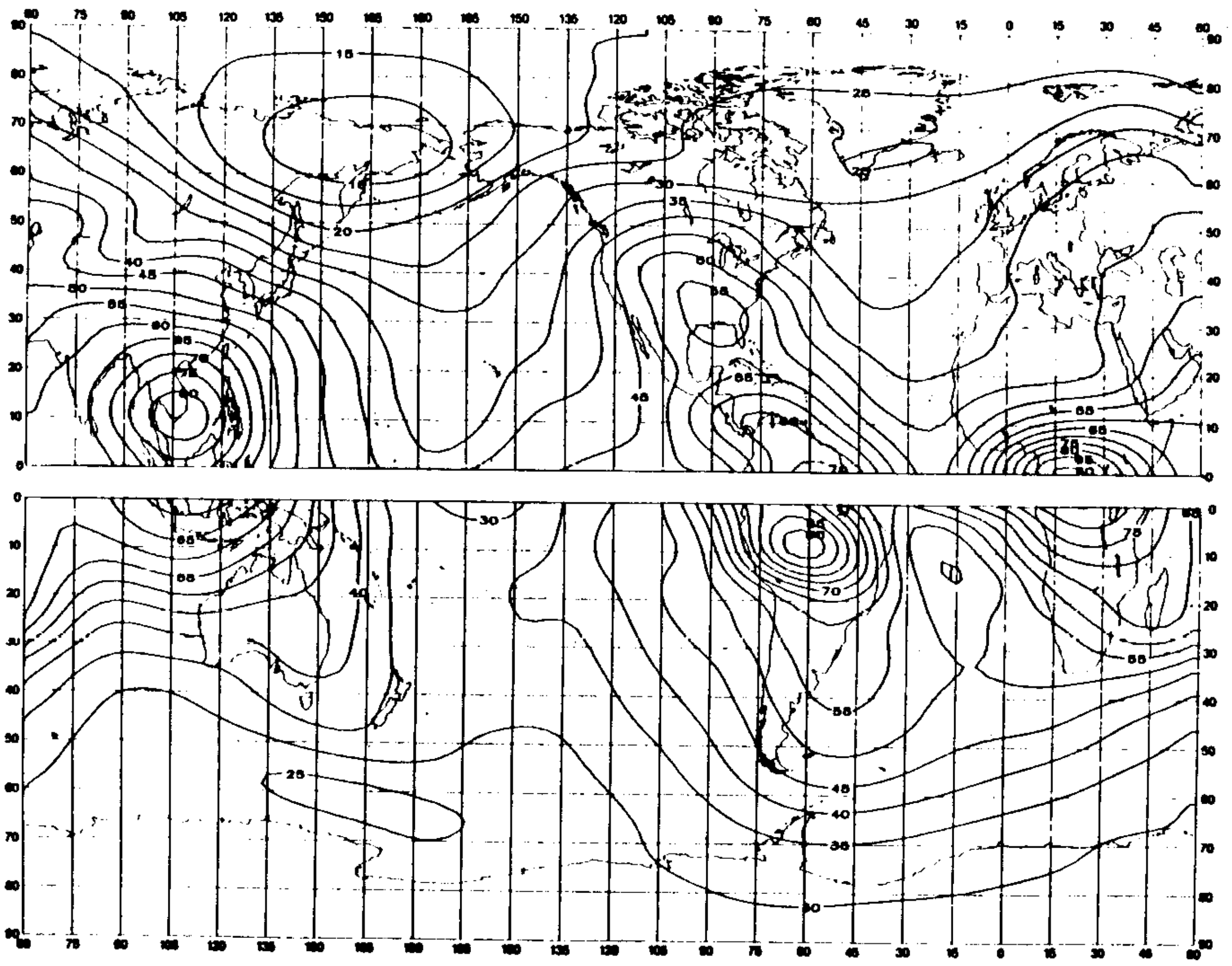
60
75
90
105
120
135
150
165
180
165
150
135
120
105
90
75
60
45
30
15
0
15
30
45
60
90
80
70
60
50
40
30
20
10
0
10
20
30
40
50
60
70
80
90

FIGURE 11a – *Valeurs attendues du bruit atmosphérique radioélectrique, $F_{am}$, en dB au-dessus de $kT_0b$ à 1 MHz (Printemps; 1200-1600 heure locale)*

FIGURE 11a – *Expected values of atmospheric radio noise, $F_{am}$ (dB above $kT_0b$ at 1 MHz) (Spring; 1200-1600 LT)*

FIGURA 11a – *Valores probables del ruido atmosférico, $F_{am}$, en dB por encima de $kT_0b$ en 1 MHz (Primavera; 1200-1600 hora local)*

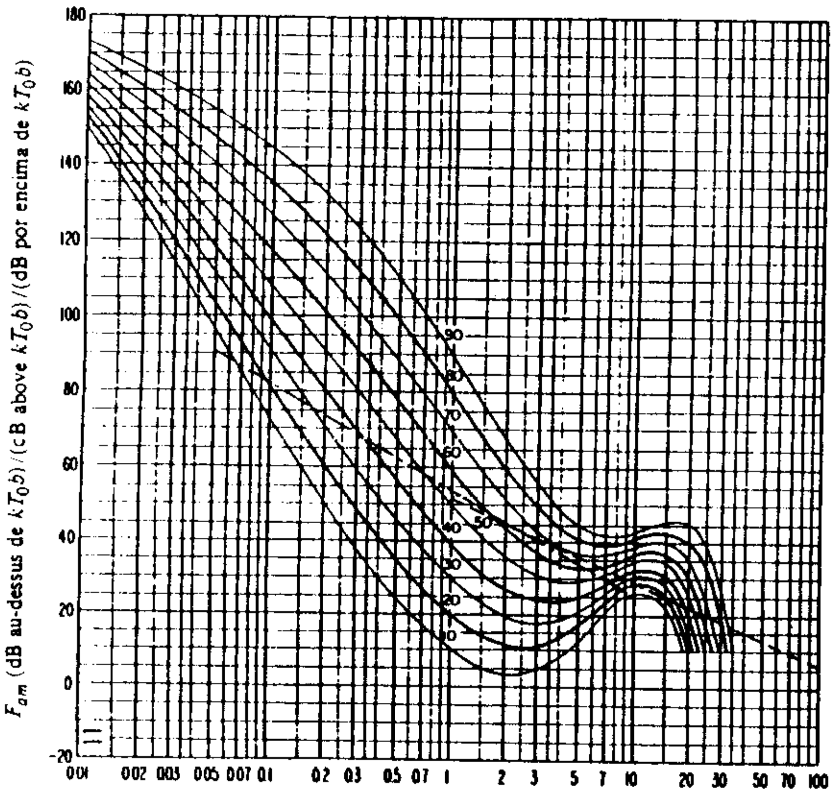

Fréquence/Frequency/Frecuencia (MHz)

FIGURE 11b – *Variation du bruit radioélectrique en fonction de la fréquence (Printemps; 1200-1600 heure locale)*

FIGURE 11b – *Variation of radio noise with frequency (Spring; 1200-1600 LT)*

FIGURA 11b – *Variaciones del ruido radioeléctrico con la frecuencia (Primavera; 1200-1600 hora local)*

Voir la légende de la Fig. 2b/See legend of Fig. 2b/Véase la leyenda de la fig. 2b

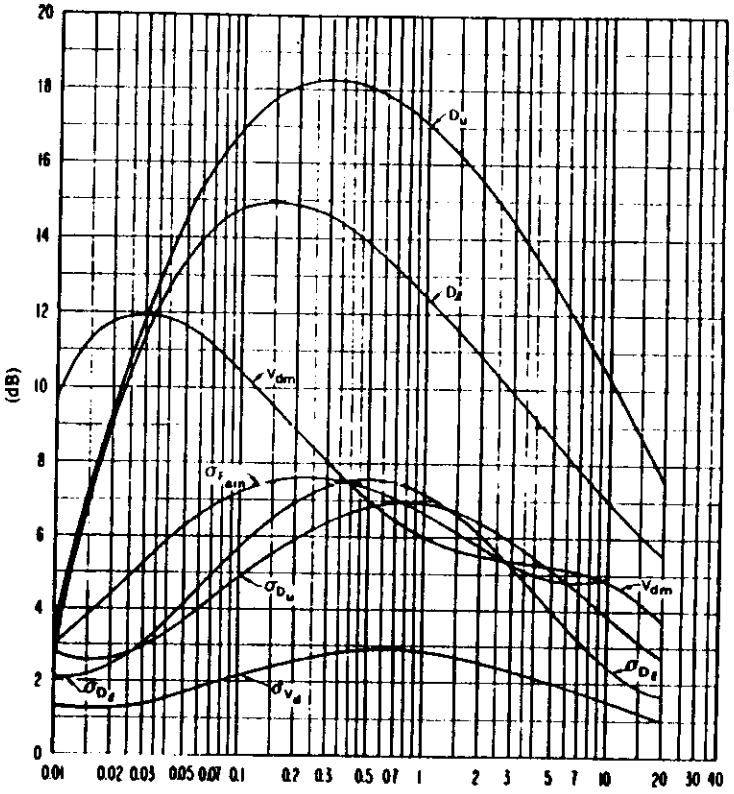

Fréquence/Frequency/Frecuencia (MHz)

FIGURE 11c – *Données sur la variabilité et le caractère du bruit (Printemps; 1200-1600 heure locale)*

FIGURE 11c – *Data on noise variability and character (Spring; 1200-1600 LT)*

FIGURA 11c – *Datos sobre la variabilidad y el carácter del ruido (Primavera; 1200-1600 hora local)*

Voir la légende de la Fig. 2c/See legend of Fig. 2c/Véase la leyenda de la fig. 2c

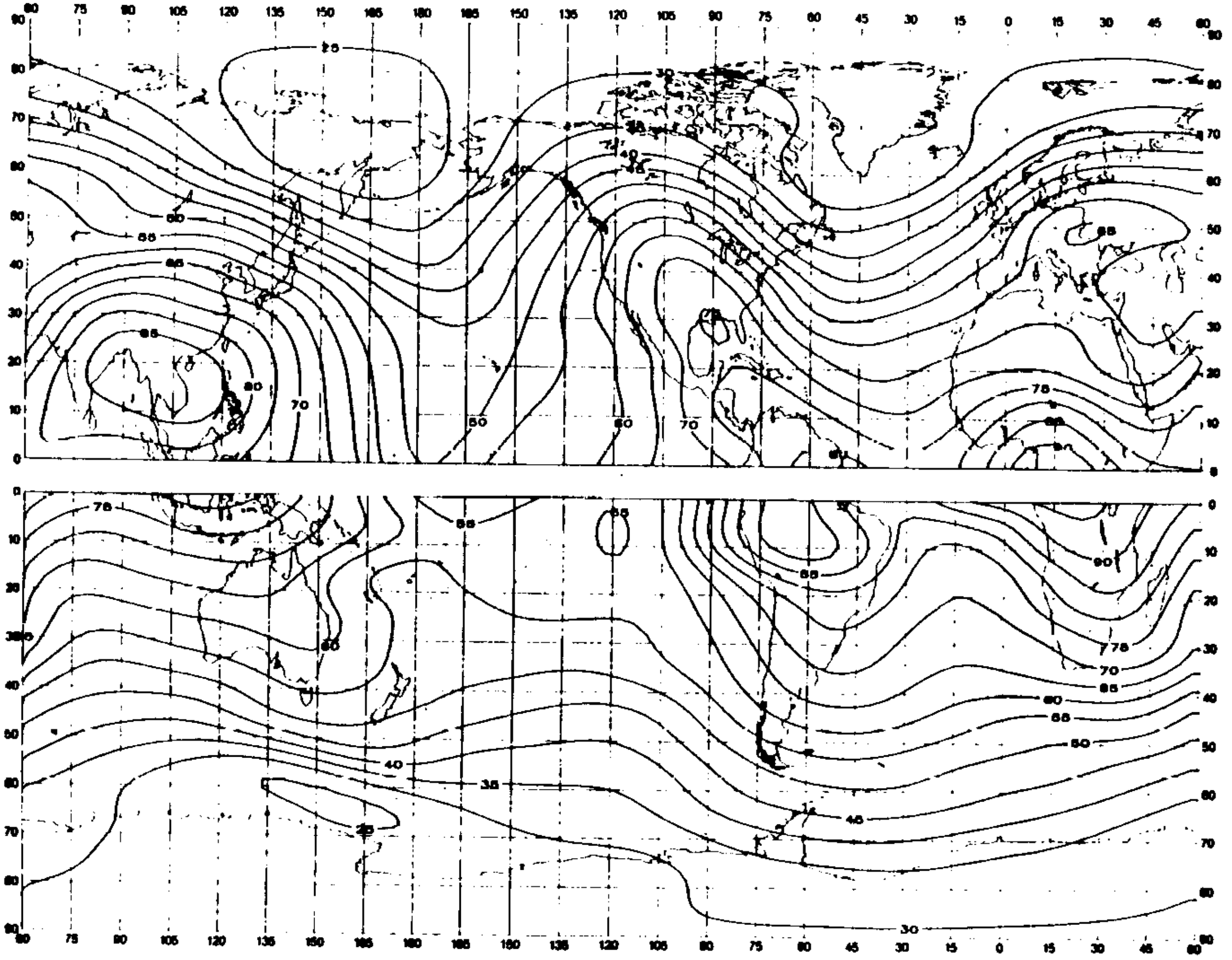
60 75 90 105 120 135 150 165 180 165 150 135 120 105 90 75 60 45 30 15 0 15 30 45 60
90 80 70 60 50 40 30 20 10 0
0 10 20 30 40 50 60 70 80 90
25
30
40
45
50
55
60
65
70
75
80
85
90
35
20

FIGURE 12a – *Valeurs attendues du bruit atmosphérique radioélectrique, $F_{am}$, en dB au-dessus de $kT_0b$ à 1 MHz (Printemps; 1600-2000 heure locale)*

FIGURE 12a – *Expected values of atmospheric radio noise, $F_{am}$ (dB above $kT_0b$ at 1 MHz) (Spring; 1600-2000 LT)*

FIGURA 12a – *Valores probables del ruido atmosférico, $F_{am}$, en dB por encima de $kT_0b$ en 1 MHz (Primavera; 1600-2000 hora local)*

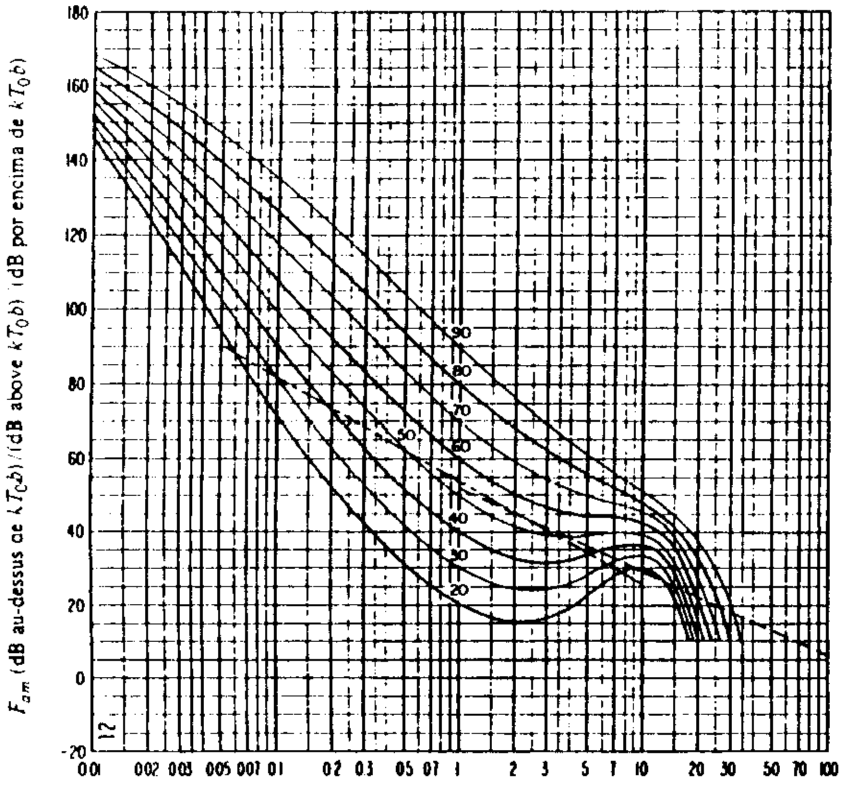

Fréquence/Frequency/Frecuencia (MHz)

FIGURE 12b – *Variation du bruit radioélectrique en fonction de la fréquence (Printemps; 1600-2000 heure locale)*

FIGURE 12b – *Variation of radio noise with frequency (Spring; 1600-2000 LT)*

FIGURA 12b – *Variaciones del ruido radioeléctrico con la frecuencia (Primavera; 1600-2000 hora local)*

Voir la legende de la Fig. 2b/See legend of Fig. 2b/Vease la leyenda de la fig. 2b

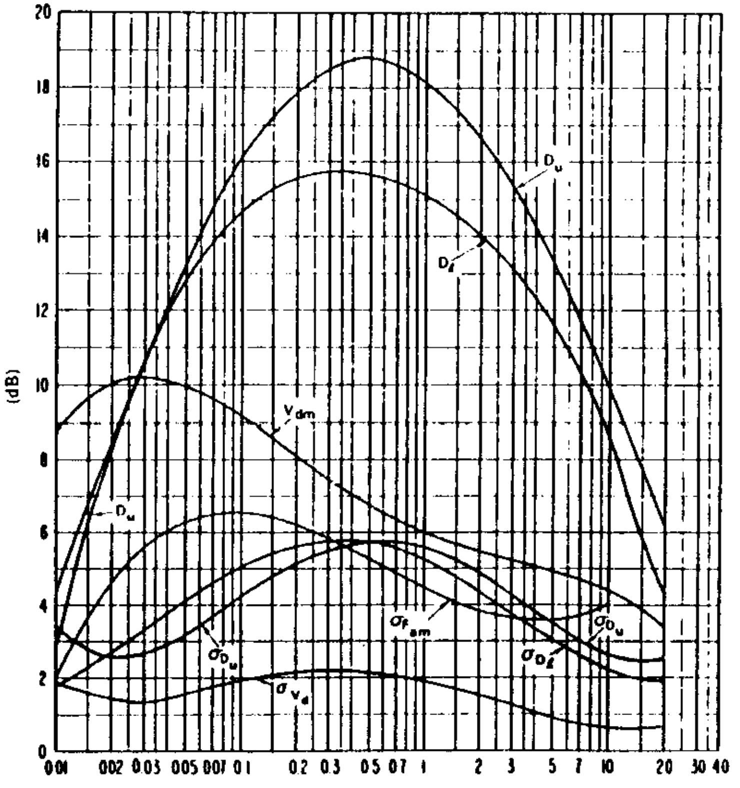

Fréquence/Frequency/Frecuencia (MHz)

FIGURE 12c – *Données sur la variabilité et le caractère du bruit (Printemps; 1600-2000 heure locale)*

FIGURE 12c – *Data on noise variability and character (Spring; 1600-2000 LT)*

FIGURA 12c – *Datos sobre la variabilidad y el carácter del ruido (Primavera; 1600-2000 hora local)*

Voir la legende de la Fig. 2c/See legend of Fig. 2c/Vease la leyenda de la fig. 2c

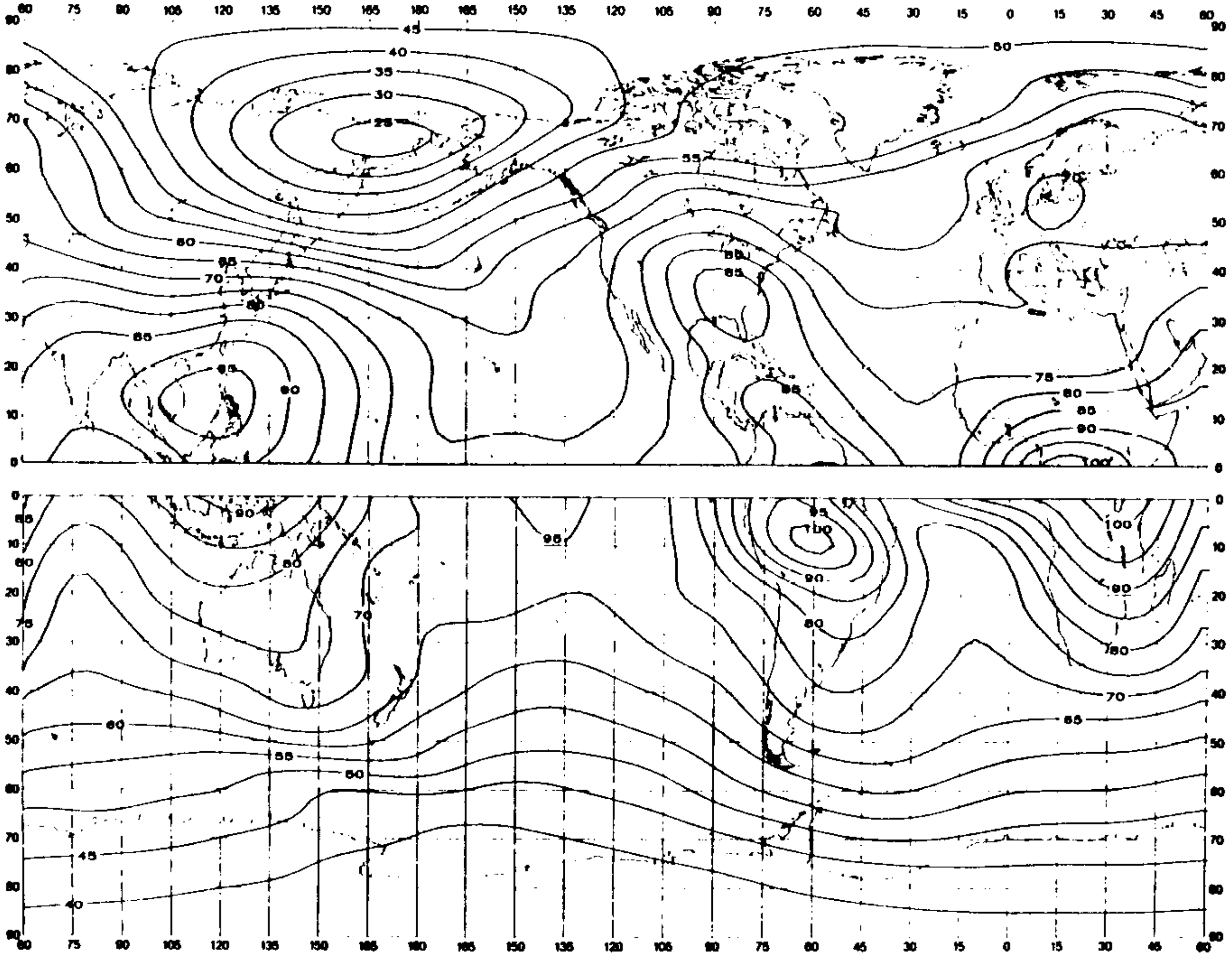
60 75 90 105 120 135 150 165 180 165 150 135 120 105 90 75 60 45 30 15 0 15 30 45 60
90 80 70 60 50 40 30 20 10 0 0 10 20 30 40 50 60 70 80 90
45
40
35
30
25
50
55
60
65
70
80
85
90
75
100
95
60
55
45
40

FIGURE 13a – *Valeurs attendues du bruit atmosphérique radioélectrique, $F_{am}$, en dB au dessus de $kT_0b$ à 1 MHz (Printemps; 2000-2400 heure locale)*

FIGURE 13a – *Expected values of atmospheric radio noise, $F_{am}$ (dB above $kT_0b$ at 1 MHz) (Spring; 2000-2400 LT)*

FIGURA 13a – *Valores probables del ruido atmosférico, $F_{am}$, en dB por encima de $kT_0b$ en 1 MHz (Primavera, 2000-2400 hora local)*

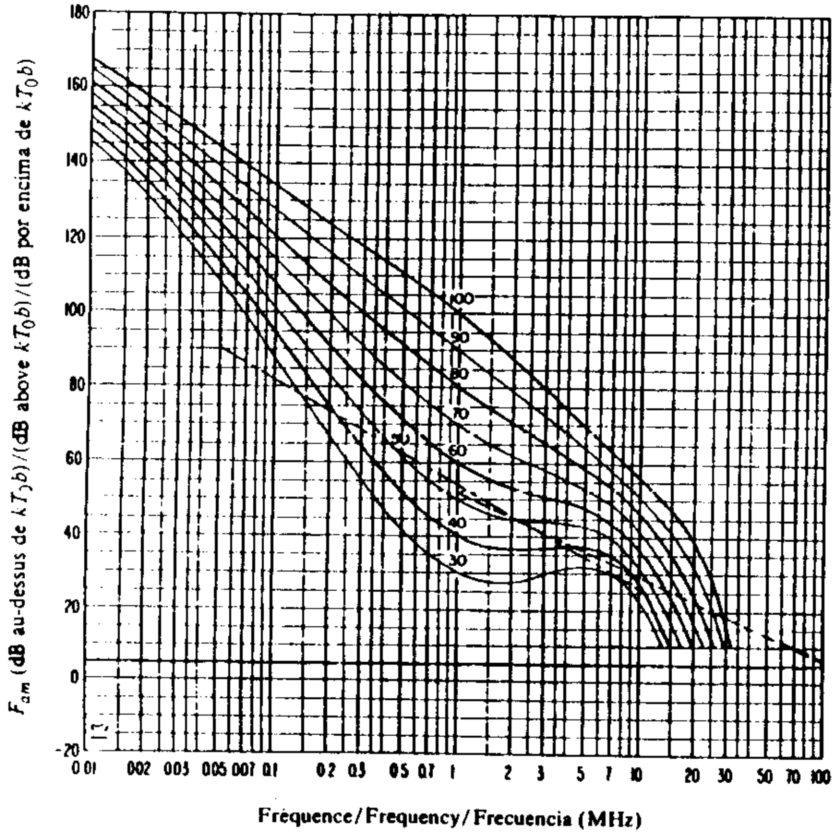

FIGURE 13b – *Variation du bruit radioélectrique en fonction de la fréquence (Printemps; 2000-2400 heure locale)*

FIGURE 13b – *Variation of radio noise with frequency (Spring; 2000-2400 LT)*

FIGURA 13b – *Variaciones del ruido radioeléctrico con la frecuencia (Primavera; 2000-2400 hora local)*

Voir la légende de la Fig. 2b/See legend of Fig. 2b/Véase la leyenda de la fig. 2b

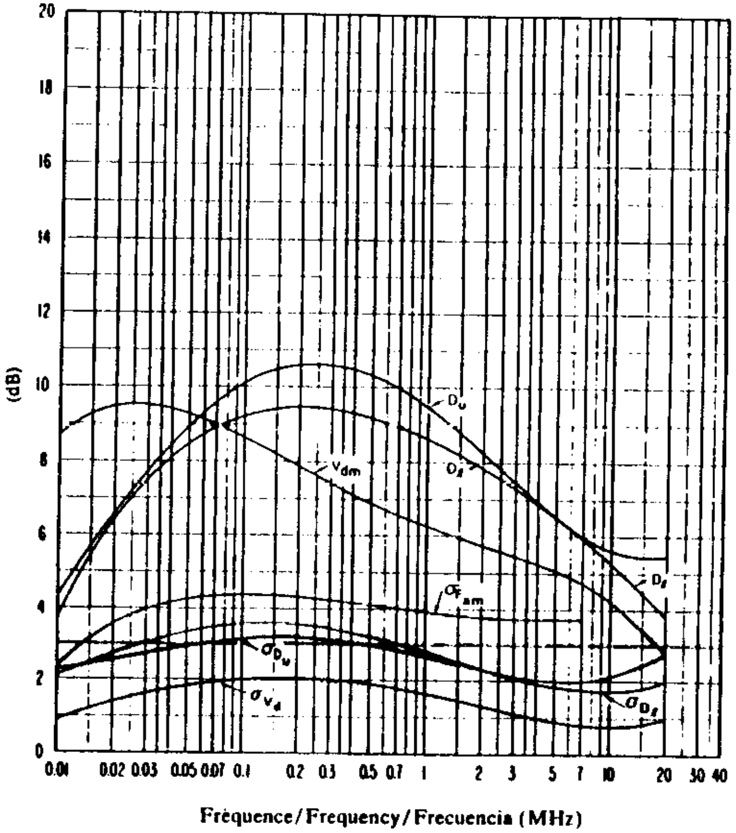

FIGURE 13c – *Données sur la variabilité et le caractère du bruit (Printemps; 2000-2400 heure locale)*

FIGURE 13c – *Data on noise variability and character (Spring; 2000-2400 LT)*

FIGURA 13c – *Datos sobre la variabilidad y el carácter del ruido (Primavera; 2000-2400 hora local)*

Voir la légende de la Fig. 2c/See legend of Fig. 2c/Véase la leyenda de la fig. 2c

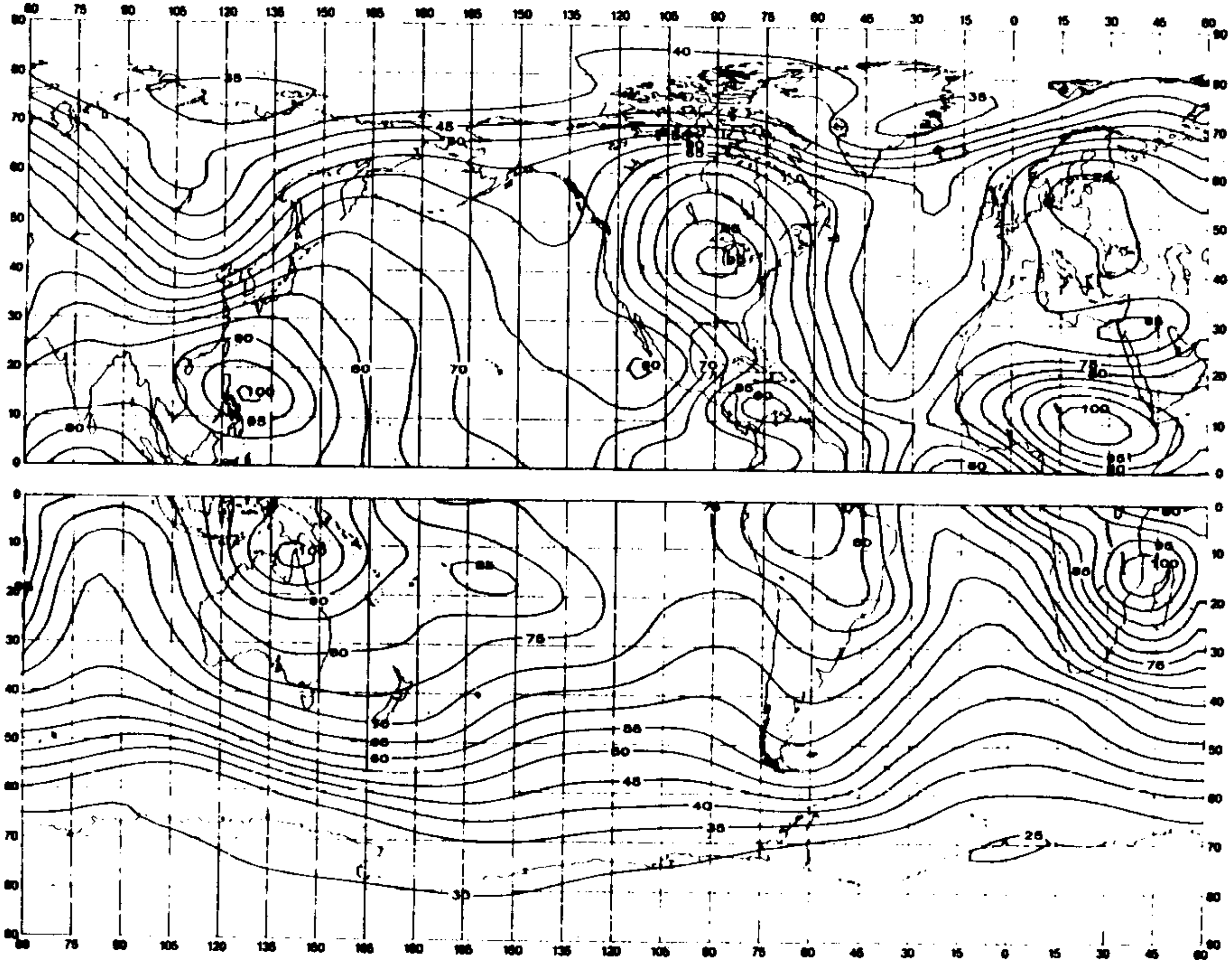
60
75
90
105
120
135
150
165
180
165
150
135
120
105
90
75
60
45
30
15
0
15
30
45
60
90
80
70
60
50
40
30
20
10
0
10
20
30
40
50
60
70
80
90
40
35
45
50
38
80
100
88
80
70
70
60
85
80
75
100
88
80
100
85
80
75
86
80
60
100
76
76
80
55
50
46
40
35
26
30

FIGURE 14a — *Valeurs attendues du bruit atmosphérique radioélectrique, $F_{am}$, en dB au-dessus de $kT_0b$ à 1 MHz (Eté; 0000 0400 heure locale)*

FIGURE 14a — *Expected values of atmospheric radio noise, $F_{am}$ (dB above $kT_0b$ at 1 MHz) (Summer; 0000-0400 LT)*

FIGURA 14a — *Valores probables del ruido atmosférico, $F_{am}$, en dB por encima de $kT_0b$ en 1 MHz (Verano; 0000-0400 hora local)*

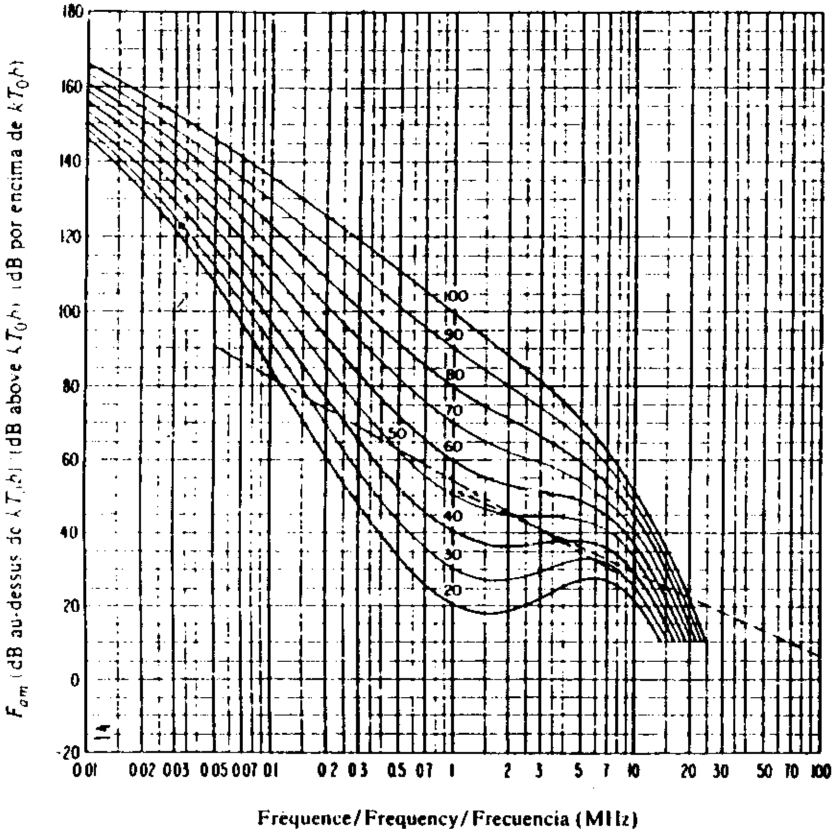

FIGURE 14b – *Variation du bruit radioélectrique en fonction de la fréquence (Eté; 0000-0400 heure locale)*

FIGURE 14b – *Variation of radio noise with frequency (Summer; 0000-0400 LT)*

FIGURA 14b – *Variaciones del ruido radioeléctrico con la frecuencia (Verano; 0000-0400 hora local)*

Voir la legende de la Fig. 2b/See legend of Fig. 2b/Véase la leyenda de la fig. 2b

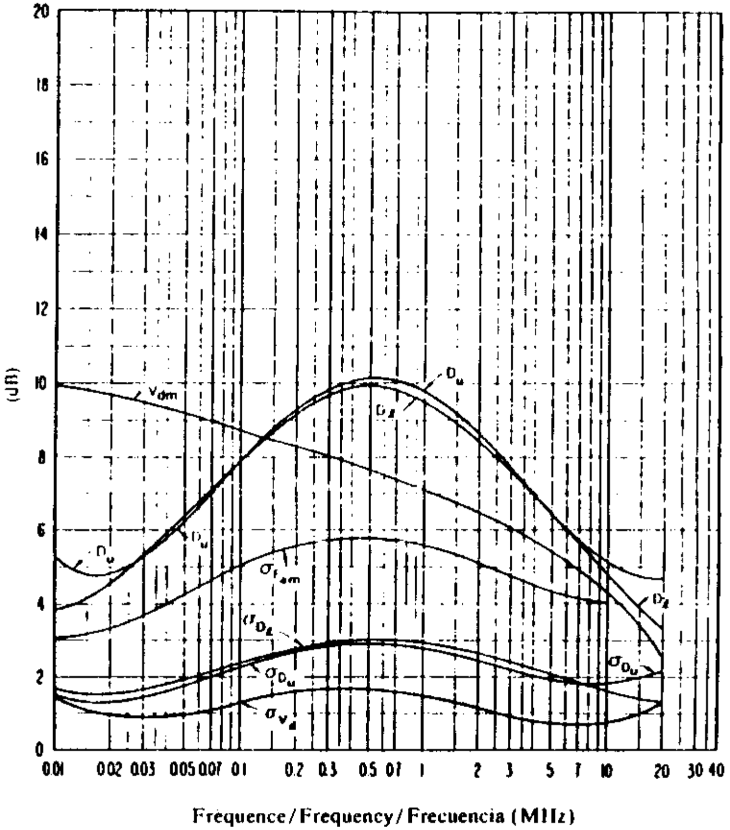

FIGURE 14c – *Données sur la variabilité et le caractère du bruit (Eté; 0000-0400 heure locale)*

FIGURE 14c – *Data on noise variability and character (Summer; 0000-0400 LT)*

FIGURA 14c – *Datos sobre la variabilidad y el carácter del ruido (Verano; 0000-0400 hora local)*

Voir la legende de la Fig. 2c/See legend of Fig. 2c/Véase la leyenda de la fig. 2c

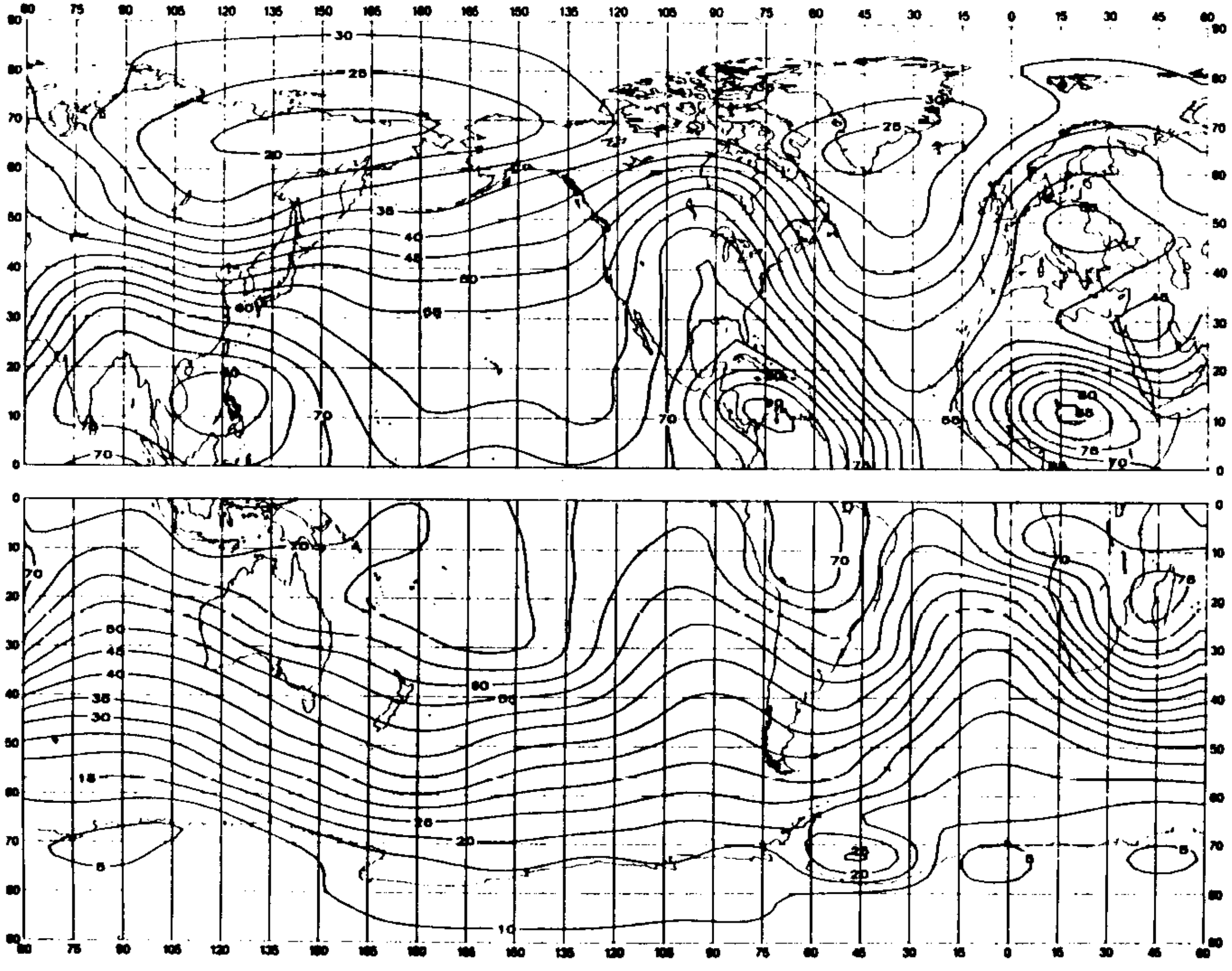

FIGURE 15a – *Valeurs attendues du bruit atmosphérique radioélectrique, $F_{am}$, en dB au-dessus de $kT_0b$ à 1 MHz (Eté; 0400-0800 heure locale)*
FIGURE 15a – *Expected values of atmospheric radio noise, $F_{am}$ (dB above $kT_0b$ at 1 MHz) (Summer; 0400-0800 LT)*
FIGURA 15a – *Valores probables del ruido atmosférico, $F_{am}$, en dB por encima de $kT_0b$ en 1 MHz (Verano; 0400-0800 hora local)*

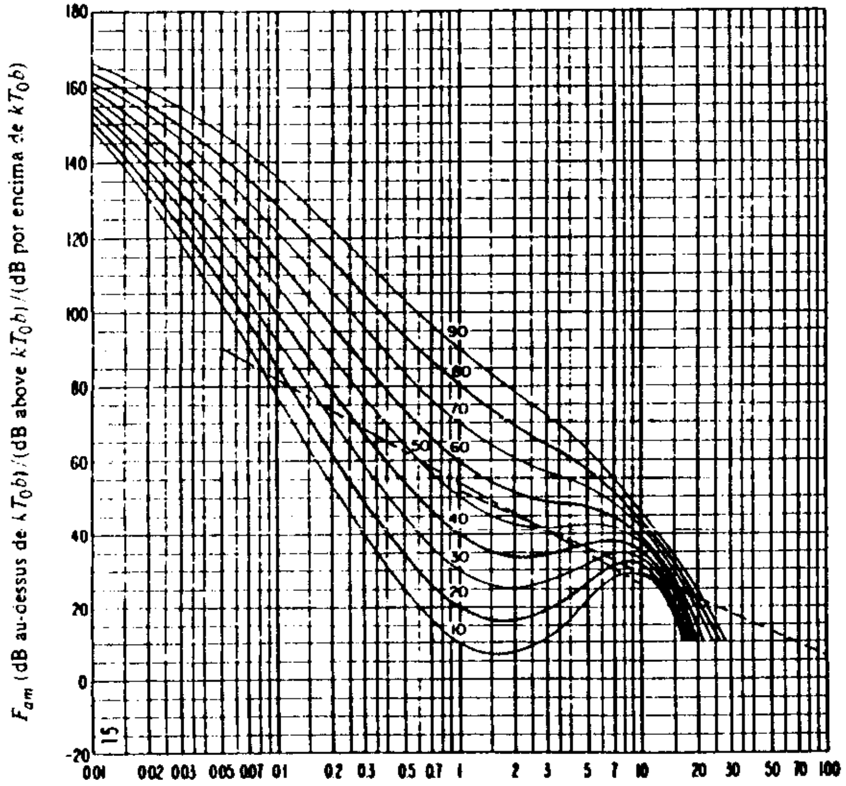

FIGURE 15b – *Variation du bruit radioélectrique en fonction de la fréquence (Eté; 0400-0800 heure locale)*

FIGURE 15b – *Variation of radio noise with frequency (Summer; 0400-0800 LT)*

FIGURA 15b – *Variaciones del ruido radioeléctrico con la frecuencia (Verano; 0400-0800 hora local)*

Voir la légende de la Fig. 2b/See legend of Fig. 2b/Véase la leyenda de la fig. 2b

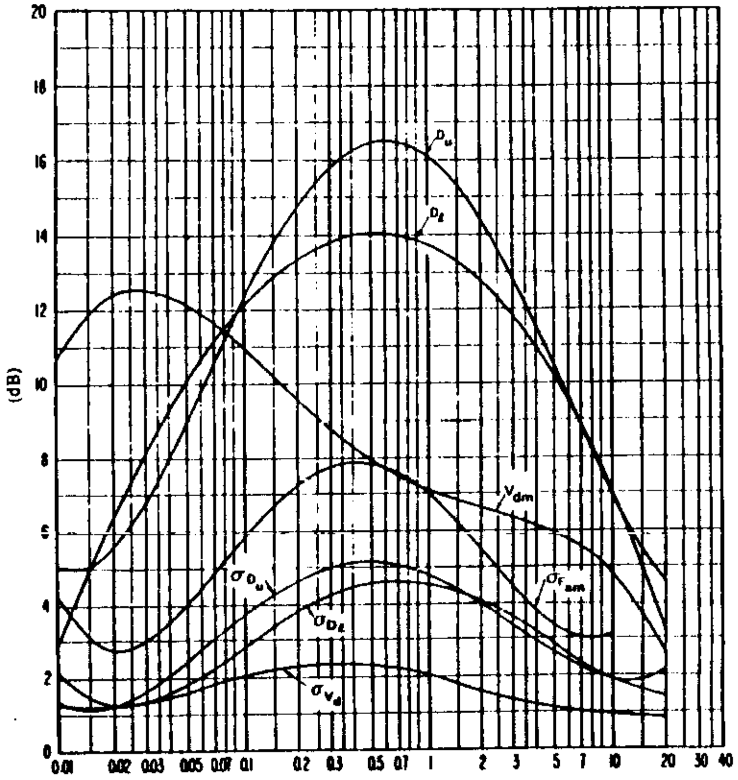

FIGURE 15c – *Données sur la variabilité et le caractère du bruit (Eté; 0400-0800 heure locale)*

FIGURE 15c – *Data on noise variability and character (Summer; 0400-0800 LT)*

FIGURA 15c – *Datos sobre la variabilidad y el carácter del ruido (Verano; 0400-0800 hora local)*

Voir la légende de la Fig. 2c/See legend of Fig. 2c/Véase la leyenda de la fig. 2c

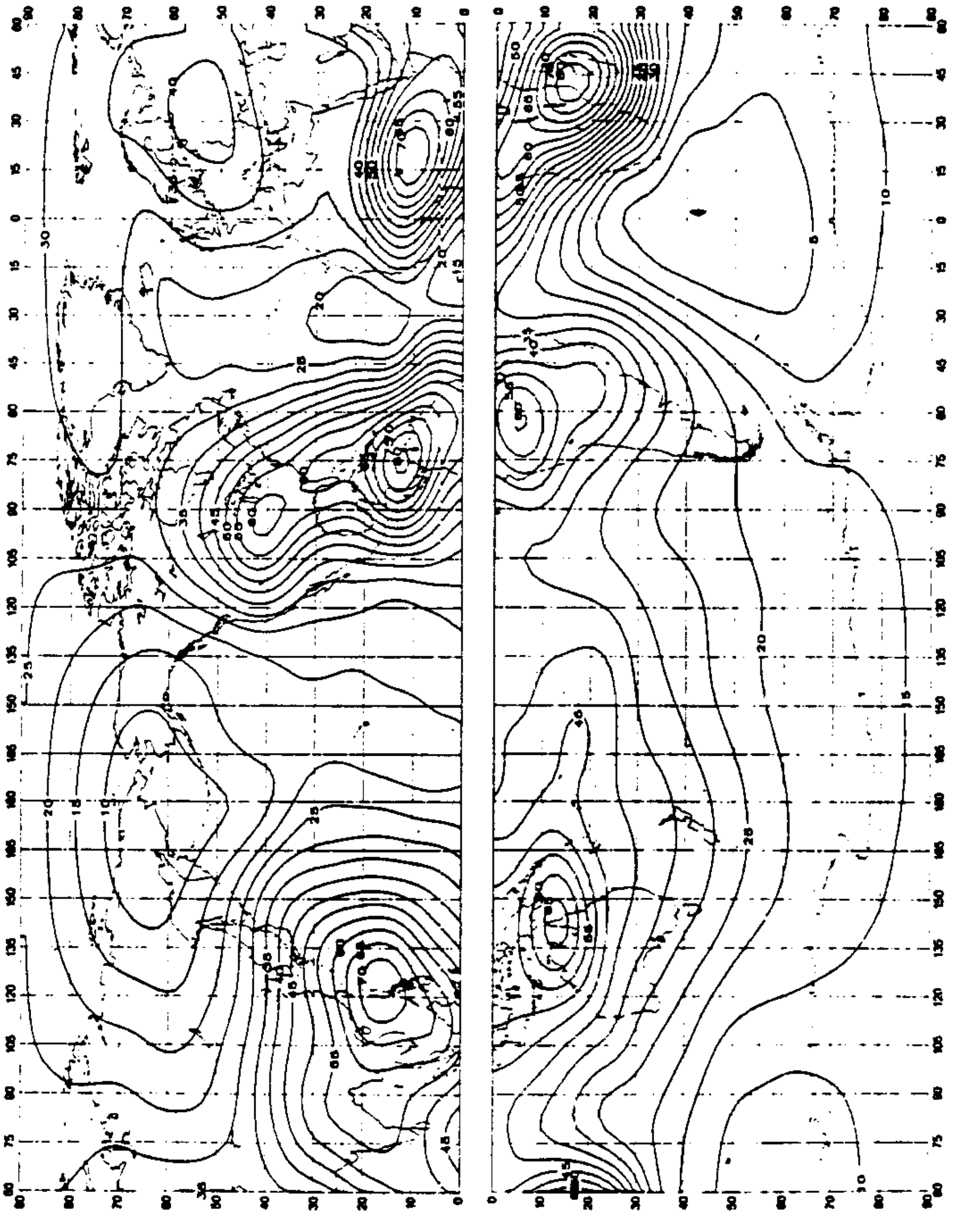
90
80
70
60
50
40
30
20
10
0
60
45
30
15
0
15
30
45
60
75
90
105
120
135
150
165
180
165
150
135
120
105
90
75
60

FIGURE 16a – *Valeurs attendues du bruit atmosphérique radioélectrique, $F_{am}$, en dB au-dessus de $kT_0b$ à 1 MHz (Eté; 0800-1200 heure locale)*
FIGURE 16a – *Expected values of atmospheric radio noise, $F_{am}$ (dB above $kT_0b$ at 1 MHz) (Summer; 0800-1200 LT)*
FIGURA 16a – *Valores probables del ruido atmosférico, $F_{am}$, en dB por encima de $kT_0b$ en 1 MHz (Verano; 0800-1200 hora local)*

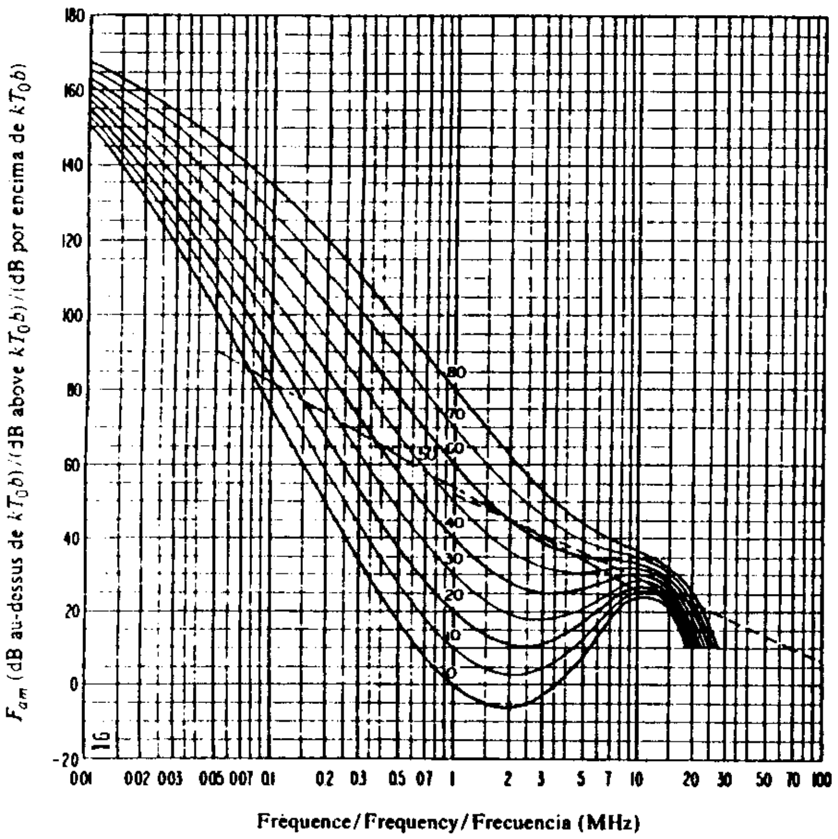

FIGURE 16b – *Variation du bruit radioélectrique en fonction de la fréquence (Eté; 0800-1200 heure locale)*

FIGURE 16b – *Variation of radio noise with frequency (Summer; 0800-1200 LT)*

FIGURA 16b – *Variaciones del ruido radioeléctrico con la frecuencia (Verano; 0800-1200 hora local)*

Voir la légende de la Fig. 2b/See legend of Fig. 2b/Véase la leyenda de la fig. 2b

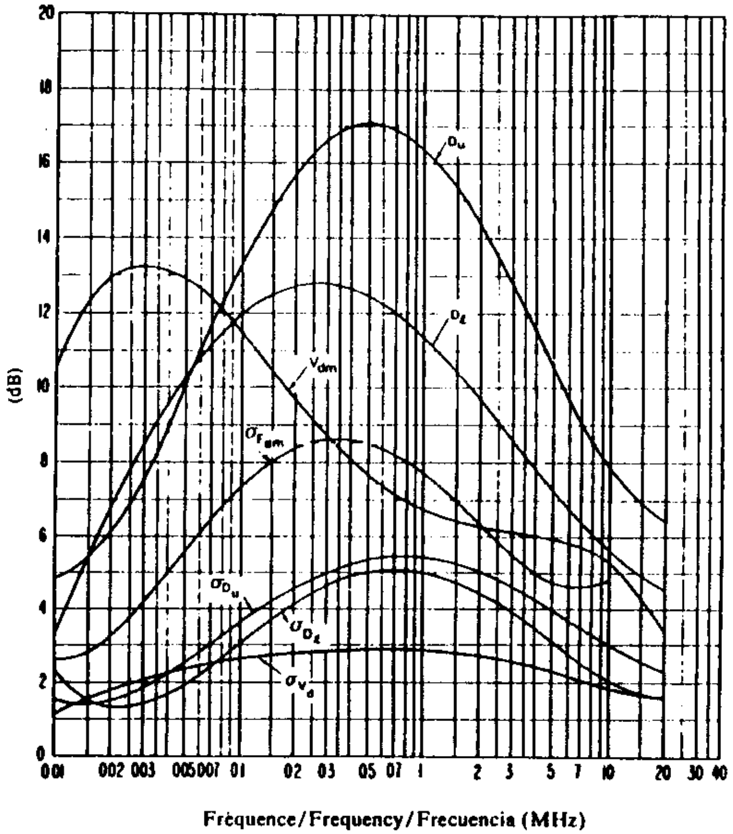

FIGURE 16c – *Données sur la variabilité et le caractère du bruit (Eté; 0800-1200 heure locale)*

FIGURE 16c – *Data on noise variability and character (Summer; 0800-1200 LT)*

FIGURA 16c – *Datos sobre la variabilidad y el carácter del ruido (Verano; 0800-1200 hora local)*

Voir la légende de la Fig. 2c/See legend of Fig. 2c/Véase la leyenda de la fig. 2c

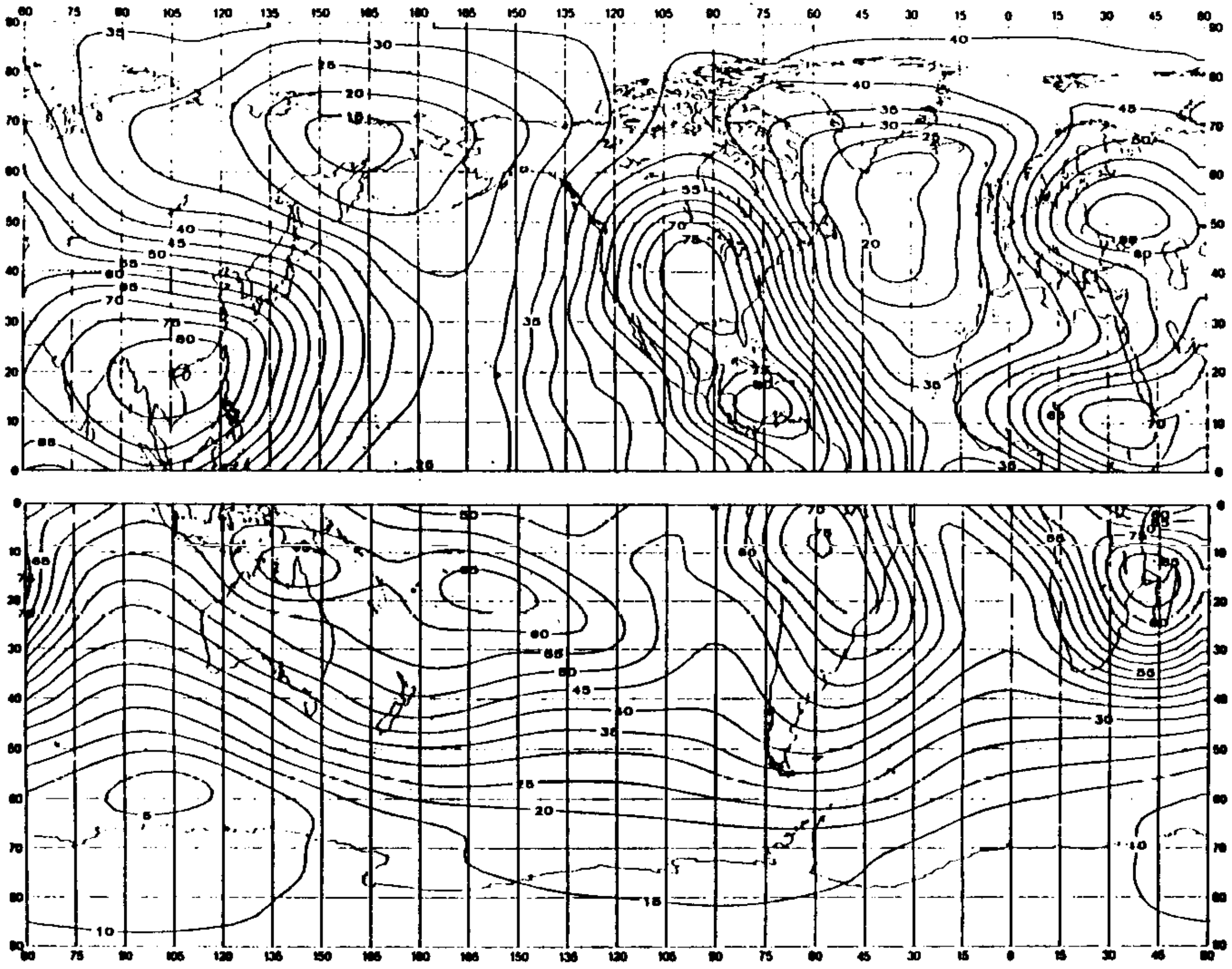
80
75
90
105
120
135
150
165
180
165
150
135
120
105
90
75
60
45
30
15
0
15
30
45
60
70
50
40
30
20
10
0
40
35
30
25
20
15
10
5
45
50
55
60
65
70
75
80

FIGURE 17a – *Valeurs attendues du bruit atmosphérique radioélectrique, $F_{am}$, en dB au-dessus de $kT_0b$ à 1 MHz (Eté; 1200-1600 heure locale)*

FIGURE 17a – *Expected values of atmospheric radio noise, $F_{am}$ (dB above $kT_0b$ at 1 MHz) (Summer; 1200-1600 LT)*

FIGURA 17a – *Valores probables del ruido atmosférico, $F_{am}$, en dB por encima de $kT_0b$ en 1 MHz (Verano; 1200-1600 hora local)*

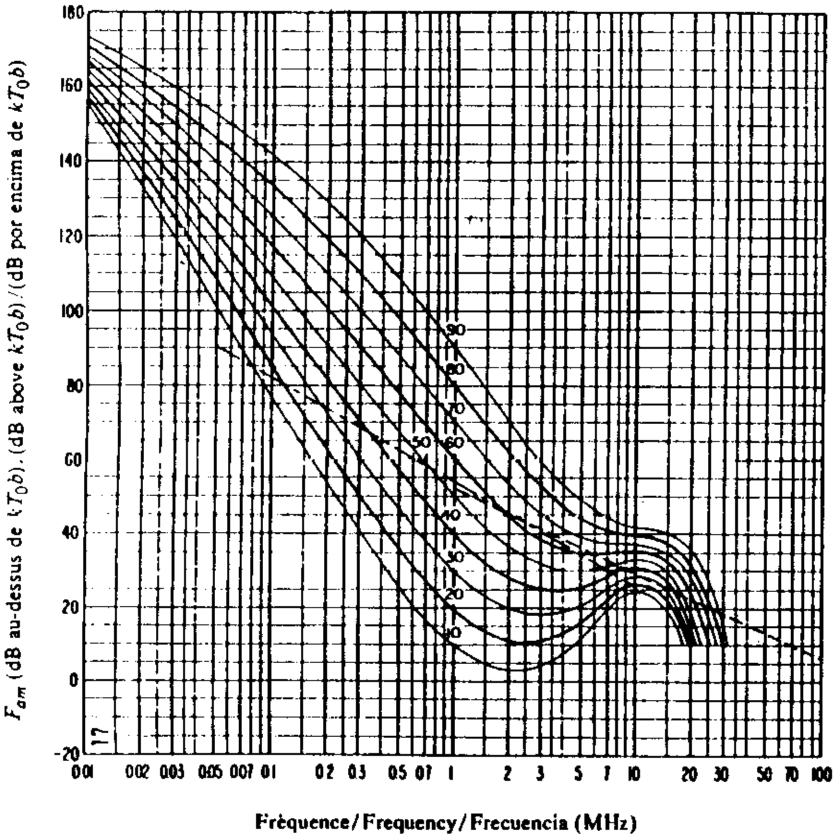

FIGURE 17b – *Variation du bruit radioélectrique en fonction de la fréquence (Eté; 1200-1600 heure locale)*

FIGURE 17b – *Variation of radio noise with frequency (Summer; 1200-1600 LT)*

FIGURA 17b – *Variaciones del ruido radioeléctrico con la frecuencia (Verano; 1200-1600 hora local)*

Voir la légende de la Fig. 2b/See legend of Fig. 2b/Véase la leyenda de la fig. 2b

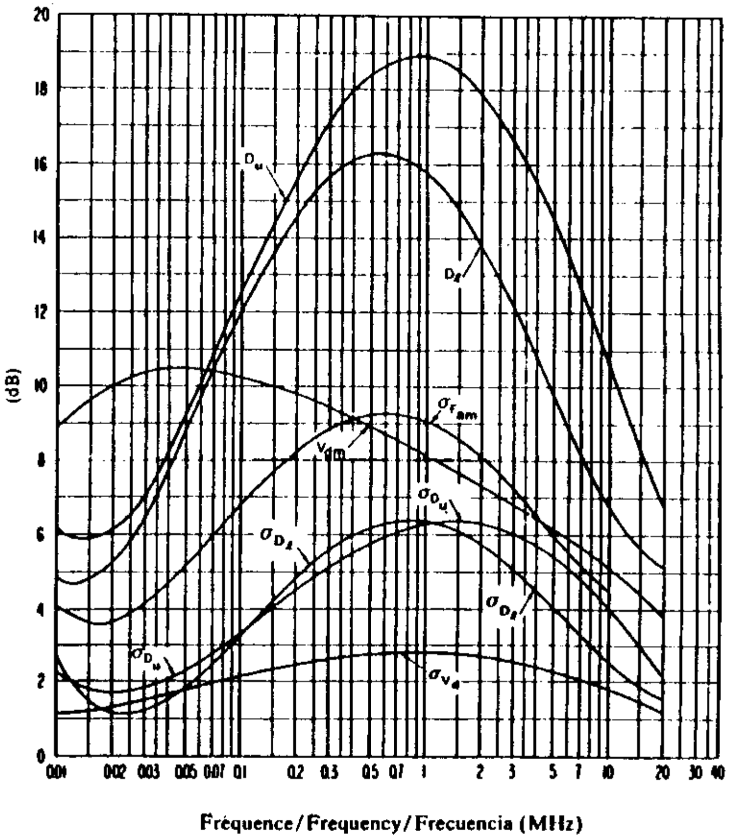

FIGURE 17c – *Données sur la variabilité et le caractère du bruit (Eté; 1200-1600 heure locale)*

FIGURE 17c – *Data on noise variability and character (Summer; 1200-1600 LT)*

FIGURA 17c – *Datos sobre la variabilidad y el carácter del ruido (Verano; 1200-1600 hora local)*

Voir la légende de la Fig. 2c/See legend of Fig. 2c/Véase la leyenda de la fig. 2c

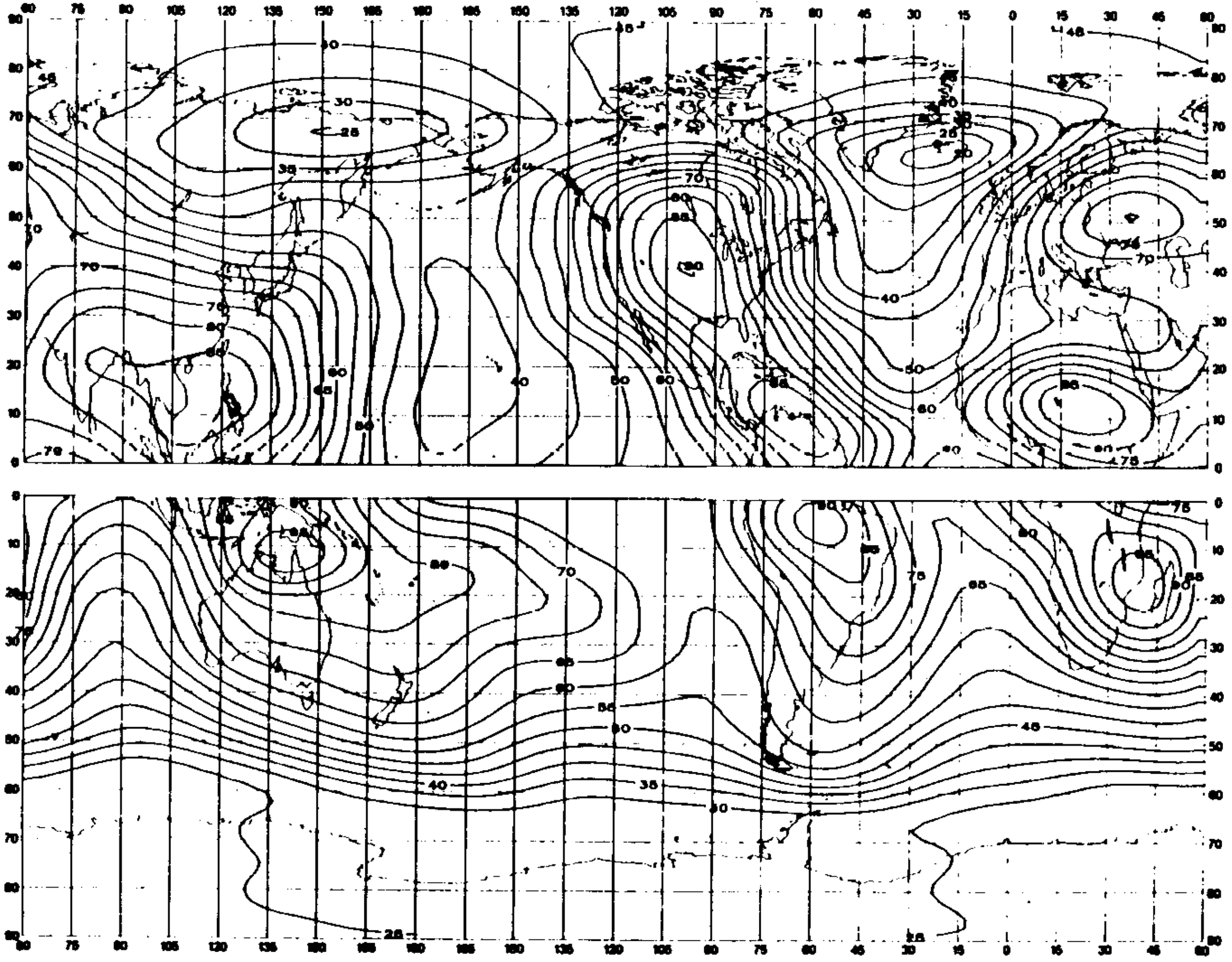
60 75 90 105 120 135 150 165 180 165 150 135 120 105 90 75 60 45 30 15 0 15 30 45 60
90 80 70 60 50 40 30 20 10 0
0 10 20 30 40 50 60 70 80 90
30
25
35
70
80
86
90
40
50
60
75
85
65
45
28

FIGURE 18a – *Valeurs attendues du bruit atmosphérique radioélectrique, $F_{am}$, en dB au-dessus de $kT_0b$ à 1 MHz (Eté; 1600-2000 heure locale)*

FIGURE 18a – *Expected values of atmospheric radio noise, $F_{am}$ (dB above $kT_0b$ at 1 MHz) (Summer; 1600-2000 LT)*

FIGURA 18a – *Valores probables del ruido atmosférico, $F_{am}$, en dB por encima de $kT_0b$ en 1 MHz (Verano; 1600-2000 hora local)*

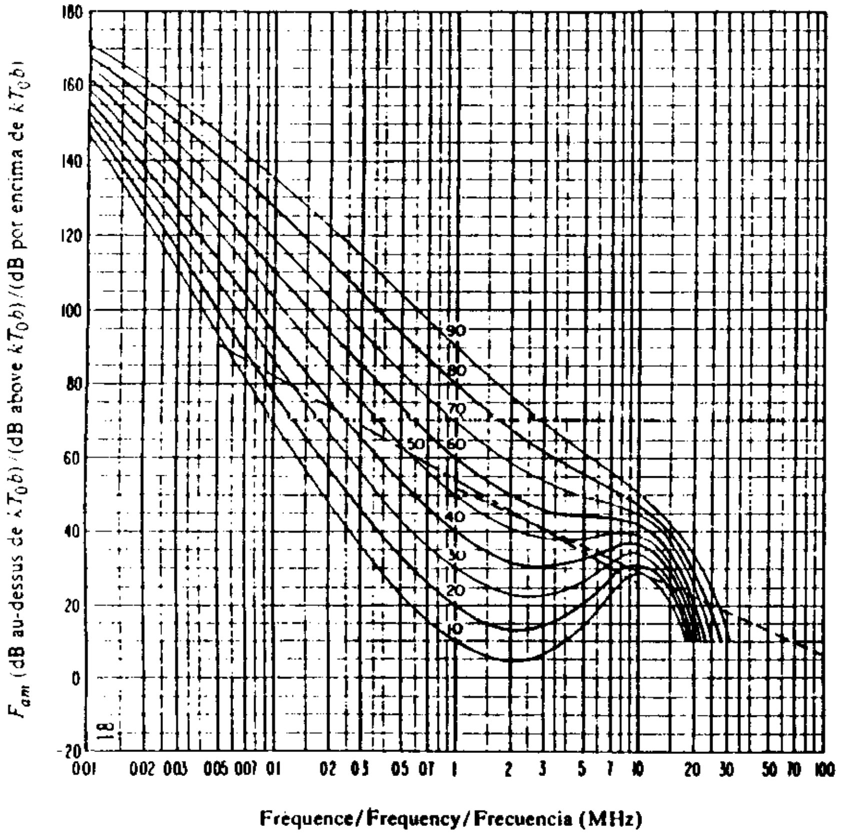

FIGURE 18b – *Variation du bruit radioélectrique en fonction de la fréquence (Eté; 1600-2000 heure locale)*

FIGURE 18b – *Variation of radio noise with frequency (Summer; 1600-2000 LT)*

FIGURA 18b – *Variaciones del ruido radioeléctrico con la frecuencia (Verano; 1600-2000 hora local)*

Voir la légende de la Fig. 2b/See legend of Fig. 2b/Véase la leyenda de la fig. 2b

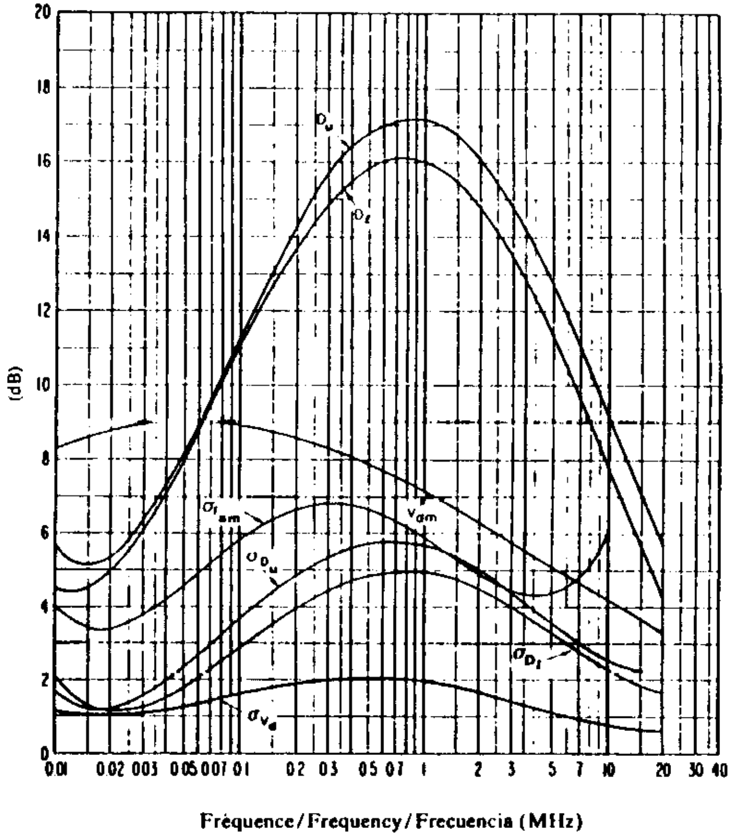

FIGURE 18c – *Données sur la variabilité et le caractère du bruit (Eté; 1600-2000 heure locale)*

FIGURE 18c – *Data on noise variability and character (Summer; 1600-2000 LT)*

FIGURA 18c – *Datos sobre la variabilidad y el carácter del ruido (Verano; 1600-2000 hora local)*

Voir la légende de la Fig. 2c/See legend of Fig. 2c/Véase la leyenda de la fig. 2c

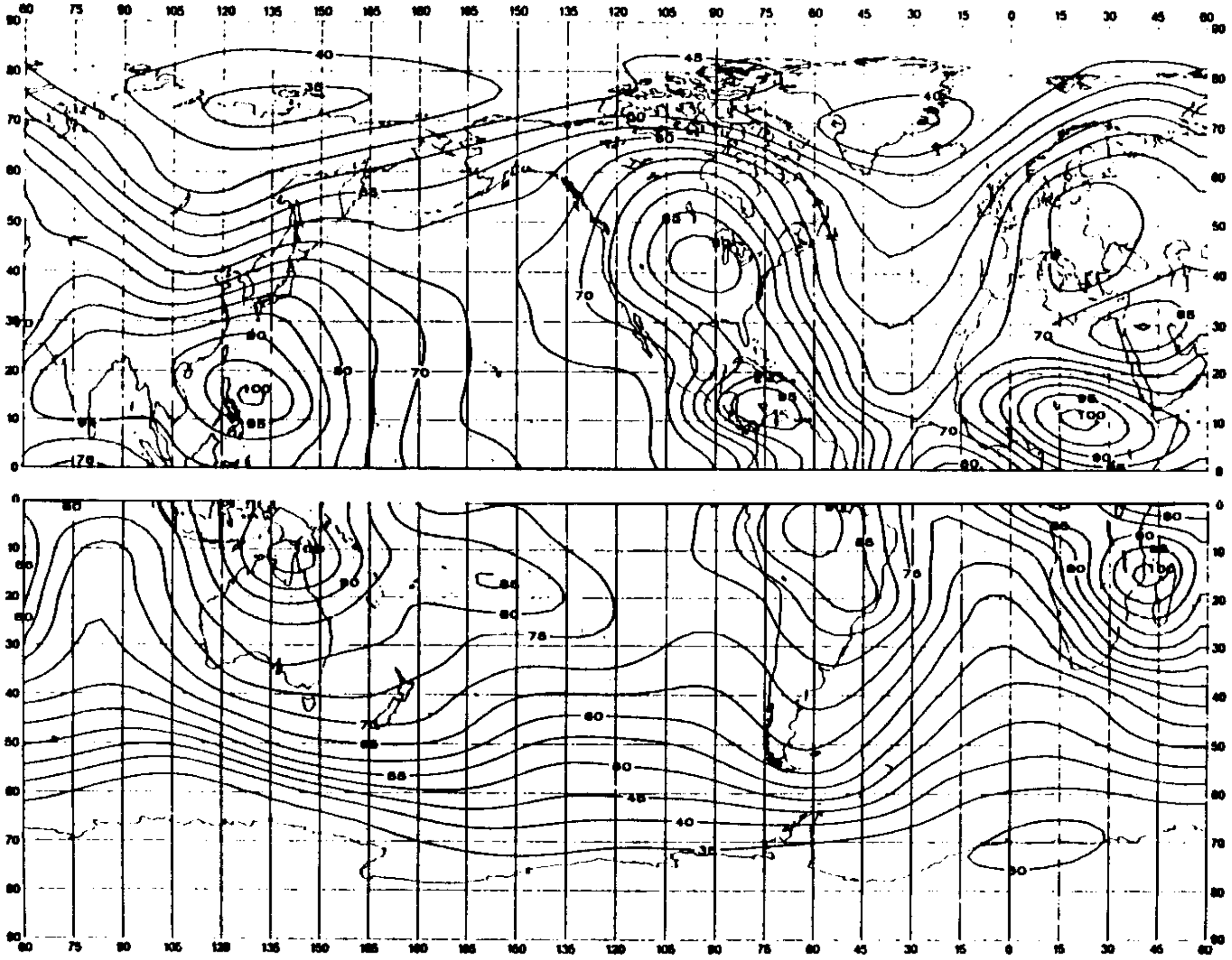
60 75 90 105 120 135 150 165 180 165 150 135 120 105 90 75 60 45 30 15 0 15 30 45 60
90 80 70 60 50 40 30 20 10 0
0 10 20 30 40 50 60 70 80 90
40
35
45
40
60
50
65
70
80
100
95
70
75
65
90
90
85
80
75
60
65
45
40
35
30

FIGURE 19a – *Valeurs attendues du bruit atmosphérique radioélectrique, $F_{am}$, en dB au-dessus de $kT_0b$ à 1 MHz (Eté; 2000-2400 heure locale)*
FIGURE 19a – *Expected values of atmospheric radio noise, $F_{am}$ (dB above $kT_0b$ at 1 MHz) (Summer; 2000-2400 LT)*
FIGURA 19a – *Valores probables del ruido atmosférico, $F_{am}$, en dB por encima de $kT_0b$ en 1 MHz (Verano; 2000-2400 hora local)*

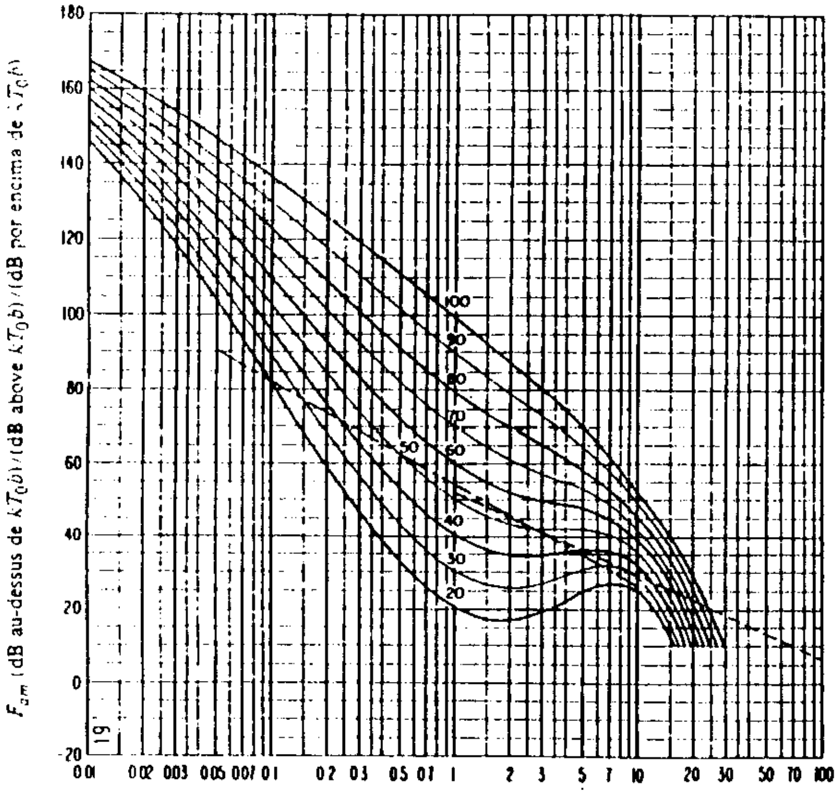

Fréquence/Frequency/Frecuencia (MHz)

FIGURE 19b – *Variation du bruit radioélectrique en fonction de la fréquence (Eté; 2000-2400 heure locale)*

FIGURE 19b – *Variation of radio noise with frequency (Summer; 2000-2400 LT)*

FIGURA 19b – *Variaciones del ruido radioeléctrico con la frecuencia (Verano; 2000-2400 hora local)*

Voir la légende de la Fig. 2b/See legend of Fig. 2b/Véase la leyenda de la fig. 2b

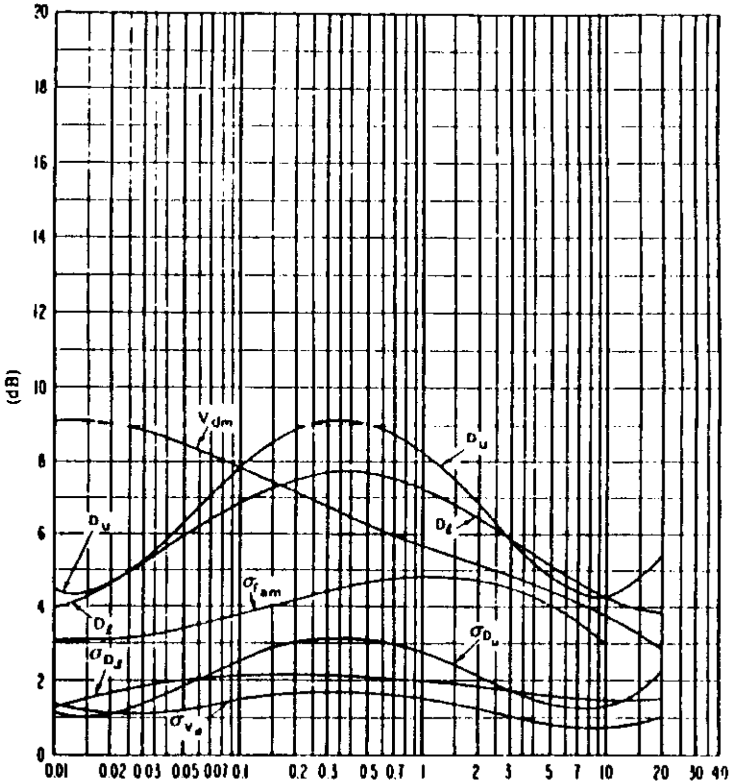

Fréquence/Frequency/Frecuencia (MHz)

FIGURE 19c – *Données sur la variabilité et le caractère du bruit (Eté; 2000-2400 heure locale)*

FIGURE 19c – *Data on noise variability and character (Summer; 2000-2400 LT)*

FIGURA 19c – *Datos sobre la variabilidad y el carácter del ruido (Verano; 2000-2400 hora local)*

Voir la légende de la Fig. 2c/See legend of Fig. 2c/Véase la leyenda de la fig. 2c

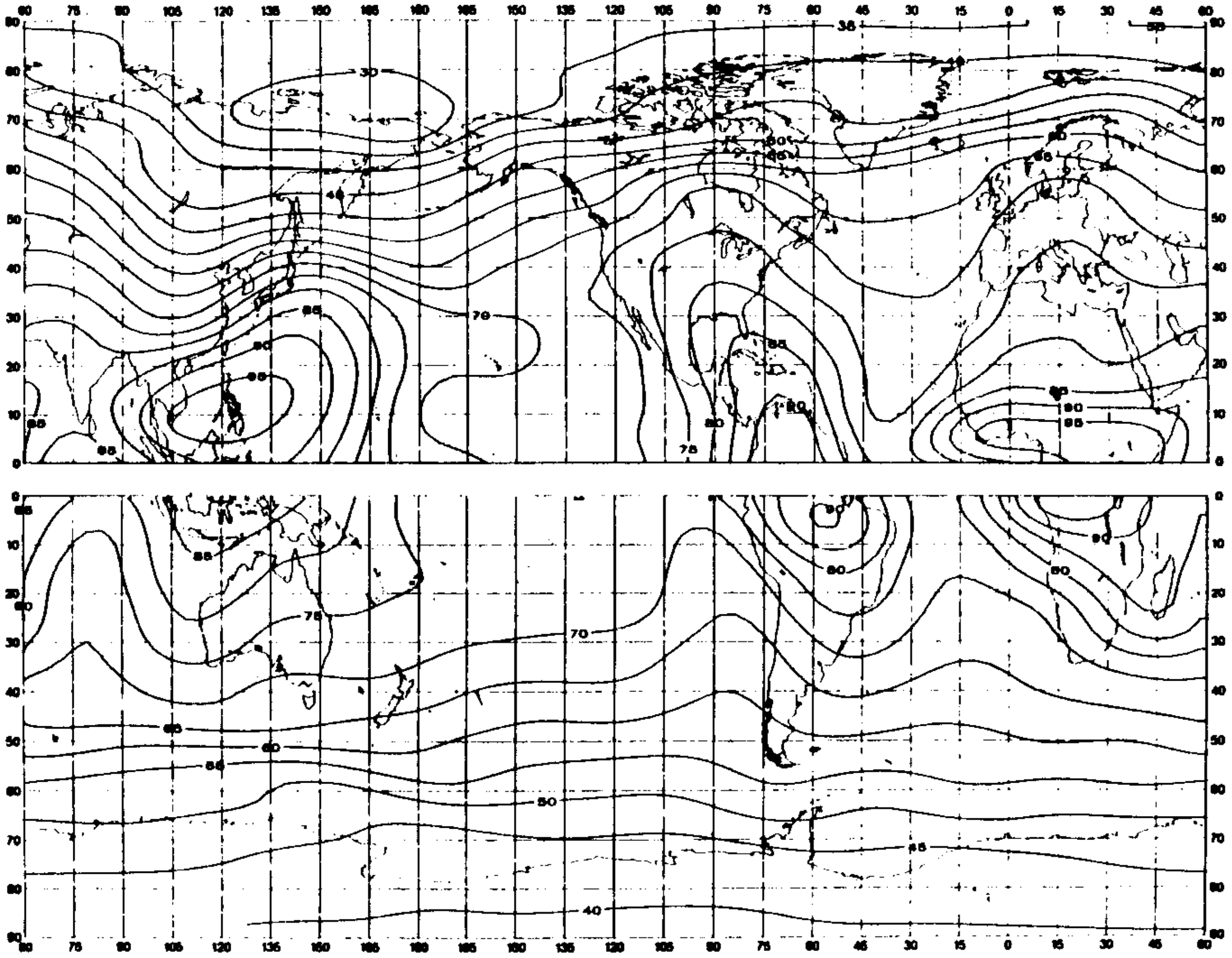
60
75
90
105
120
135
150
165
180
165
150
135
120
105
90
75
60
45
30
15
0
15
30
45
60
90
80
70
60
50
40
30
20
10
0
30
36
40
50
65
70
75
80
85
90

FIGURE 20a – *Valeurs attendues du bruit atmosphérique radioélectrique, $F_{am}$, en dB au-dessus de $kT_0b$ à 1 MHz (Automne; 0000-0400 heure locale)*
FIGURE 20a – *Expected values of atmospheric radio noise, $F_{am}$ (dB above $kT_0b$ at 1 MHz) (Autumn; 0000-0400 LT)*
FIGURA 20a – *Valores probables del ruido atmosférico, $F_{am}$, en dB por encima de $kT_0b$ en 1 MHz (Otoño; 0000-0400 hora local)*

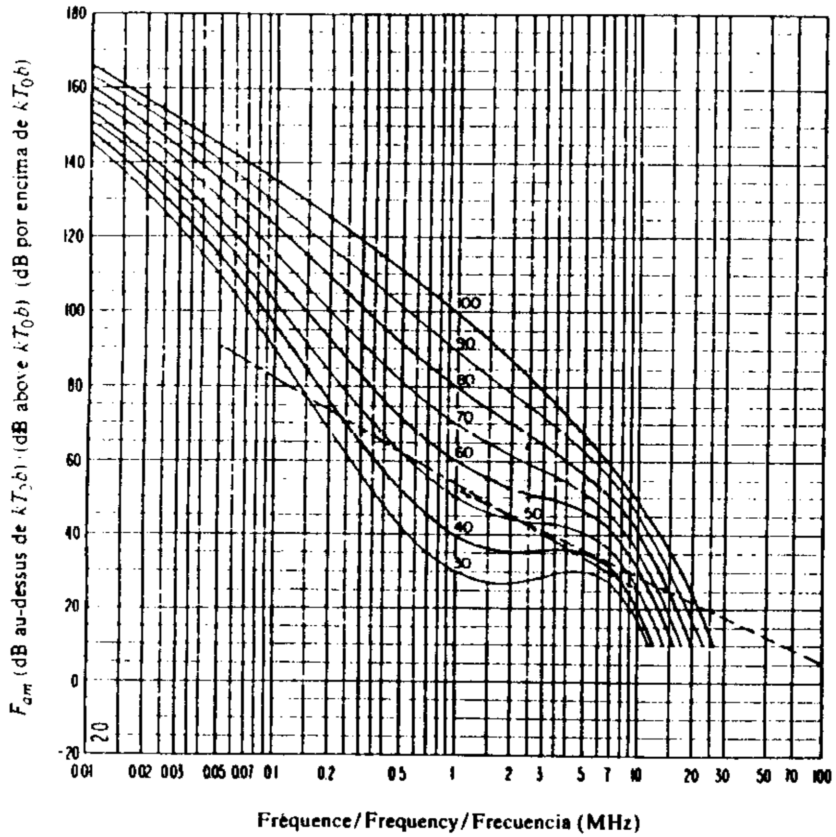

FIGURE 20b – *Variation du bruit radioélectrique en fonction de la fréquence (Automne; 0000-0400 heure locale)*

FIGURE 20b – *Variation of radio noise with frequency (Autumn; 0000-0400 LT)*

FIGURA 20b – *Variaciones del ruido radioeléctrico con la frecuencia (Otoño; 0000-0400 hora local)*

Voir la legende de la Fig. 2b/ See legend of Fig. 2b/ Véase la leyenda de la fig. 2b

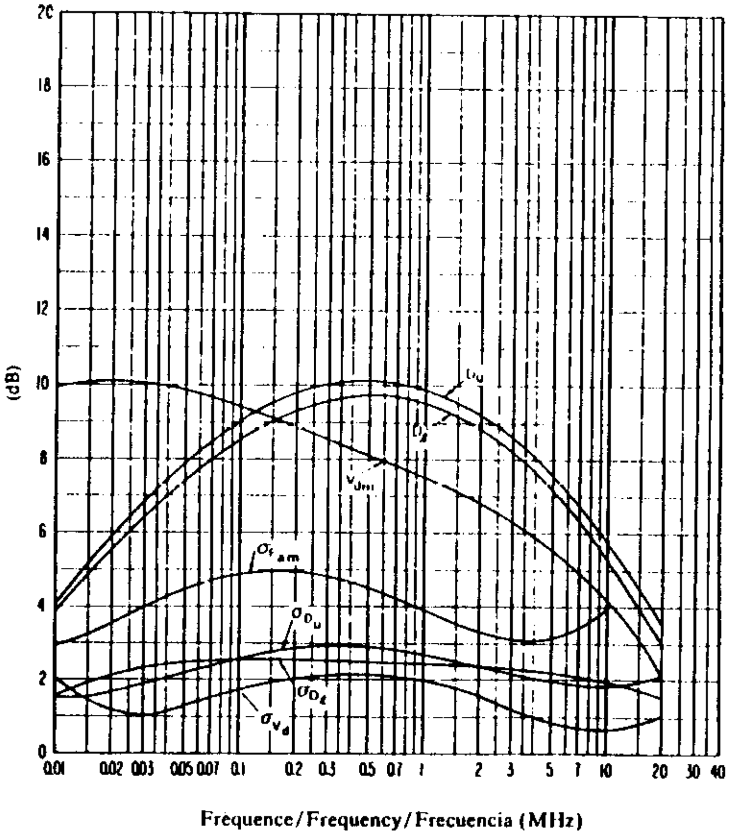

FIGURE 20c – *Données sur la variabilité et le caractère du bruit (Automne; 0000-0400 heure locale)*

FIGURE 20c – *Data on noise variability and character (Autumn; 0000-0400 LT)*

FIGURA 20c – *Datos sobre la variabilidad y el carácter del ruido (Otoño; 0000-0400 hora local)*

Voir la légende de la Fig. 2c/ See legend of Fig. 2c/ Véase la leyenda de la fig. 2c

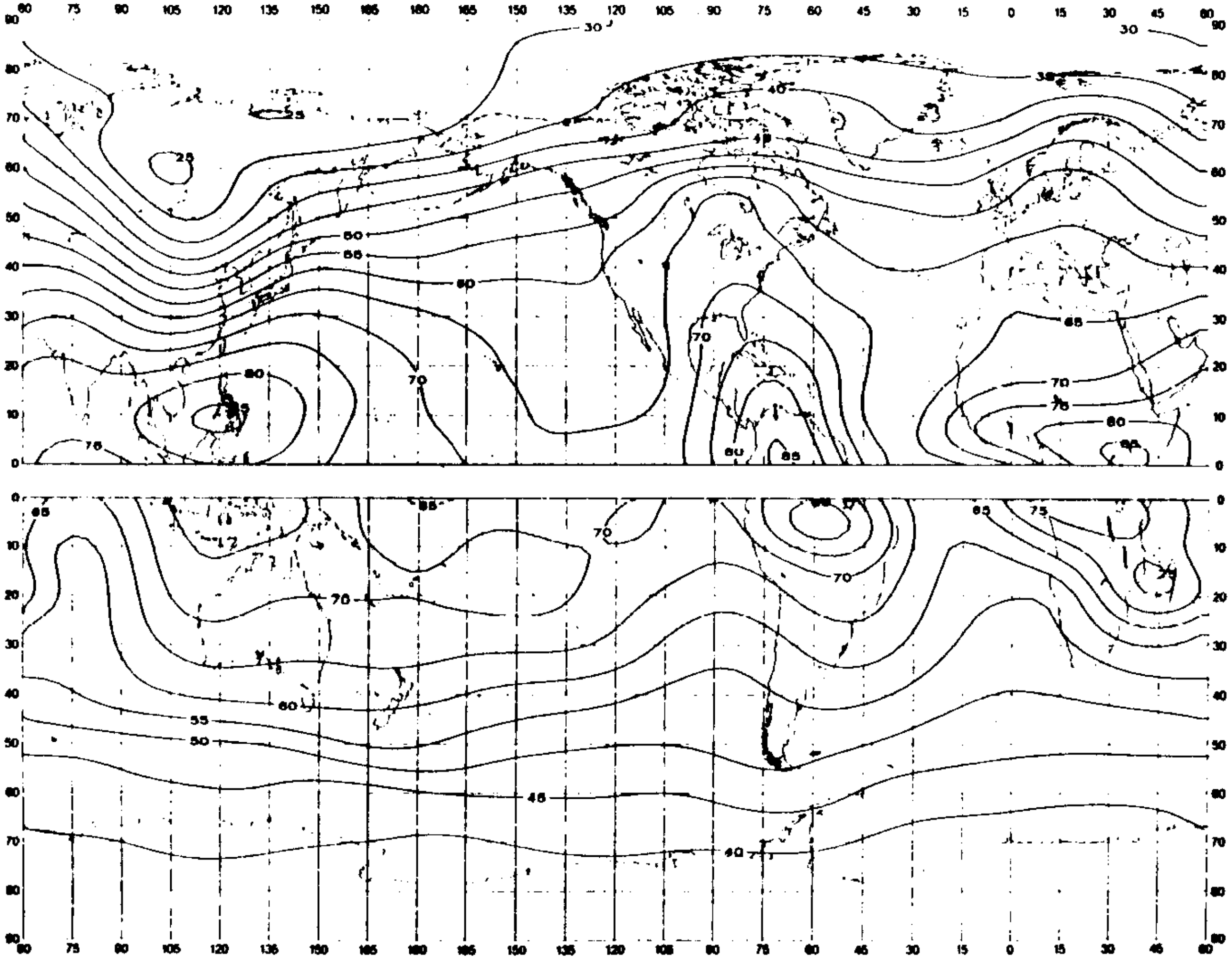

FIGURE 21a – *Valeurs attendues du bruit atmosphérique radioélectrique, $F_{am}$, en dB au-dessus de $kT_0b$ à 1 MHz (Automne; 0400-0800 heure locale)*

FIGURE 21a – *Expected values of atmospheric radio noise, $F_{am}$ (dB above $kT_0b$ at 1 MHz) (Autumn; 0400-0800 LT)*

FIGURA 21a – *Valores probables del ruido atmosférico, $F_{am}$, en dB por encima de $kT_0b$ en 1 MHz (Otoño; 0400-0800 hora local)*

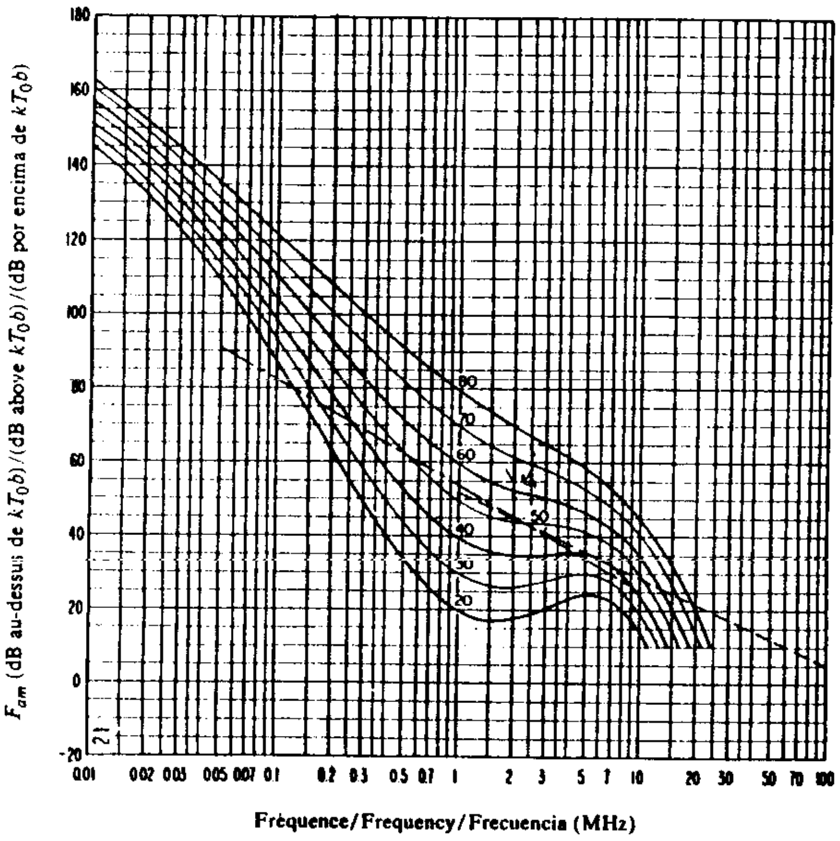

FIGURE 21b – *Variation du bruit radioélectrique en fonction de la fréquence (Automne; 0400-0800 heure locale)*

FIGURE 21b – *Variation of radio noise with frequency (Autumn; 0400-0800 LT)*

FIGURA 21b – *Variaciones del ruido radioeléctrico con la frecuencia (Otoño; 0400-0800 hora local)*

Voir la légende de la Fig. 2b/See legend of Fig. 2b/Véase la leyenda de la fig. 2b

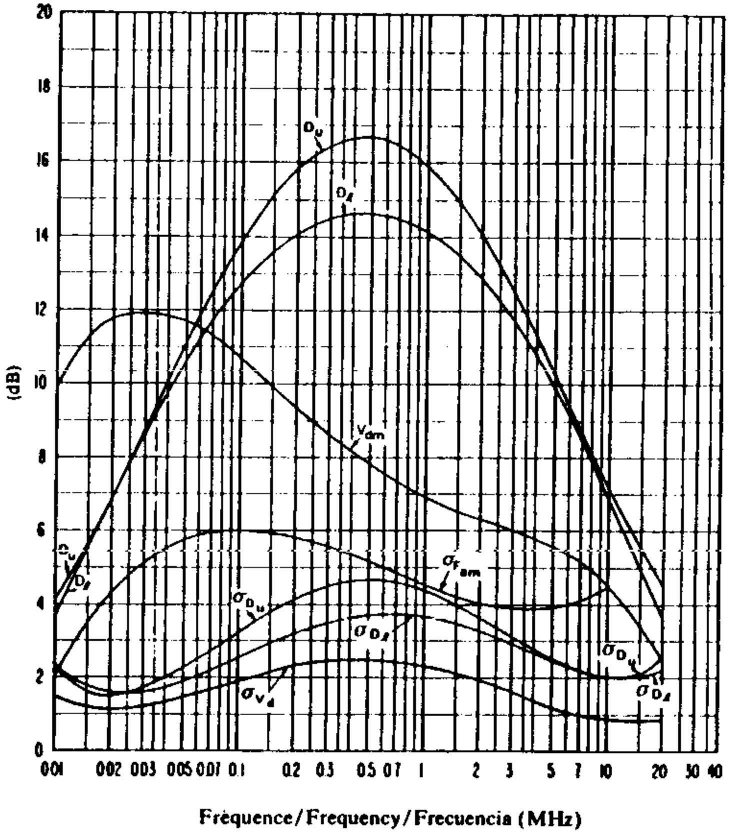

FIGURE 21c – *Données sur la variabilité et le caractère du bruit (Automne; 0400-0800 heure locale)*

FIGURE 21c – *Data on noise variability and character (Autumn; 0400-0800 LT)*

FIGURA 21c – *Datos sobre la variabilidad y el carácter del ruido (Otoño; 0400-0800 hora local)*

Voir la légende de la Fig. 2c/See legend of Fig. 2c/Véase la leyenda de la fig. 2c

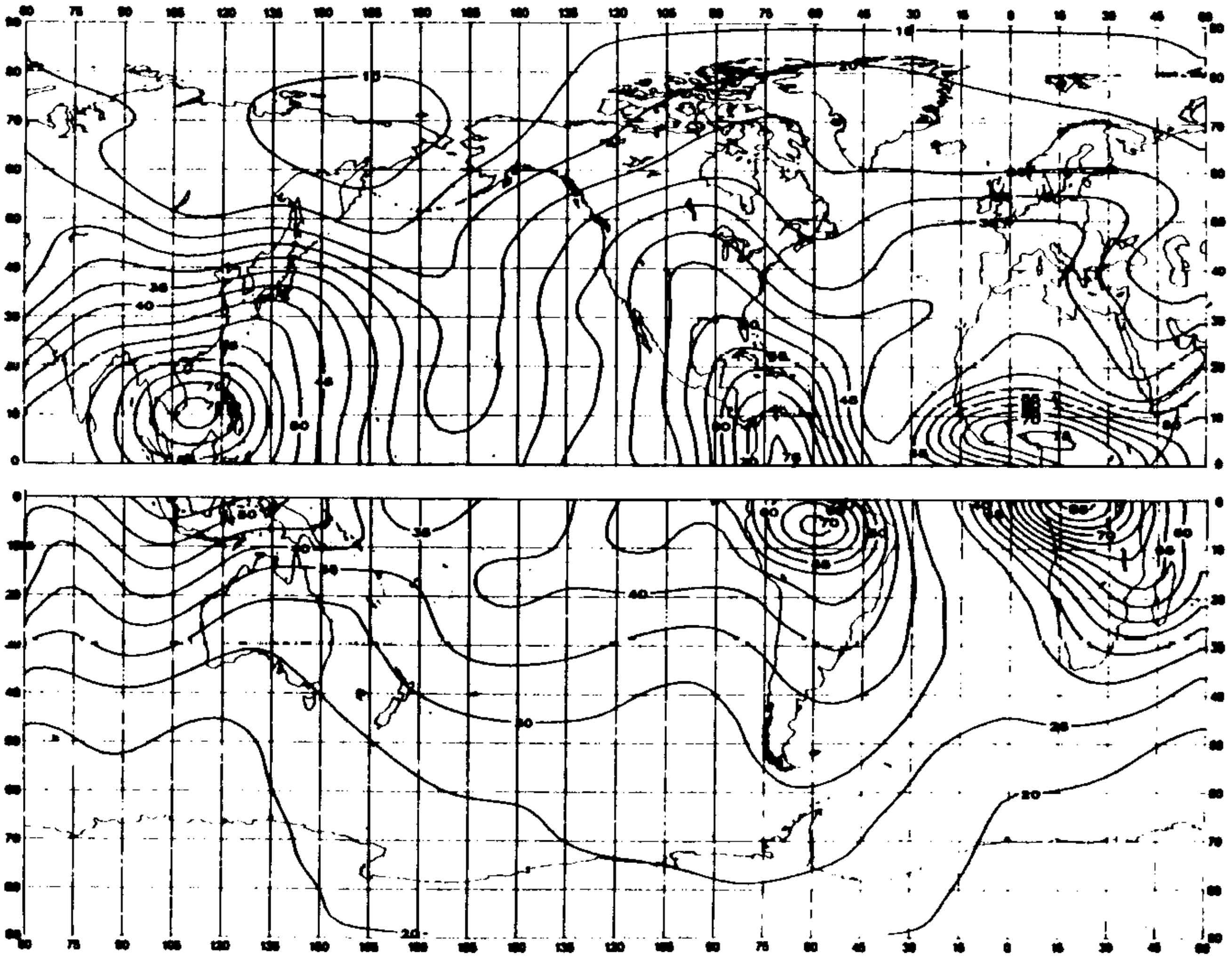
90
75
60
45
30
15
0
10
20
30
40
50
60
70
80
90
60
75
90
105
120
135
150
165
180
165
150
135
120
105
90
75
60
45
30
15
0
15
30
45
60
10
20
30
40
60
70
75
80

FIGURE 22a – *Valeurs attendues du bruit atmosphérique radioélectrique, $F_{am}$, en dB au-dessus de $kT_0b$ à 1 MHz (Automne; 0800-1200 heure locale)*
FIGURE 22a – *Expected values of atmospheric radio noise, $F_{am}$ (dB above $kT_0b$ at 1 MHz) (Autumn; 0800-1200 LT)*
FIGURA 22a – *Valores probables del ruido atmosférico, $F_{am}$, en dB por encima de $kT_0b$ en 1 MHz (Otoño; 0800-1200 hora local)*

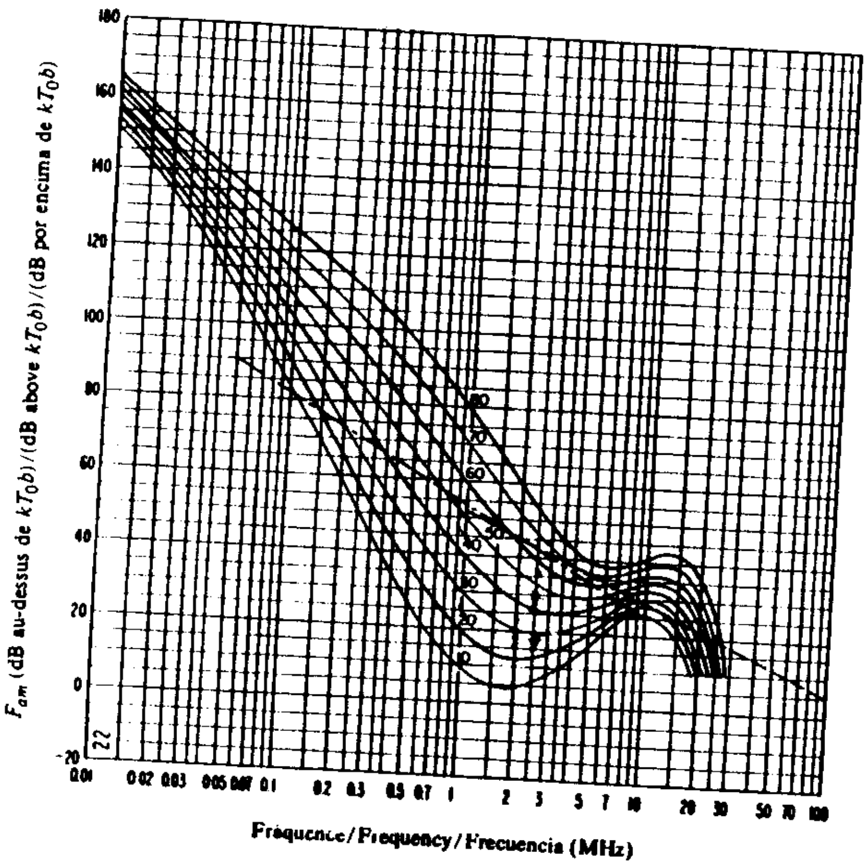

FIGURE 22b – *Variation du bruit radioélectrique en fonction de la fréquence (Automne; 0800-1200 heure locale)*

FIGURE 22b – *Variation of radio noise with frequency (Autumn; 0800-1200 LT)*

FIGURA 22b – *Variaciones del ruido radioeléctrico con la frecuencia (Otoño; 0800-1200 hora local)*

Voir la légende de la Fig. 2b/See legend of Fig. 2b/Véase la leyenda de la fig. 2b

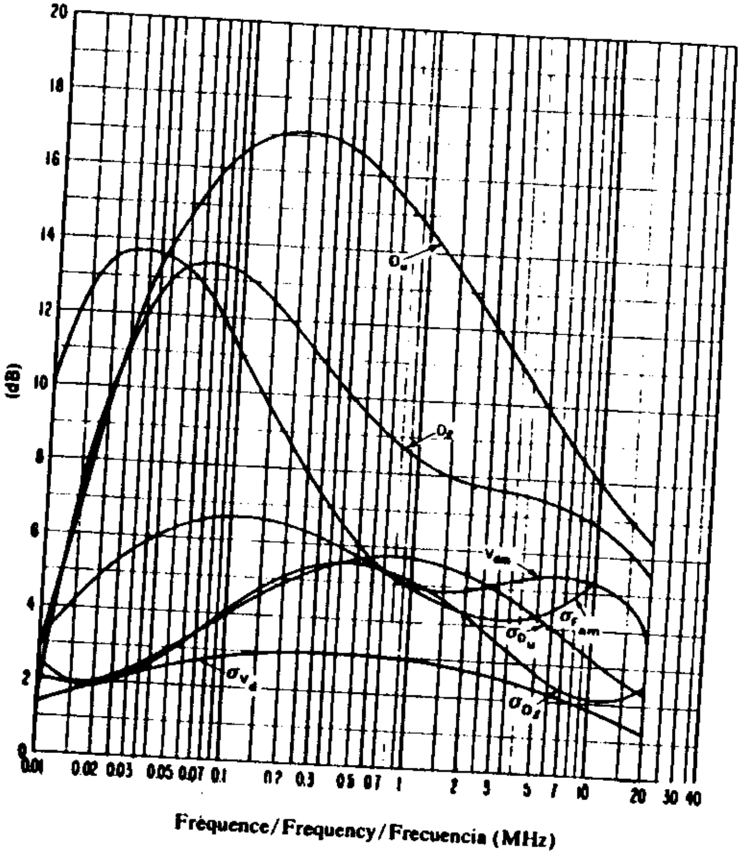

FIGURE 22c – *Données sur la variabilité et le caractère du bruit (Automne; 0800-1200 heure locale)*

FIGURE 22c – *Data on noise variability and character (Autumn; 0800-1200 LT)*

FIGURA 22c – *Datos sobre la variabilidad y el carácter del ruido (Otoño; 0800-1200 hora local)*

Voir la légende de la Fig. 2c/See legend of Fig. 2c/Véase la leyenda de la fig. 2c

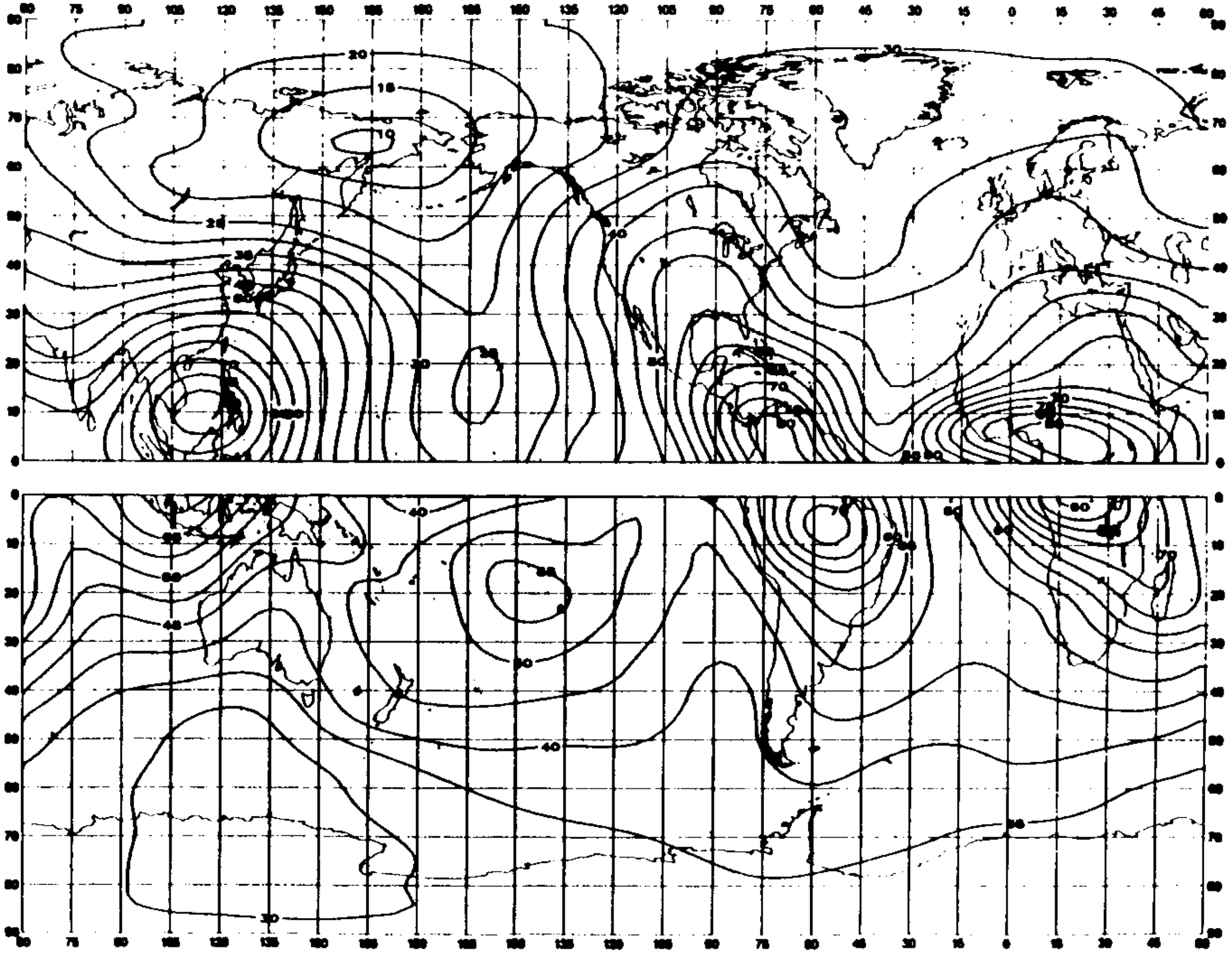
60
75
90
105
120
135
150
165
180
165
150
135
120
105
90
75
60
45
30
15
0
15
30
45
60
90
80
70
60
50
40
30
20
10
0
20
18
10
24
36
40
30
50
60
70
80
40
30

FIGURE 23a — *Valeurs attendues du bruit atmosphérique radioélectrique, $F_{am}$, en dB au-dessus de $kT_0b$ à 1 MHz (Automne; 1200-1600 heure locale)*

FIGURE 23a *Expected values of atmospheric radio noise, $F_{am}$ (dB above $kT_0b$ at 1 MHz) (Autumn; 1200-1600 L.T)*

FIGURA 23a *Valores probables del ruido atmosférico, $F_{am}$, en dB por encima de $kT_0b$ en 1 MHz (Otoño; 1200-1600 hora local)*

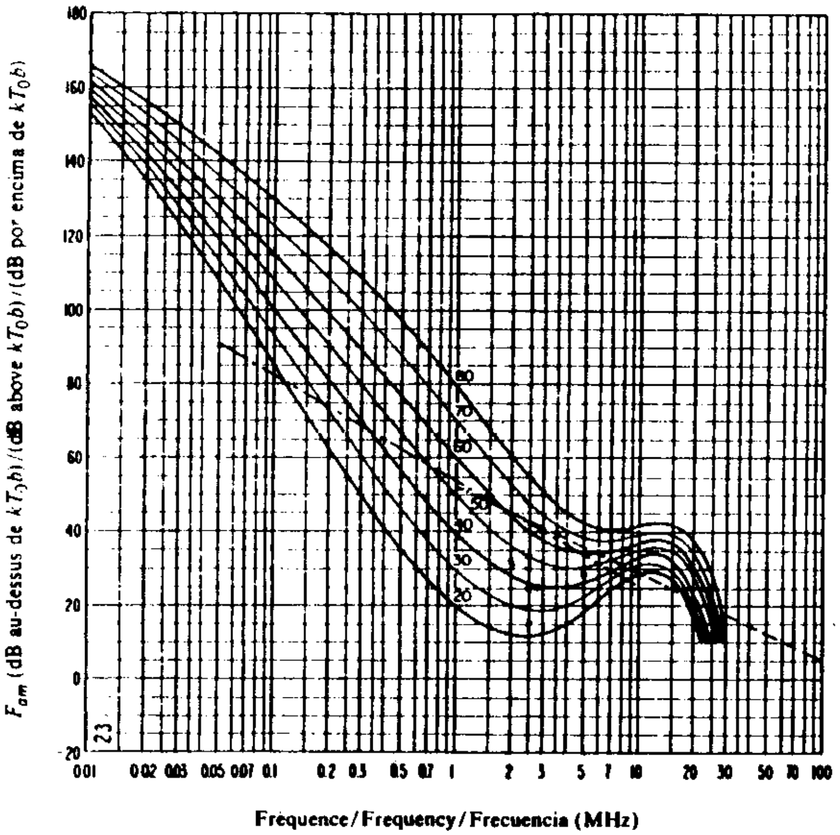

FIGURE 23b – *Variation du bruit radioélectrique en fonction de la fréquence (Automne; 1200-1600 heure locale)*

FIGURE 23b – *Variation of radio noise with frequency (Autumn; 1200-1600 LT)*

FIGURA 23b – *Variaciones del ruido radioeléctrico con la frecuencia (Otoño; 1200-1600 hora local)*

Voir la légende de la Fig. 2b/See legend of Fig. 2b/Véase la leyenda de la fig. 2b

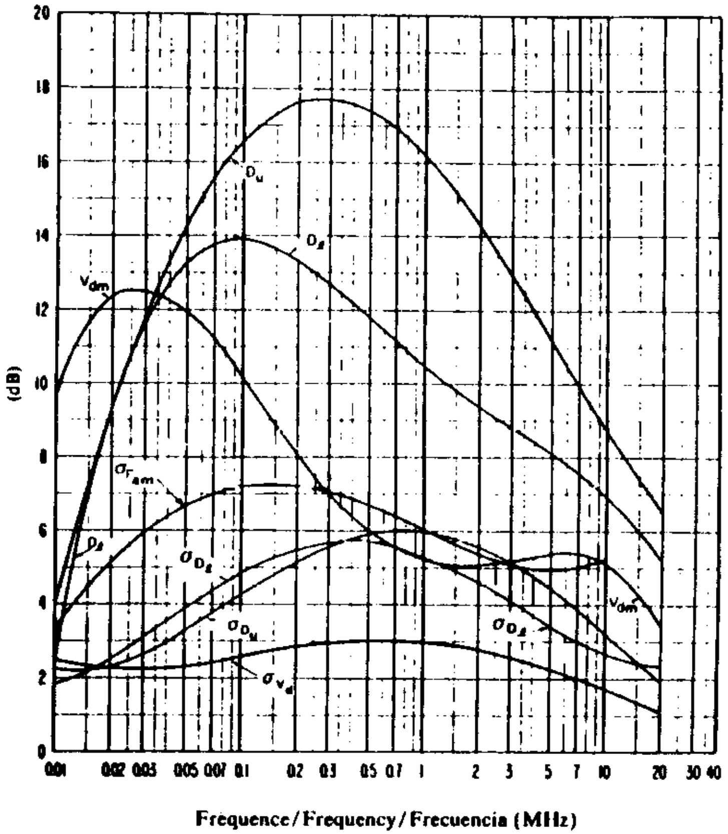

FIGURE 23c – *Données sur la variabilité et le caractère du bruit (Automne; 1200-1600 heure locale)*

FIGURE 23c – *Data on noise variability and character (Autumn; 1200-1600 LT)*

FIGURA 23c – *Datos sobre la variabilidad y el carácter del ruido (Otoño; 1200-1600 hora local)*

Voir la légende de la Fig. 2c/See legend of Fig. 2c/Véase la leyenda de la fig. 2c

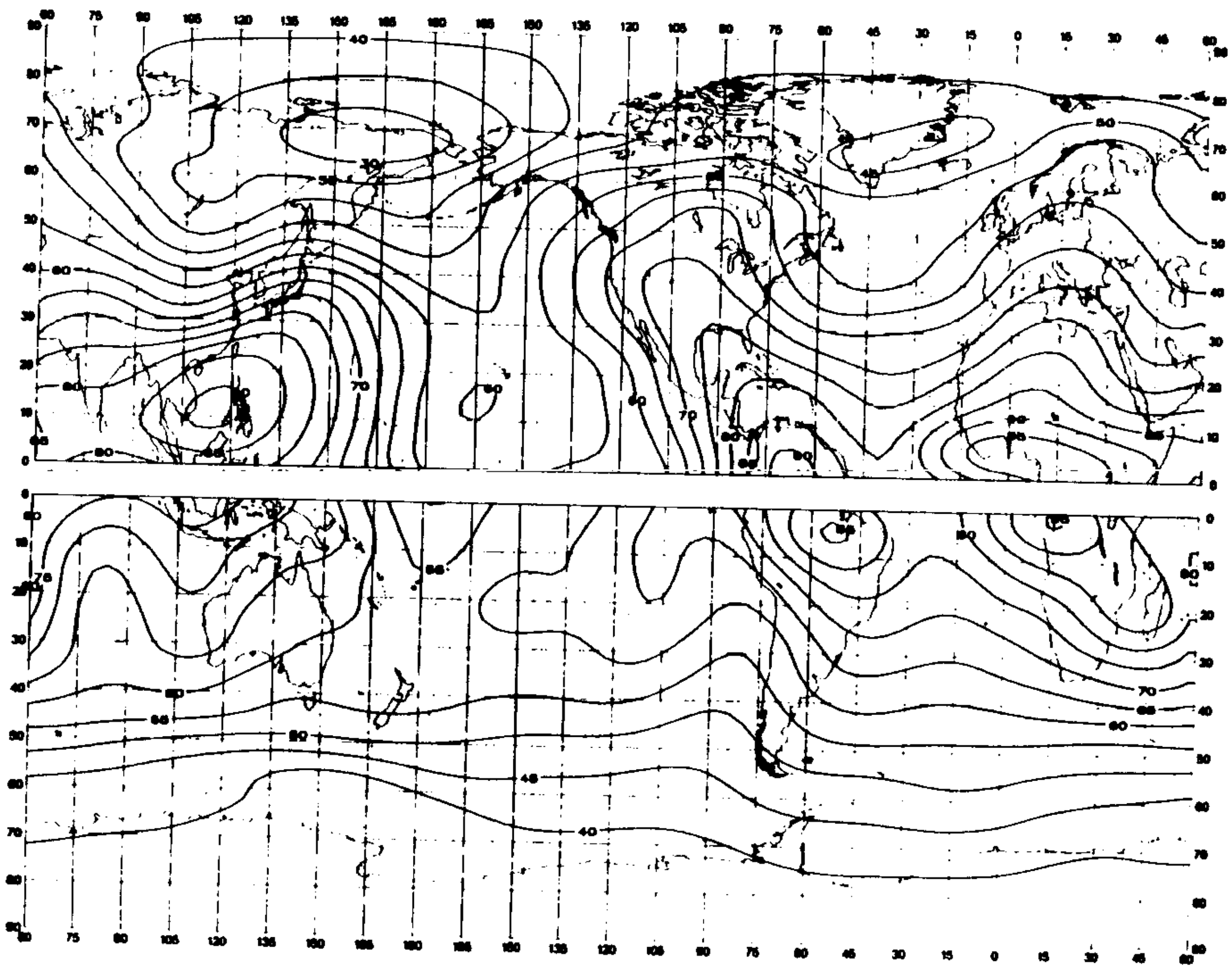
60
75
90
105
120
135
150
165
180
165
150
135
120
105
90
75
60
45
30
15
0
15
30
45
60
90
80
70
60
50
40
30
20
10
0
10
20
30
40
50
60
70
80
90
40
30
50
60
70
80
65
70
60
40

FIGURE 24a – *Valeurs attendues du bruit atmosphérique radioélectrique, $F_{am}$, en dB au-dessus de $kT_0b$ à 1 MHz (Automne; 1600-2000 heure locale)*

FIGURE 24a – *Expected values of atmospheric radio noise, $F_{am}$ (dB above $kT_0b$ at 1 MHz) (Autumn; 1600-2000 LT)*

FIGURA 24a – *Valores probables del ruido atmosférico, $F_{am}$, en dB por encima de $kT_0b$ en 1 MHz (Otoño; 1600-2000 hora local)*

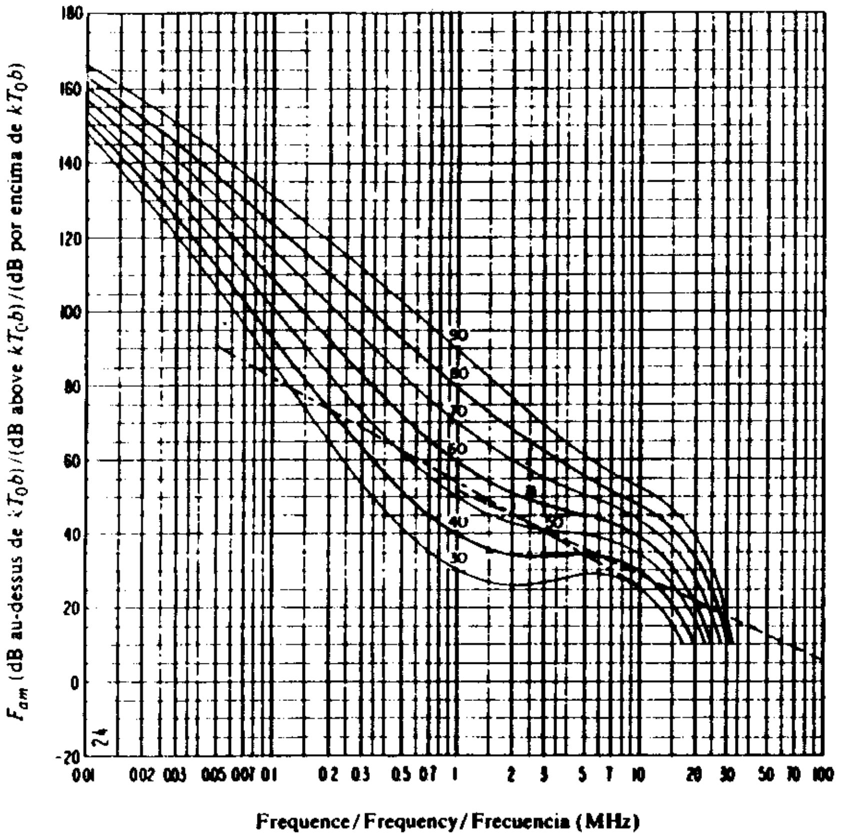

FIGURE 24b – *Variation du bruit radioélectrique en fonction de la fréquence (Automne; 1600-2000 heure locale)*

FIGURE 24b – *Variation of radio noise with frequency (Autumn; 1600-2000 LT)*

FIGURA 24b – *Variaciones del ruido radioeléctrico con la frecuencia (Otoño; 1600-2000 hora local)*

Voir la legende de la Fig. 2b/See legend of Fig. 2b/Vease la leyenda de la fig. 2b

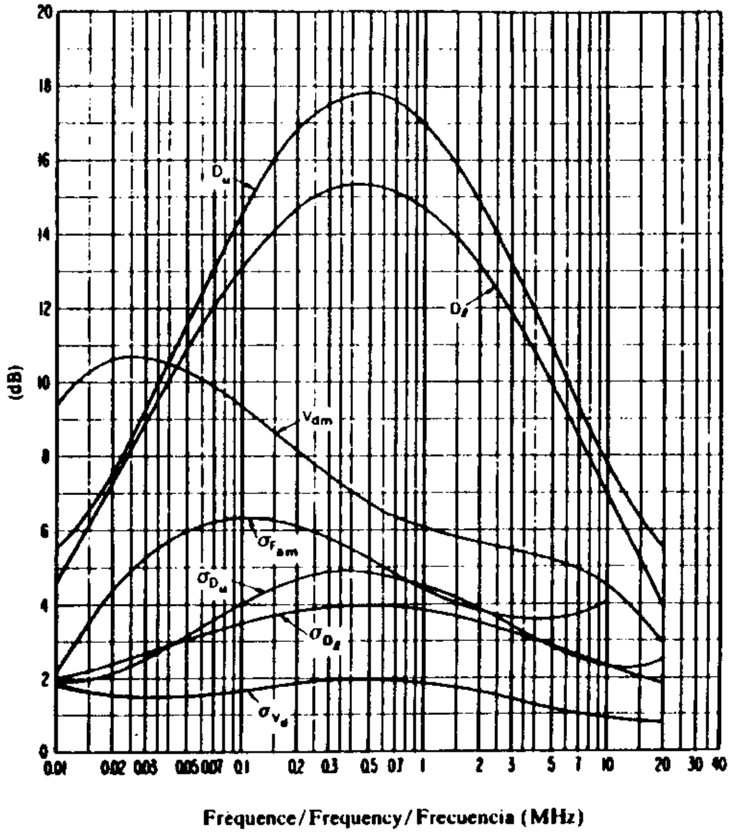

FIGURE 24c – *Données sur la variabilité et le caractère du bruit (Automne; 1600-2000 heure locale)*

FIGURE 24c – *Data on noise variability and character (Autumn; 1600-2000 LT)*

FIGURA 24c – *Datos sobre la variabilidad y el carácter del ruido (Otoño; 1600-2000 hora local)*

Voir la legende de la Fig. 2c/See legend of Fig. 2c/Vease la leyenda de la fig. 2c

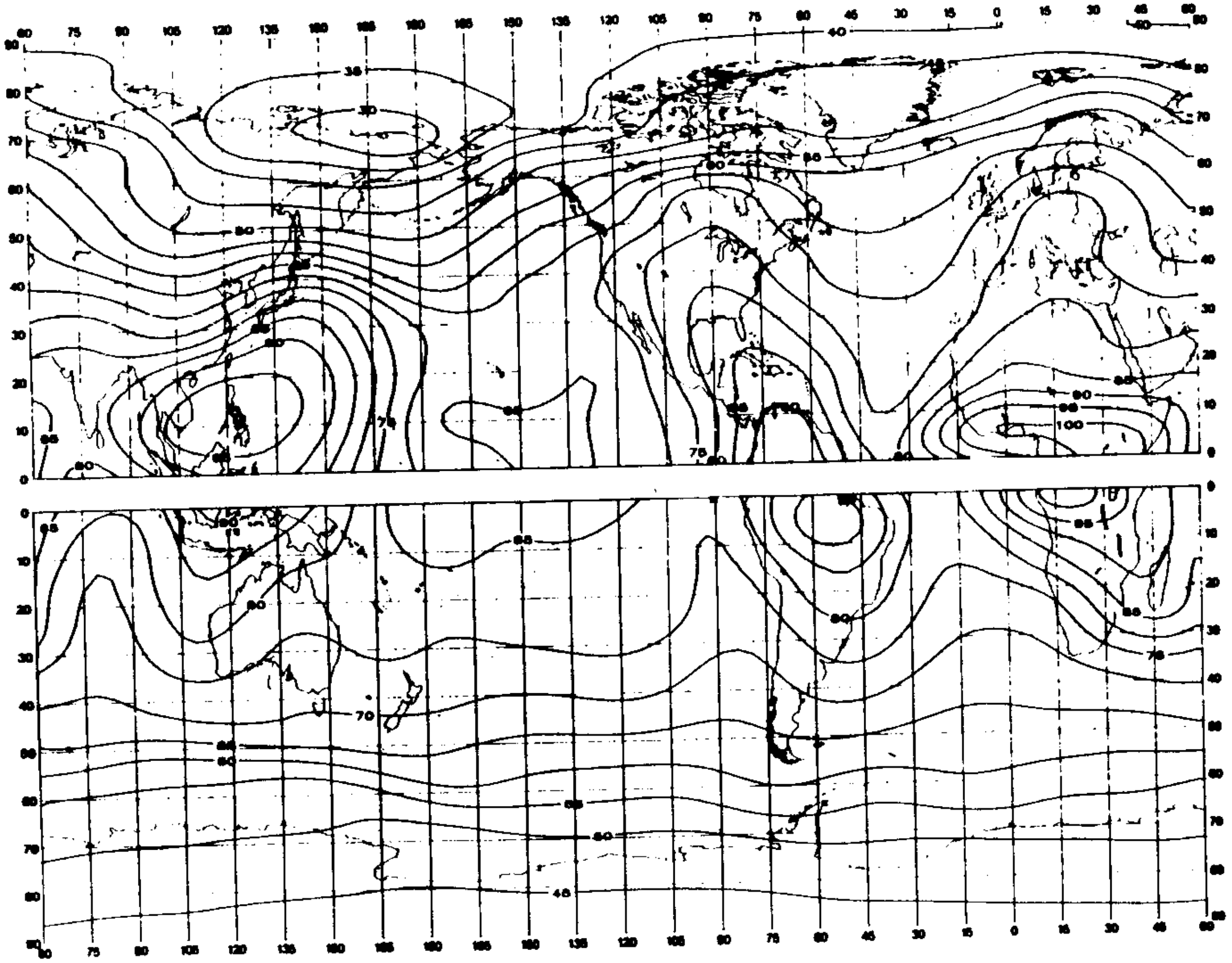
60
75
90
105
120
135
150
165
180
165
150
135
120
105
90
75
60
45
30
15
0
15
30
45
60
90
80
70
60
50
40
30
20
10
0
40
36
30
45
80
85
75
90
95
100
65
70
60
50
46

FIGURE 25a Valeurs attendues du bruit atmosphérique radioélectrique, $F_{am}$, en dB au dessus de $kT_0b$ à 1 MHz (Automne; 2000-2400 heure locale)

FIGURE 25a Expected values of atmospheric radio noise, $F_{am}$ (dB above $kT_0b$ at 1 MHz) (Autumn; 2000-2400 LT)

FIGURA 25a Valores probables del ruido atmosférico, $F_{am}$, en dB por encima de $kT_0b$ en 1 MHz (Otoño; 2000-2400 hora local)

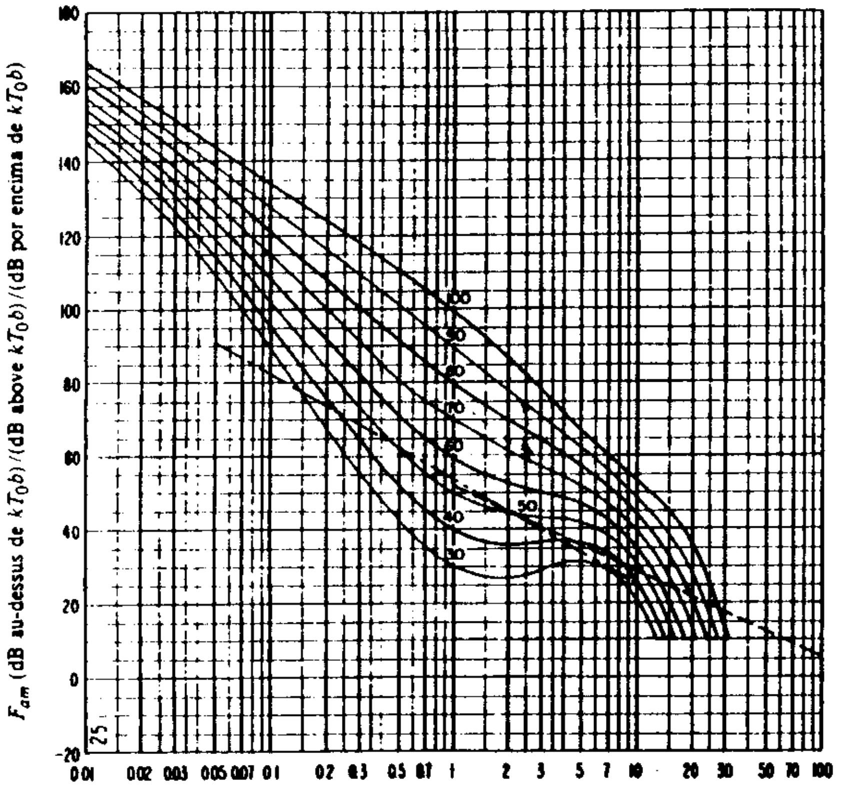

FIGURE 25b – *Variation du bruit radioélectrique en fonction de la fréquence (Automne; 2000-2400 heure locale)*

FIGURE 25b – *Variation of radio noise with frequency (Autumn; 2000-2400 LT)*

FIGURA 25b – *Variaciones del ruido radioeléctrico con la frecuencia (Otoño; 2000-2400 hora local)*

Voir la légende de la Fig. 2b/See legend of Fig. 2b/Véase la leyenda de la fig. 2b

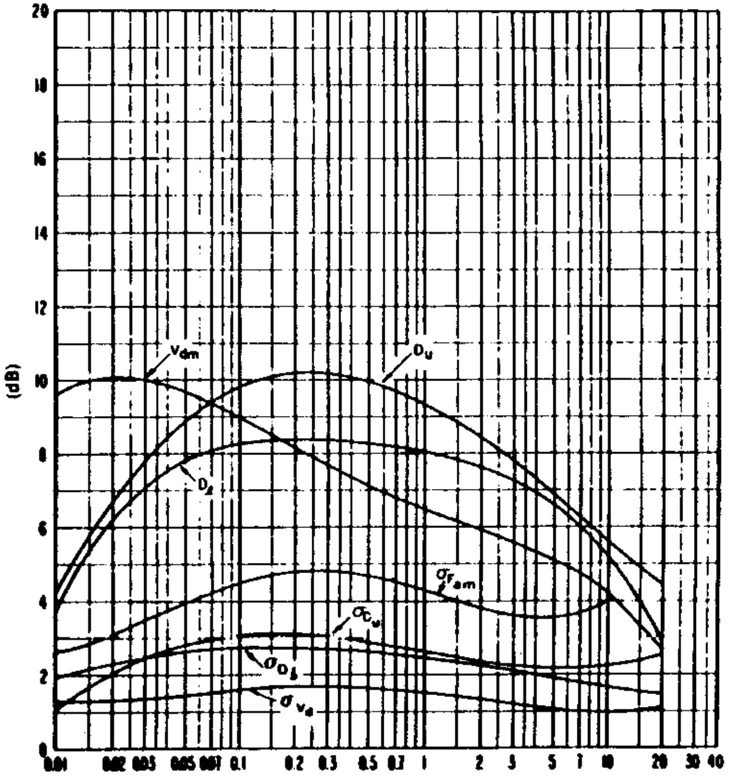

FIGURE 25c – *Données sur la variabilité et le caractère du bruit (Automne; 2000-2400 heure locale)*

FIGURE 25c – *Data on noise variability and character (Autumn; 2000-2400 LT)*

FIGURA 25c – *Datos sobre la variabilidad y el carácter del ruido (Otoño; 2000-2400 hora local)*

Voir la légende de la Fig. 2c/See legend of Fig. 2c/Véase la leyenda de la fig. 2c

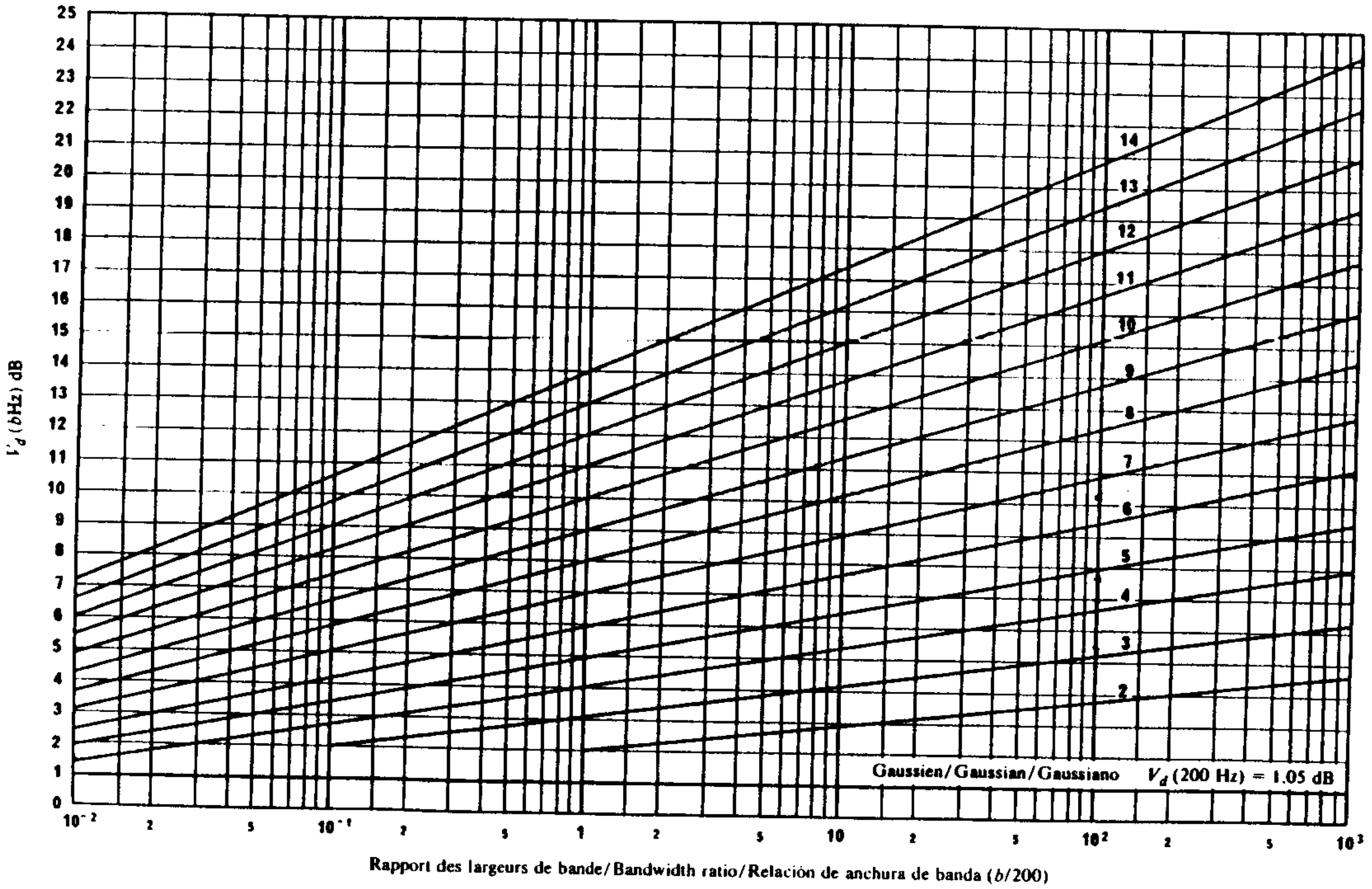

FIGURE 26 – *Conversion des valeurs de $V_d$ valables pour une largeur de bande de 200 Hz, $V_{dm}$, en valeurs de $V_d$ valables pour d'autres largeurs de bande, b*

FIGURE 26 *Translation of a 200 Hz bandwidth $V_d$, $V_{dm}$, to other bandwidths, b*

FIGURA 26 *Conversión de $V_d$ para una anchura de banda de 200 Hz, $V_{dm}$, en valores para otras anchuras de banda, b*

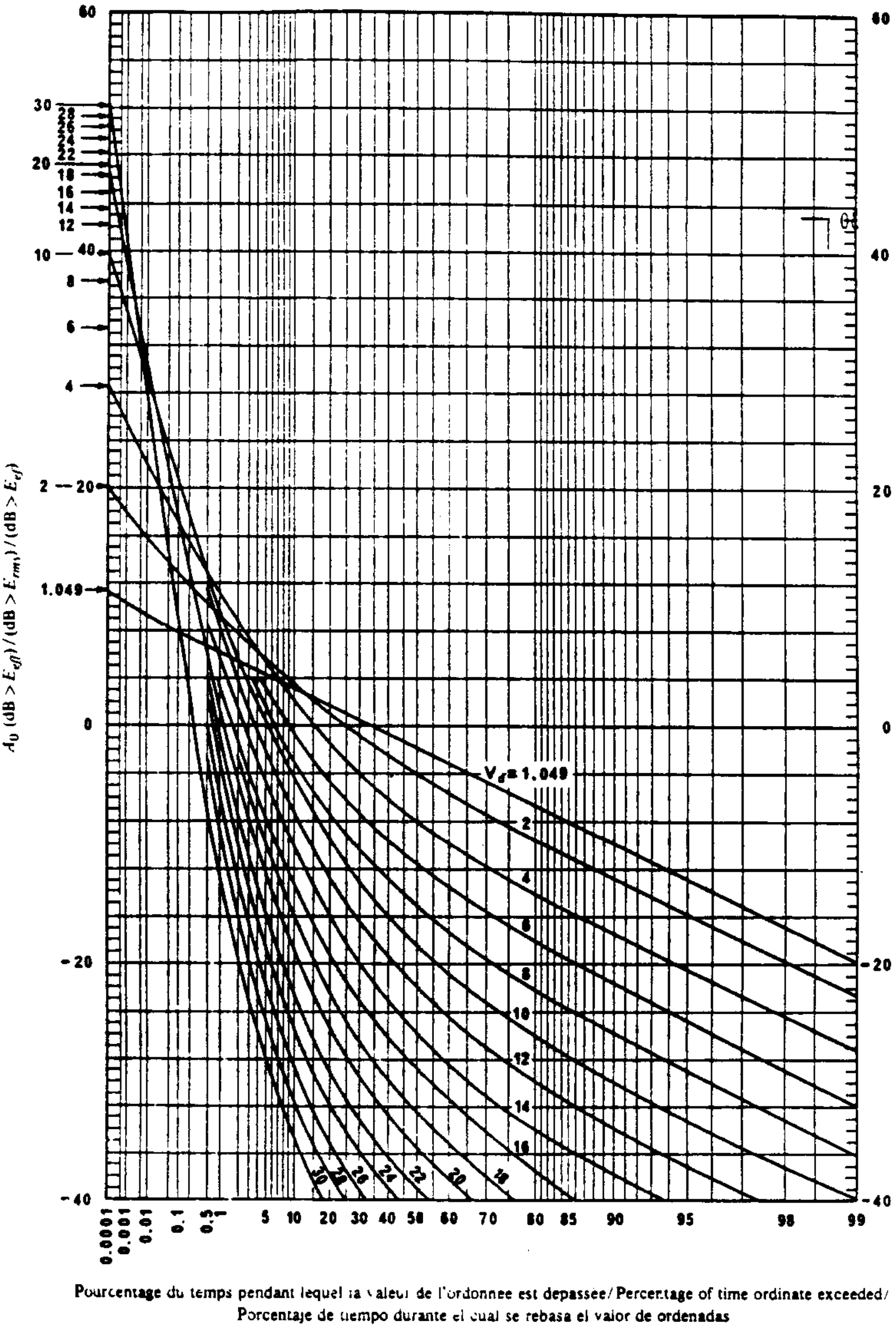

FIGURE 27 – *Distributions de probabilite d'amplitude du bruit atmospherique radioelectrique pour differentes valeurs de $V_d$*

FIGURE 27 – *Amplitude probability distributions for atmospheric radio noise for various values of $V_d$*

FIGURA 27 – *Distribuciones de la probabilidad de amplitud (DPA) del ruido radioelectrico atmosférico para* [illegible]

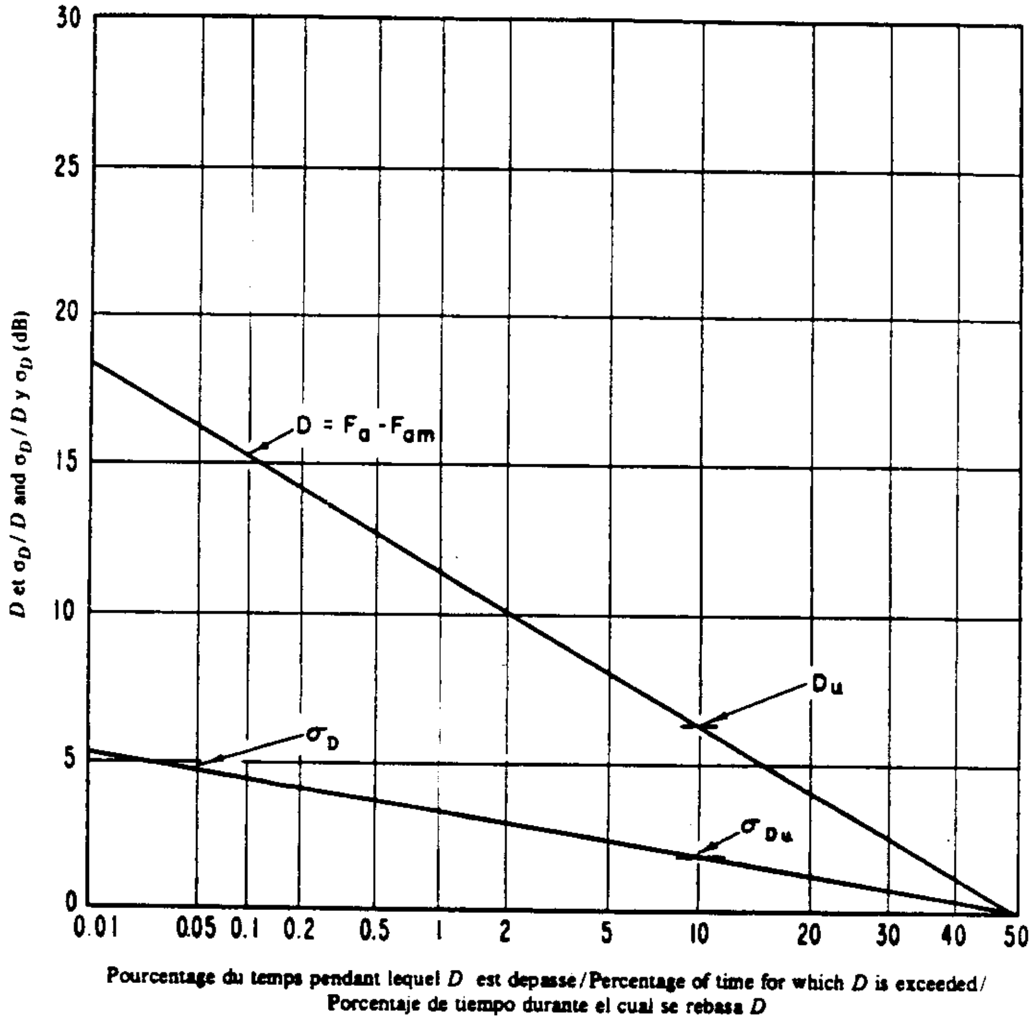

FIGURE 28 – *Valeurs attendues de D et de leurs écarts types* $\sigma_D$
FIGURE 28 – *Expected values of D and their standard deviations* $\sigma_D$
FIGURA 28 – *Valores probables de D y de sus desviaciones típicas,* $\sigma_D$

| | | |
|---|---|---|
| Eté: 2000-2400 heure locale | Summer: 2000-2400 LT | Verano: 2000-2400 hora local |
| Fréquence: 50 kHz | Frequency: 50 kHz | Frecuencia: 50 kHz |

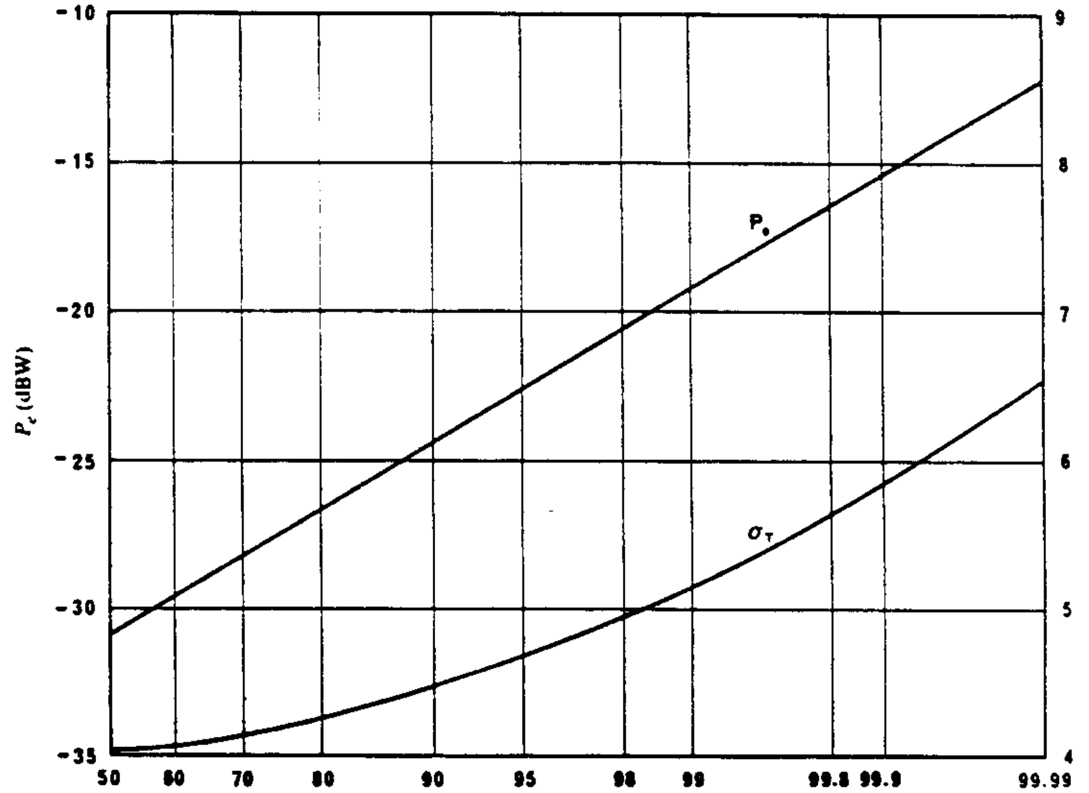

Durée de service satisfaisant/Time availability/Disponibilidad en el tiempo (%)

FIGURE 29 – *Valeurs de $P_e$ et de leurs écarts types $\sigma_T$*
FIGURE 29 – *Values of $P_e$ and their standard deviations $\sigma_T$*
FIGURA 29 – *Valores de $P_e$ y de sus desviaciones típicas, $\sigma_T$*

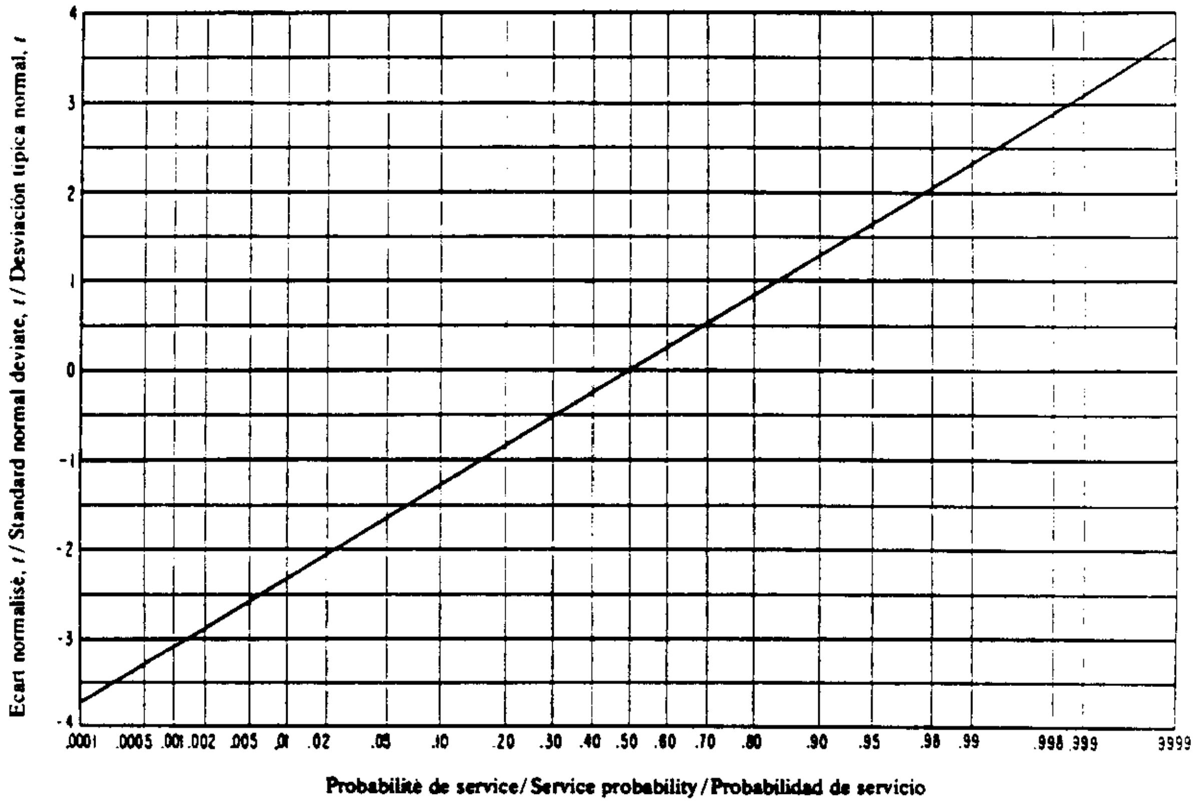

FIGURE 30 – *Probabilité de service en fonction de l'écart normalisé t*
FIGURE 30 – *Service probability as a function of the standard normal deviate, t*
FIGURA 30 – *Probabilidad de servicio en función de la desviacion tipica normal, t*

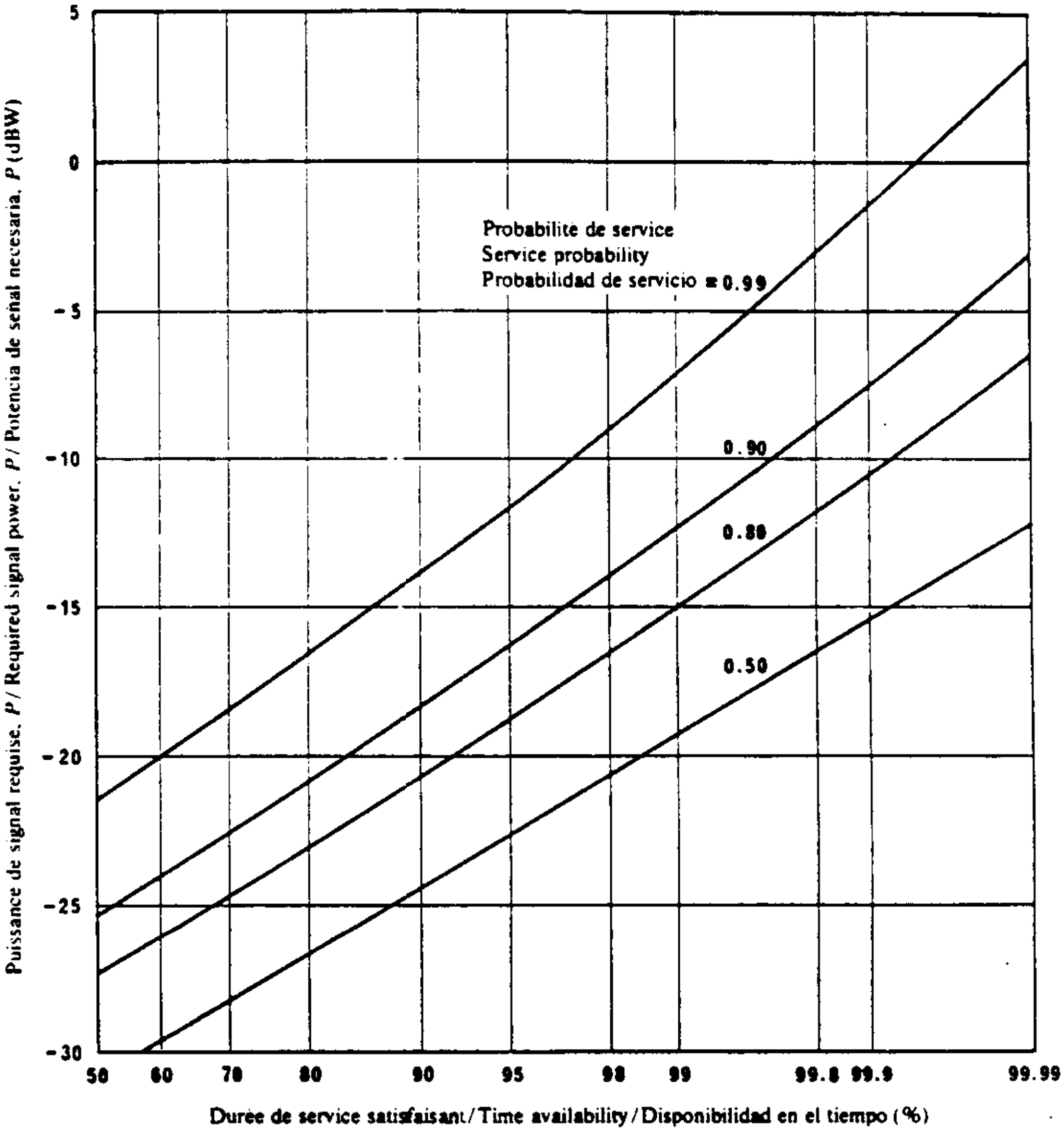

FIGURE 31 – *Puissance de signal requise en fonction de la duree de service satisfaisant, pour differentes probabilites de service (niveaux de confiance)*

FIGURE 31 – *Required signal power versus time availability for various service probabilities (confidence levels)*

FIGURA 31 – *Potencia de señal necesaria P, en funcion de la disponibilidad en el tiempo para diversos valores de la probabilidad de servicio (niveles de confianza)*

| | | |
|---|---|---|
| Geneve, Suisse | Geneva, Switzerland | Ginebra, Suiza |
| Ete: 2000-2400 heure locale | Summer: 2000-2400 LT | Verano: 2000-2400 hora local |
| Frequence: 50 kHz | Frequency: 50 kHz | Frecuencia: 50 kHz |
| Largeur de bande: 100 Hz | Bandwidth: 100 Hz | Anchura de banda: 100 Hz |
| Erreur binaire: $5 \times 10^{-4}$ | Binary errors: $5 \times 10^{-4}$ | Errores binarios: 0.05% |
| Type de service: non coherent a MDF | Type of service: NCFSK | Tipo de servicio: MDF no coherente |

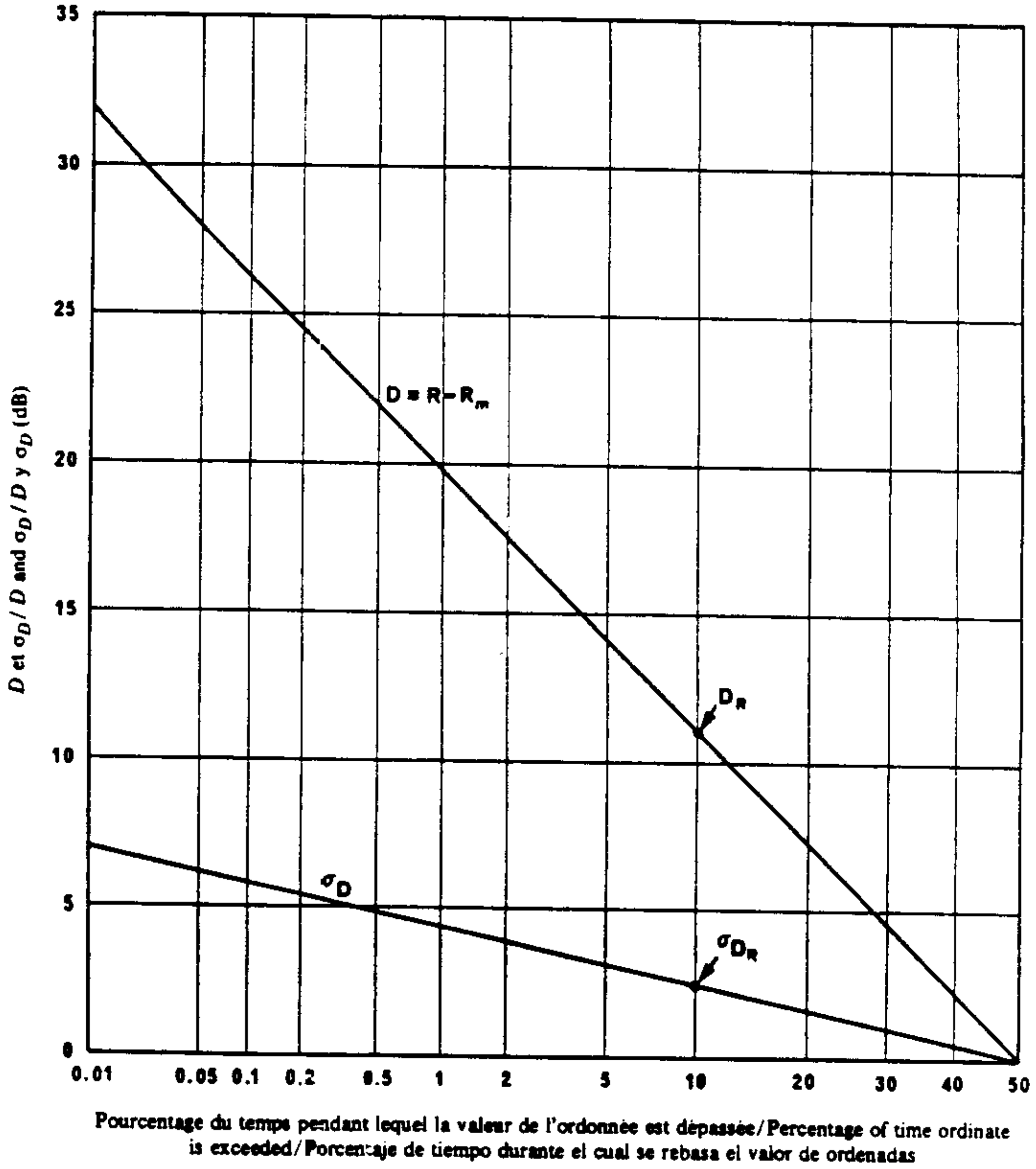

FIGURE 32 – *Valeurs de D et de leurs écarts types* $\sigma_D$
FIGURE 32 – *Values of D and their standard deviations* $\sigma_D$
FIGURA 32 – *Valores de D y de sus desviaciones típicas,* $\sigma_D$

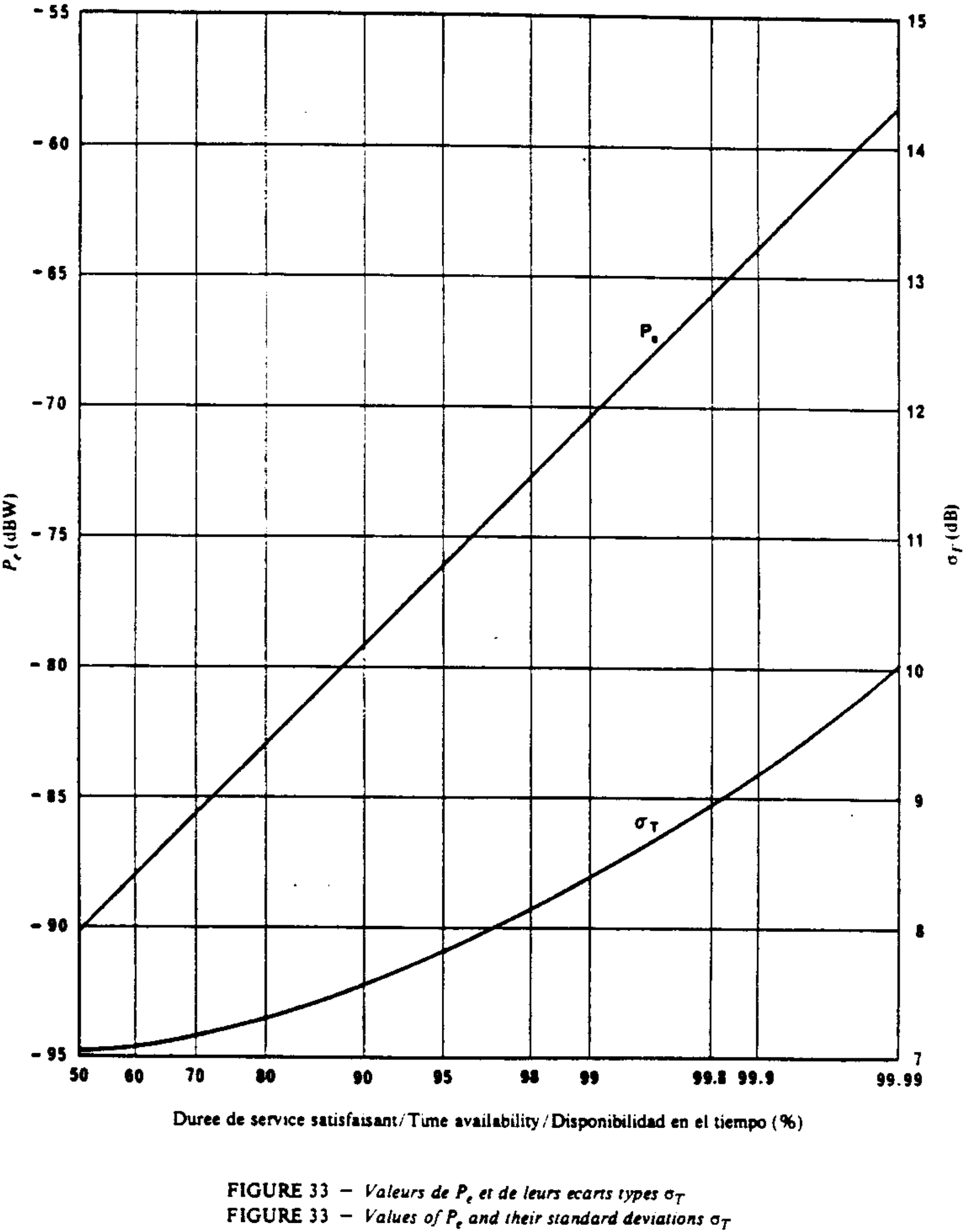

FIGURE 33 – *Valeurs de $P_e$ et de leurs ecarts types $\sigma_T$*
FIGURE 33 – *Values of $P_e$ and their standard deviations $\sigma_T$*
FIGURA 33 – *Valores de $P_e$ y de sus desviaciones tipicas, $\sigma_T$*

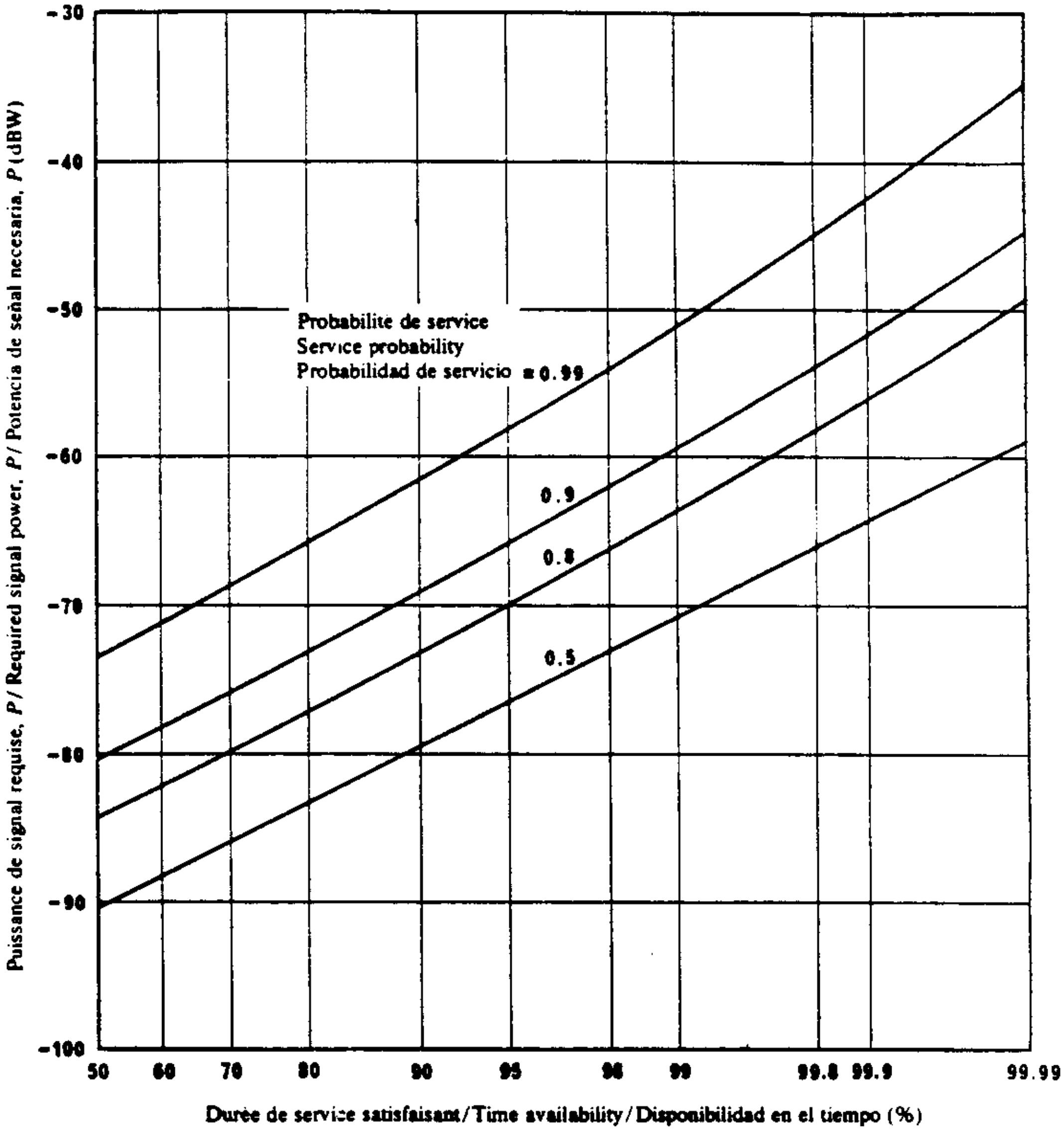

FIGURE 34 – *Puissance de signal requise en fonction de la durée de service satisfaisant, pour différentes probabilités de service (niveaux de confiance)*

FIGURE 34 – *Required signal power versus time availability for various service probabilities (confidence levels)*

FIGURA 34 – *Potencia de señal necesaria, P, en función de la disponibilidad en el tiempo para diversos valores de la probabilidad de servicio (niveles de confianza)*

| | | |
|---|---|---|
| Genève, Suisse | Geneva, Switzerland | Ginebra, Suiza |
| Eté: 2000-2400 heure locale | Summer: 2000-2400 LT | Verano: 2000-2400 hora local |
| Fréquence: 5 MHz | Frequency: 5 MHz | Frecuencia: 5 MHz |
| Largeur de bande: 6 kHz | Bandwidth: 6 kHz | Anchura de banda: 6 kHz |
| Téléphonie A3E, qualité tout juste commerciale | A3E telephony, marginally commercial service | Telefonía A3E, servicio marginalmente comercial |